ABSTRACT

Title of Document: IDENTIFICATION AND CHARACTERIZATION OF HRG-1 HEME TRANSPORTERS IN EUKARYOTES

Abbhirami Rajagopal, Doctor of Philosophy, 2008

Directed By: Assistant professor Dr. Iqbal Hamza, Department of Animal and Avian sciences & Molecular and Cellular Biology Program (MOCB)

Heme is a prosthetic group in proteins that perform diverse biological functions including respiration, gas sensing, xenobiotic detoxification, cell differentiation, circadian clock control and micro RNA processing. In most eukaryotes, heme is synthesized through a multi-step pathway with defined intermediates that are highly conserved through evolution. Despite our extensive knowledge about heme biosynthesis and degradation, the molecules and pathways involved in intracellular heme trafficking are unknown, primarily due to the inability to dissociate the tightly regulated processes of heme biosynthesis and degradation from intracellular trafficking events. *Caenorhabditis elegans* and related helminths are natural heme auxotrophs that rely solely on exogenous heme for normal development and reproduction. We performed a genome-wide microarray analysis and identified 288 genes that are regulated by heme at the transcriptional level in *C. elegans*. Here, we characterize two heme-responsive genes, *hrg-1* and its paralog *hrg-4*, that are highly upregulated at low heme concentrations and

demonstrate that HRG-1 and HRG-4 are heme transporters. Depletion of *hrg-1* and *hrg-4* in worms by RNAi results in the disruption of organismal heme homeostasis and abnormal response to heme analogs. HRG-4 traffics to the plasma membrane, and HRG-1 localizes to endo-lysosomal compartments. While *hrg-4* appears to be specific to worms, *hrg-1* has homologs in vertebrates. Knock-down of *hrg-1* in zebrafish results in severe anemia and profound developmental defects, which are fully rescued by worm *hrg-1*. Human and worm HRG-1 proteins localize together. CeHRG-1, hHRG1 and CeHRG-4 all bind and transport heme. To further understand the *in vivo* functions of *hrg-1* and *hrg-4*, we characterize the genetic deletions of these genes in *C. elegans*. Preliminary experiments suggest that the deletion mutants respond abnormally to heme analogs, although these results do not phenocopy the RNAi knock-down studies. We speculate that the deletion strains may have developed compensatory mechanisms in response to the genetic lesions in *hrg-1* and *hrg-4*. Taken together, the studies described herein lay the foundation for identifying the molecular mechanisms for heme transport by the HRG-1 proteins in metazoans and delineating the heme trafficking pathways in *C. elegans*.

IDENTIFICATION AND CHARACTERIZATION OF HRG-1 HEME TRANSPORTERS IN EUKARYOTES

By

Abbhirami Rajagopal

Dissertation submitted to the Faculty of the Graduate School of the
University of Maryland, College Park, in partial fulfillment
of the requirements for the degree of
Doctor of Philosophy
2008

Advisory Committee:
Dr. Iqbal Hamza, Chair
Dr. Eric Haag
Dr. Gerald Deitzer
Dr. Michael Krause
Dr. Tom Porter
Dr. Carol Keefer, Dean's Representative

© Copyright by
Abbhirami Rajagopal
2008

Dedication

TO MY SISTER, WHO LIVES ON, IN OUR MEMORIES

Acknowledgements

These past few years have been a wonderful learning experience for me and for that I would like to thank my mentor Dr. Iqbal Hamza. He has always believed in me and has been very supportive of me even through some of my worst days. He has trained me to think critically and his passion for his work has finally trickled down to me! I will always be grateful for all that he has done.

I thank my committee members Dr. Eric Haag, Dr. Gerald Deitzer, Dr. Michael Krause, Dr. Tom Porter for their help and suggestions through out the course of this work. Their suggestions have always been very constructive and have helped shape my scientific thinking. I thank Dr. Carol Keefer for serving as the Dean's Representative on my committee.

These few years in the Hamza lab would not have been so much fun if not for the wonderful lab members, past and present. When I first joined the lab, it was just Anita (former post-doc), Melissa (the former lab technician) and me. I must thank Anita Rao and Melissa Winn, for all the discussions that have kept me going all these years. I am fortunate to be in a lab that works together so closely. I must thank the lab members: Scott, Tamika (the newest member of the lab), Neely, Caiyong, Jason, Xiaojing, Caitlin and Jon (the newest grad student). It has been really fun working with all of you! Scott has helped me with not just writing this dissertation (he has had to go through his document several times!) but also helping me to "hang-in-there". The pep talks over Starbucks have been helpful. Thank you Scott! I must thank Caitlin for helping me with mammalian experiments and going over my thesis in a record day and a half. Xiaojing was the "go-to" person in helping me with some of

my experiments while I was trying to write. Jon and the undergrads- Talia and Yike, have been very helpful- whenever I needed help, I could count on them.

I thank Donna (ex-MOCB secretary), Sarah (current MOCB secretary) and Sheryl Grey (Animal Science). Any sort of paperwork, they were there to take care of it!

I thank all my friends in the Animal Sciences department and the MOCB program for all their support and encouragement.

To my family, especially my parents and grandma- could not have done this without you. You have been and will always be my inspiration and my pillars of support. To my friends- thank you, you have been my mirror- I could think aloud, talk aloud, and express myself in front of you.

To Ashok, this would not have been possible but for you. Thank you for just being there when I most needed.

Table of contents

List of Tables

Chapter 3

List of Figures

Chapter 1

Chapter 3

Chapter 4

Chapter 5

Chapter 1 Introduction

Iron, one of the most abundant transition metal present in the Earth, is also a critical micronutrient. With its ability to readily accept and donate electrons, it participates in a wide variety of biochemical reactions as an oxidant or reductant. Iron deficiency is a major diet-related health problem world-wide [1]. Iron-deficiency anemia affects up to two billion people and can exacerbate other health problems. Iron deficiency impairs physical and mental development in children. In developing countries, serious complications from nutritional iron deficiency are compounded by malaria and hookworm infestations. Hookworms cause anemia by feeding on blood from lacerated capillaries in the intestinal mucosa. The malarial parasite, *Plasmodium falciparum*, contributes to the etiology of anemia through several mechanisms including direct destruction of parasitized red blood cells, reduction in iron absorption due to increased parasite load and even sequestration of iron by the parasite. As a result, therapeutic regimens for treating both hookworm infections and malaria include iron supplements [2-5].

Despite being one of the Earth's most abundant metals, iron-deficiency anemia is a major health risk factor in both developed and developing countries for two reasons. The first reason for such high incidence of iron deficiency anemia is that, under physiological pH, elemental Fe (II) oxidizes to Fe (III), which then precipitates to form ferric hydroxide or hydroxyl-iron dimers that are absorbed poorly by the small intestine. The second reason is that plant compounds such as tannins and phytates can chelate free iron to form insoluble complexes that prevent iron absorption [6]. By contrast, heme, or iron-protoporphyrin IX, is more readily

absorbed than inorganic iron and is the source for two-thirds of body iron even though heme constitutes only one-third of total dietary iron [7, 8]. This can be attributed to the fact that heme is soluble in the alkaline pH of the small intestine where most absorption occurs and heme uptake is not influenced by plant compounds that interfere with iron absorption [9]. Despite the importance of heme as a dietary source of iron, the mechanism by which heme absorption occurs through the intestinal cells is poorly understood. While biochemical studies have shown that heme is absorbed via the brush border present on the enterocytes, the proteins responsible for heme uptake are unclear [10-12].

Heme is a prosthetic group of proteins that perform diverse functions such as oxygen transport (globins), xenobiotic detoxification (cytochrome P450s), oxidative metabolism (cytochrome *c* oxidase), gas sensing (guanylate cyclases), circadian rhythm (nuclear hormone, Rev-erb α) and thyroid hormone synthesis (thyroperoxidase) [13]. Heme has also been shown to directly regulate processes such as cell differentiation and gene expression [14, 15]. It has also been proposed that heme may function as an acute cell-signaling molecule because it has been shown to bind the large-conductance calcium-dependent Slo1 BK channels (a class of ion channel) with high affinity [16]. Heme is synthesized through a highly conserved, eight-step pathway in most prokaryotes and eukaryotes. Tight control of cellular heme level is achieved by maintaining a balance between heme biosynthesis and catabolism by the enzyme heme oxygenase.

Although heme biosynthesis and its regulation have been extensively studied, very little is known about the intracellular trafficking of heme. Once heme is

synthesized, it has to be transported across the mitochondrial inner membrane for incorporation into cytochromes present in the mitochondrial intermembrane space. Also, heme has to be transported out of the mitochondria to be incorporated into hemoproteins found in the cytosol, nucleus, endoplasmic reticulum and other organelles. Free heme is hydrophobic and cytotoxic due to its inherent peroxidase activity [17]. Thus, a *prima facie* argument can be made that specific molecules and pathways exist to transport heme from the site of synthesis to other cellular compartments where hemoproteins are present.

Heme biosynthesis

Heme is synthesized in most eukaryotic cells via a series of eight highly conserved enzymatic steps. The first step in the heme biosynthetic pathway is the condensation of succinyl CoA and glycine to form 5-aminolevulinic acid (ALA) catalyzed by ALA synthase (ALA-S). This reaction occurs in the matrix of the mitochondria. ALA is transported out of the mitochondria to the cytosol for the subsequent four steps of heme biosynthesis. ALA dehydratase (ALA-D) converts 2 molecules of ALA to porphobilinogen (PBG), an intermediate with only one pyrrole ring. Porphobilinogen deaminase catalyzes the conversion of 4 molecules of PBG to an unstable polymer hydroxymethylbilane and uroporphyrinogen synthase (UPO-S) converts hydroxymethylbilane to uroporphyrinogen III (UPO III), a cyclic tetrapyrrole. In the next step, UPO III is decarboxylated by uroporphyrinogen decarboxylase (UPO-D) to form coproporphyrinogen III (CPO III). CPO III is transported into the mitochondria, where coproporphyrinogen oxidase (CPO), an enzyme found in the mitochondrial intermembrane space, catalyzes the formation of

protoporphyrinogen IX (PPO IX). In the final step, ferrochelatase (FECH) catalyzes the insertion of ferrous iron into the protoporphyrin IX (PPIX) ring to form protoheme or heme *b* (Figure 1).

Heme *b* is modified at the C-2 and C-8 positions to form heme *a*, the form of heme that is found in cytochrome oxidases [18]. These modifications occur in two steps involving heme *o* synthase and heme *a* synthase. Heme *c* is found in cytochromes *c1* and cytochrome *c*. Heme *c* differs from heme *b* in that heme *c* binds proteins covalently through the two vinyl side chains [19].

The universal precursor of heme biosynthesis, 5-aminolevulinic acid (ALA), is synthesized from succinyl CoA and glycine in most eukaryotes but in some prokaryotes and all higher plants, ALA is synthesized via the glutamate C-5 pathway [20]. ALA synthesis occurs in three steps. Glutamate is converted to glutamyl-tRNA. Glutamate-1-semialdehyde is synthesized from glutamyl-tRNA by glutamyl-tRNA reductase. Glutamate-1-semialdehyde amino-transferase catalyzes the conversion of glutamate-1-semialdehyde to 5-aminolevulinic acid (ALA), after which the heme biosynthetic pathway is similar to its mammalian counterpart. Higher plants synthesize four major tetrapyrrole compounds and they are heme, siroheme, chlorophyll and phytochromobilin [21, 22]. Uroporphyrinogen III is the branch point for pathways leading to the synthesis of these different tetrapyrrole molecules. Methylation of UPO III and the subsequent insertion of iron (Fe^{+2}), results in the formation of siroheme. Protoporphyrin IX is synthesized in plants in a manner similar to other eukaryotes. Insertion of Fe^{+2} into PP IX is the final step in heme biosynthesis, while Mg^{+2} insertion into PP IX is the first step in the synthesis of chlorophyll [20].

Figure 1. Heme biosynthesis in eukaryotes

Heme biosynthesis is an eight-step enzymatic pathway that begins with the synthesis of ALA in the mitochondria. ALA is then transported from the mitochondria into the cytosol where the subsequent four steps occur. The intermediate coproporphyrinogen III is transported back into the mitochondria for the final three steps. The final step is the insertion of ferrous iron into the protoporphyrin IX ring and this reaction is catalyzed by ferrochelatase. Mitochondrial enzymes are in green and cytosolic enzymes are in red.

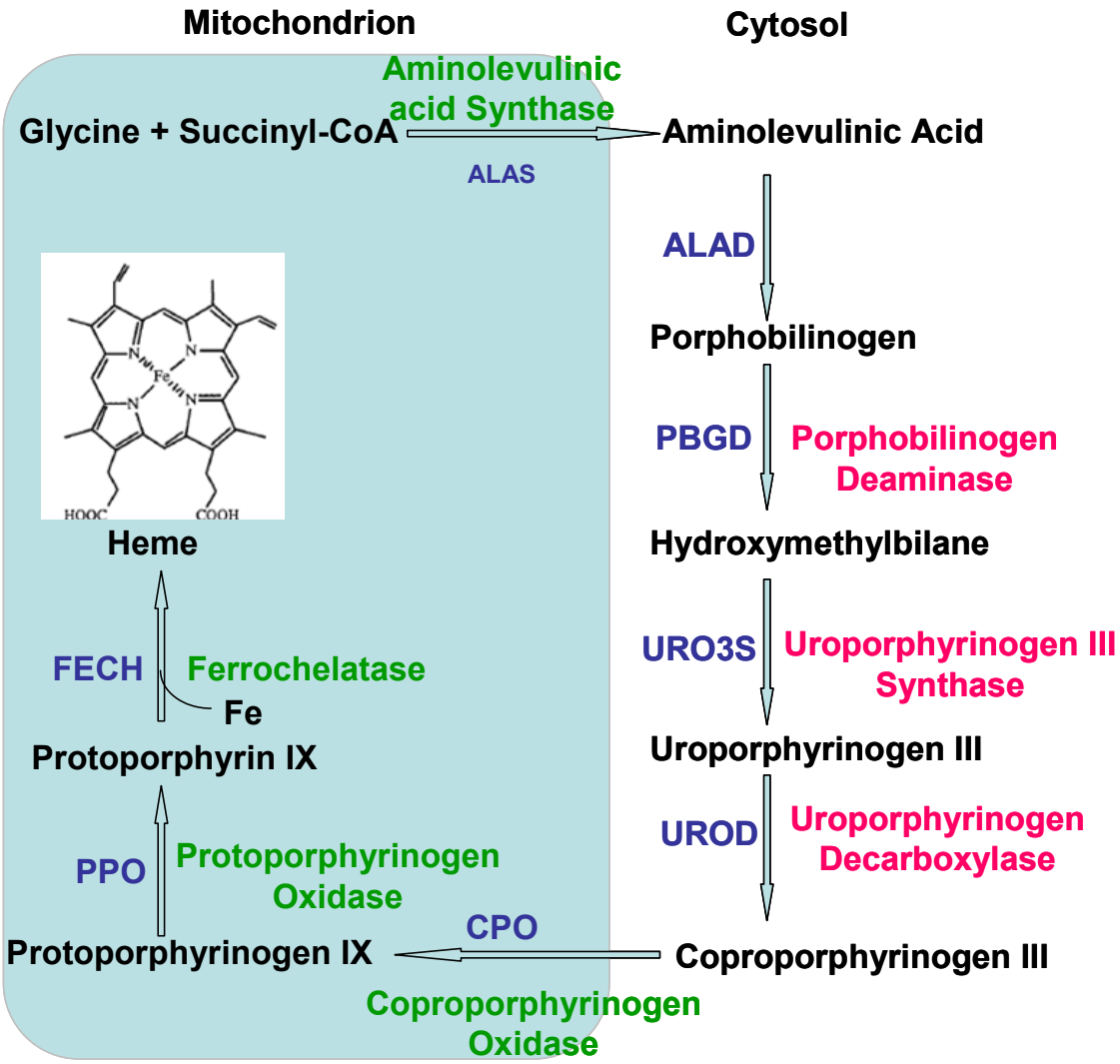

Adapted from BBA-Molecular Cell Research , 2006. 1763 (77):p. 723-736

Regulation of heme biosynthesis

Heme biosynthesis is regulated by several factors including iron availability, oxygen and by heme levels and has been extensively studied in many model organisms. In the bacterium *Bradyrhizobium japonicum*, heme biosynthesis is tightly coordinated with iron availability [23]. It has been shown that mutations in the Iron Response Regulator (*irr*) gene resulted in accumulation of toxic levels of porphyrin, and increased expression of *hemB*, or ALA dehydratase, an iron-dependent enzyme in the heme biosynthetic pathway that encodes ALA-D, under iron-limiting conditions in *B. japonicum*. Bacteria carrying the mutations in *irr* also had a deficiency in high affinity iron transport indicating that Irr might also play a role in maintaining cellular iron levels. Irr was found to accumulate only in conditions when iron was limiting and turned over rapidly when there was an abundant supply of iron. These results suggested that Irr is involved in iron homeostasis and the coordination of heme biosynthesis with iron availability [23].

A previous study in *Saccharomyces cerevisiae* (baker's yeast) showed that when oxygen levels fall below submicromolar concentrations, heme synthesis declines [24]. It has been shown in baker's yeast that transcription of *HEM13;* a gene that encodes for coproporphyrinogen III oxidase, is repressed by heme and oxygen [25, 26]. While in *S. cerevisiae* heme is used as a measure of oxygen supply, in fission yeast *Schizosaccharomyces pombe*, sterol regulatory element binding protein (SREBP or Sre1p), an oxygen sensor, monitors sterol synthesis as an indirect measurement of oxygen supply [27]. Sre1p is an oxygen-dependent transcription

factor that allows for adaptations of *S. pombe* when oxygen levels are fluctuating. A transcriptional profiling study done in wild-type and Δ*sre1p S. pombe* during anaerobiosis identified heme biosynthesis genes as some of the primary targets of Sre1p [27]. The authors have shown significant induction of three of the heme biosynthetic genes, coproporphyrinogen III oxidase, protoporphyrinogen oxidase and ferrochelatase in mutants of *S. pombe* lacking Sre1p.

All of the genes encoding for mammalian heme biosynthetic pathway enzymes have been cloned and studied extensively. Two different genes encode for the first enzyme of heme biosynthesis, ALA synthase [28]. *ALA-S1* is expressed ubiquitously and is encoded for by the *ALA-S1* gene present on chromosome 3. *ALA-S2* on the X chromosome, encodes for the erythroid-specific *ALA-S2*. It is not surprising that the regulation of these genes is also very different. Expression of *ALA-S1* is regulated by the transcription factor NPAS2, a neuronal Pas domain region 2 protein, which also plays an important role in the circadian clock[29]. Heme-bound NPAS2 heterodimerizes with BMAL1; this complex binds to the *ALA-S1* promoter, thereby upregulating heme biosynthesis [29]. Increased levels of heme in the cell induce heme oxygenase. Degradation of heme results in the formation of carbon monoxide, biliverdin and iron. In the presence of carbon monoxide, the transcription factor complex NPAS2-BMAL1 cannot bind DNA, thus preventing the expression of *ALA-S1* [29].

It has also been shown that transcription of *ALA-S1* is upregulated by peroxisome proliferator-activated coactivator 1α, PGC-1α [30]. Interactions of PGC-1α with NRF-1 (nuclear regulatory factor) and FOXO1 (a fork head family member),

both of which bind the *ALA-S1* promoter, are important for the activation of the *ALA-S1* promoter. Even though high intake of glucose has been used as a treatment for porphyrias such as acute intermittent porphyria (AIP), the mechanism by which glucose helped alleviate the symptoms of AIP was not understood. This study was the first to reveal a link between glucose metabolism and heme homeostasis.

Han *et al* have shown that *ALAS-2* is transcriptionally regulated by histone acetyltransferase p300 in erythroid cells [31]. Erythroid-specific transcription factor GATA1 recruits the transcriptional regulator, and the interaction between these two proteins induces the *ALAS-2* promoter. In murine erythroleukemia cells, the regulation of translation ALA-S2 occurs in an iron-dependent manner by the Iron Responsive Element/ Iron Regulatory Protein (IRE/ IRP) system. Of the two forms of IRP, only IRP2 has been shown to regulate *ALA-S2* [32]. Under iron-depleted conditions, IRP2 binds IRE in the 5' untranslated region of *ALA-S2* mRNA, inhibits translation and prevents heme synthesis [33].

ALA dehydratase is the second enzyme in heme biosynthesis and catalyzes the conversion of ALA to PBG. There are no known tissue-specific isozymes for ALA-D. A single *ALA-D* gene in humans is located on chromosome 9. This gene consists of two alternatively spliced non-coding exons (1A and 1B) and eleven coding exons. Although the level of ALA-D is higher in the erythroid cells than all other cell types, there are only very subtle differences in the 5' untranslated regions between the ubiquitous and erythroid-specific *ALA-D*. While the housekeeping promoter is located upstream from exon 1A, the erythroid-specific promoter is found between exons 1A

and 1B. It has been shown that the promoter of erythroid-specific *ALA-D* has GATA1 binding sites [34].

PBG-D, the third enzyme in the biosynthesis of heme exists as two different isoforms; one expressed ubiquitously and the other expressed only in erythroid cells. The two different isoforms are encoded by one *PBG-D* gene found on chromosome 11. Two different promoters control the expression of "housekeeping" and erythroid-specific forms of *PBG-D*.

Uroporphyrinogen III is decarboxylated to coproporphyrinogen III (CPO III) by uroporphyrinogen decarboxylase (*URO-D*). Despite the marked increase in the level of *URO-D* mRNA in erythroid cells, the molecular mechanisms for this upregulation are unclear. Coproporphyrinogen oxidase found on the mitochondrial intermembrane space catalyzes the conversion of CPO III to protoporphyrinogen IX (PPO IX). Both oxygen-dependent and oxygen-independent forms of this enzyme exist. Eukaryotes and some prokaryotes utilize the oxygen-dependent form of CPO. The promoter of human *CPO* gene has a Sp-1 like element, GATA-1 binding site and a novel regulatory element, all of which interact to upregulate the expression of *CPO* in erythroid cells [35]. The enzyme that converts PPO IX to protoporphyrin IX (PP IX) is protoporphyrinogen oxidase (PPO). The gene resides on chromosome 1 and the 5' flanking region contains a GATA-1 binding site, suggesting a possible regulation by GATA-1 in erythroid cells [34].

Ferrochelatase (FECH), the last enzyme in the biosynthesis of heme, catalyzes the addition of iron into PP IX. The crystal structure of FECH revealed that the enzyme functions as a homodimer and that there is a potential binding site for an iron

donor protein on the matrix side of the homodimer [36, 37]. It has been shown that frataxin, a nuclear-encoded protein targeted to the mitochondrial matrix, important for mitochondrial iron metabolism, interacts with ferrochelatase. This interaction results in the transfer of iron from frataxin to FECH [38]. Taketani *et al* demonstrated that expression of ferrochelatase is regulated by intracellular iron levels through the iron-sulfur cluster that resides at the carboxyl-terminus of the enzyme [39]. *FECH* has been shown to be upregulated under hypoxia [40]. *FECH* has two Hypoxia Inducible Factor-1 binding sites, and, therefore, it is possible that the increase in level of *FECH* expression is due to a mechanism that involves HIF-1 [40].

Pathology of heme biosynthesis

Defects in any of the heme biosynthetic pathway enzymes, except *ALA-S2*, are clinically known as porphyrias. The classification of porphyrias is based on the site of defect (hepatic versus erythropoietic) and by the enzyme that is defective [41]. Most porphyrias result in accumulation of porphyrin intermediates. While symptoms vary depending on the type of porphyria, some of the major symptoms associated with porphyria include abdominal pain, light sensitivity (photodermatitis) and neuro-muscular symptoms such as muscle pain, muscle weakness or paralysis and numbness or tingling sensations [42].

Mutations in *ALA-S2* lead to sideroblastic anemias. This type of anemia is characterized by excessive deposits of non-heme iron within the mitochondria of a pathologic erythroid precursor.

The most common hereditary hepatic porphyria is known as acute intermittent porphyria (AIP). AIP, an autosomal dominant disorder, occurs due to the deficiency of both the ubiquitous housekeeping and erythroid-specific isoforms of porphobilinogen deaminase (PBG-D). Gastrointestinal and neuropathic symptoms such as abdominal pain and paralysis are characteristic of AIP.

An extremely rare disease called congenital erythropoietic porphyria or Gunther's disease results from mutations in uroporphyrinogen synthase. Anemia occurs as a result of a shortened life span of red blood cells, and symptoms can occasionally appear during infancy [43]. Defects in protoporphyrinogen oxidase lead to variegate porphyria. This porphyria is characterized by skin photosensitivity and skin eruptions on exposure to sun due to accumulation of porphyrins [41].

A deficiency in uroporphyrinogen decarboxylase (URO-D) causes porphyria cutanea tarda (PCT). This disease is most often acquired, but, in some individuals PCT develops due to inheritance of autosomal dominant deficiency of URO-D [44]. This is one of the hepatic porphyrias and large amounts of porphyrins build up in the liver when the disease becomes active. Factors such as iron deficiency and alcohol use influence PCT disease progression. PCT is the most treatable of porphyrias. Removal of blood or a phlebotomy to reduce iron load is the most recommended form of treatment.

Deficiency of ferrochelatase activity results in erythropoietic protoporphyria (EPP), also known as protoporphyria. Patients with this disorder have reduced enzyme activity and accumulate protoporphyrin in their hepatic cells, which leads to hepatic failure. This disease is also characterized by severe photosensitivity [44]. Oral

administration of beta-carotene, vitamin A precursor and a natural plant product, has been the most effective treatment as it reduces the symptoms of photosensitivity [43].

Degradation of heme

While heme that is synthesized in most eukaryotic cells is used for incorporation into hemoproteins that perform diverse biological functions, heme is also absorbed by enterocytes as a dietary source of iron. Once heme bound to hemoglobin is absorbed through the intestine, it is broken down to biliverdin, CO and iron in two steps. The first step is breakdown of heme by the microsomal enzyme heme oxygenase (HO), into bilirubin [45]. The second step of the heme degradation pathway is the catalysis of bilirubin to biliverdin, CO and iron by biliverdin reductase.

Heme oxygenase also catalyzes the breakdown of free heme that is not bound to any protein, acting as a scavenger to prevent the toxicity from free heme. Two different genes encode two isoforms of heme oxygenase *HO-1*, the inducible form and *HO-2*, which is constitutively expressed [46]. *HO-3*, a third isoform of heme oxygenase, is brain-specific and exhibited very poor heme degradation activity when expressed in *E. coli* [47]. Results from Hayashi *et al* showed that *HO-3* is a pseudogene arising from *HO-2* because of the presence of stop codons within the coding region of *HO-2* and the lack of *HO-3* mRNA and protein expression in rat tissues.

Although HO enzymes are present in abundance in the ER, it has been shown that HO-1 associates with the plasma membrane of endothelial cells upon induction

by factors such as LPS and heme [48]. Nuclear translocation of HO-1 was observed when NIH3T3 cells were stimulated with heme, hemopexin or hypoxia [49]. Translocation to the nucleus requires a C-terminal truncation of HO-1 by an uncharacterized protease. Nuclear localization has been shown to be an important cytoprotective signaling mechanism during oxidative stress [49].

Bach-1, a mammalian transcriptional repressor that is regulated by heme, regulates *HO-1* [50]. Bach-1 is a bZIP protein that forms heterodimers with Maf proteins, binds to heme responsive elements (HRE) in the 5' untranslated region of the *HO-1* promoter and down regulates *HO-1* under low heme conditions. In human liver cells, knock-down of BACH-1 resulted in an increase in *HO-1* gene expression. Binding of heme to Bach-1 caused a conformational change and reduced the ability of Bach-1 to bind to HREs found in the promoter of *HO-1*. This, in turn, led to the binding of transcriptional activators, such as Maf and Nrf2, to HREs in the *HO-1* promoter to increase transcription of *HO-1* [50].

HO-1 belongs to a larger family of stress proteins. Although HO-1 shares no homology with heat shock proteins and does not display any protein chaperone activity, promoter regions of HOs from different species contain heat shock elements. For this reason, HO-1 is also referred to as Hsp-32. In rodents, hypothermia has been shown to induce HO-1 protein and mRNA accumulation [51].

While HO has been shown to play important cytoprotective roles, the products of heme degradation also play key roles in several cellular processes [51]. Iron released from heme by HO has been thought to enter a labile or chelatable pool of iron and can be used for iron-dependent cellular processes [52]. Studies have also

shown that levels of ferritin, an iron storage protein, increased when HO-1 was induced [53, 54]. Ferritin synthesized due to HO-1 activity has been thought to contribute to HO-1-mediated cytoprotection [55]. The other product of heme degradation is bilirubin, a yellow pigment that is secreted into the bile and rapidly eliminated. Although bilirubin is eliminated from cells, it has been shown to have a beneficial role as an antioxidant and is still under investigation as a therapeutic agent for several inflammatory diseases such as vascular injury [51].

Carbon monoxide (CO) is also generated upon degradation of heme. Despite its effects as an air pollutant, recent studies shed light on the physiological importance of CO. CO has been shown to bind directly to heme-iron of soluble guanylate cyclase, thereby stimulating the enzyme and leading to subsequent elevation in cyclic GMP levels [56]. CO has also been shown to have anti-apoptotic and anti-proliferative effects. CO has been known to possess vasodilation properties, and these dilatory effects are thought to occur by regulating cGMP levels and potassium channel activity [51].

The end products of heme degradation have been examined for their therapeutic value. For example, application of bile pigments exogenously has been shown to alleviate symptoms of transplant rejection, and inhalation of CO has been effective in several animal models including models of inflammation, vascular injury, hypertension and lung injury [51].

Heme uptake and transport

Heme uptake and transport have been well-characterized in pathogenic bacteria. In order to cause infection in the host, pathogenic bacteria must satisfy their iron demands. As a defense mechanism against pathogens, the host must restrict access to iron and heme. This restriction of iron and heme to pathogens poses a serious problem that the bacteria must overcome for survival. While most bacteria secrete high-affinity, low-molecular weight chelators to sequester iron, some have the ability to obtain their iron requirements by binding either exogenous heme or heme-containing proteins, or by secreting hemophores [57].

The general mechanisms of heme acquisition in pathogenic gram-negative bacteria are demonstrated in Figure 2. Heme uptake systems are classified into two groups *a)* those that involve direct binding of heme or hemoproteins by specific outer membrane receptors and *b)* those that involve secretion of hemophores that bind the heme source and deliver it to specific receptors [57]. There are 29 outer membrane heme receptors that have been identified from different species of gram-negative bacteria. Although these receptors share between 21% and 90% homology when compared to each other, they all share a highly conserved amino acid motif FRAP(10X)H(XX)NPL(2X)E [58]. The outer membrane receptors can be divided into subgroups. A first subgroup of outer membrane receptors is not substrate-specific and binds either heme or heme-containing proteins. Such receptors are found in *Yersinia enterocolitica*, *Escherichia coli* and *Shigella* [57]. Outer membrane receptors such as HemR in *Y. enterocolitica* bind heme and transport it actively across the outer

membrane into the bacterial periplasm. An intact Ton system, with the cytoplasmic membrane proteins ExbB and ExbD and membrane-anchored protein TonB, is required to provide energy for heme transport across the outer membrane. The TonB system uses a proton-motive force for the passage of heme into the periplasm. Heme is bound by a periplasmic heme binding protein such as HemT and then delivered to permeases on the cytoplasmic membrane, like HemU and HemV in *Y. enterocolitica* [59]. Transport of heme across the cytoplasmic membrane requires expenditure of ATP. In the cytoplasm, HemS and HemO proteins process heme to release iron.

The second subgroup of receptors is substrate-specific and binds only one or two sources of heme. These heme receptors are found in *Vibrio*, *Neisseria* and *Haemophilus* and these receptors have a high affinity binding sites for one or two particular heme sources such as hemoglobin (Hb) and or haptoglobin-hemoglobin (Hpt/Hb) complexes [57]. The neisserial Hpt-Hb and Hb receptor, HpuAB is the only system with two outer membrane receptors, HpuA and HpuB. While HpuA is an outer membrane lipoprotein, HpuB is a TonB-dependent receptor that is similar to other TonB-dependent receptors. It has been shown that both proteins are required for Hb, Hpt-Hb and apo-haptoglobin binding. But it is not clear as to whether HpuA and HpuB have similar binding affinities for holo- versus apo-haptoglobin [57].

Figure 2. Heme acquisition by gram-negative bacteria.

Hemolysin secreted by bacteria degrades red blood cells (RBC), releasing hemoglobin (Hb) and heme. Once released, heme may be transported into the bacterial cell by different mechanisms A) direct binding of hemoglobin or heme to a specific TonB-dependent outer membrane receptor results in transport of heme into the periplasm. B) Capture of hemoproteins such as hemoglobin or hemopexin by hemophores, which deliver these hemoproteins to a specific TonB-dependent outer membrane receptor. C) Degradation of hemoproteins by either membrane bound or secreted bacterial proteases to release heme. Heme bound by TonB-dependent outer membrane receptors is transported into the periplasm. TonB in association with the ExbB and ExbD proteins provide energy for this process. The transport of heme through the cytoplasmic membrane occurs via a system composed of cytoplasmic membrane-associated permease and an ATPase. Heme oxygenase-like enzymes degrade heme in the cytoplasm.

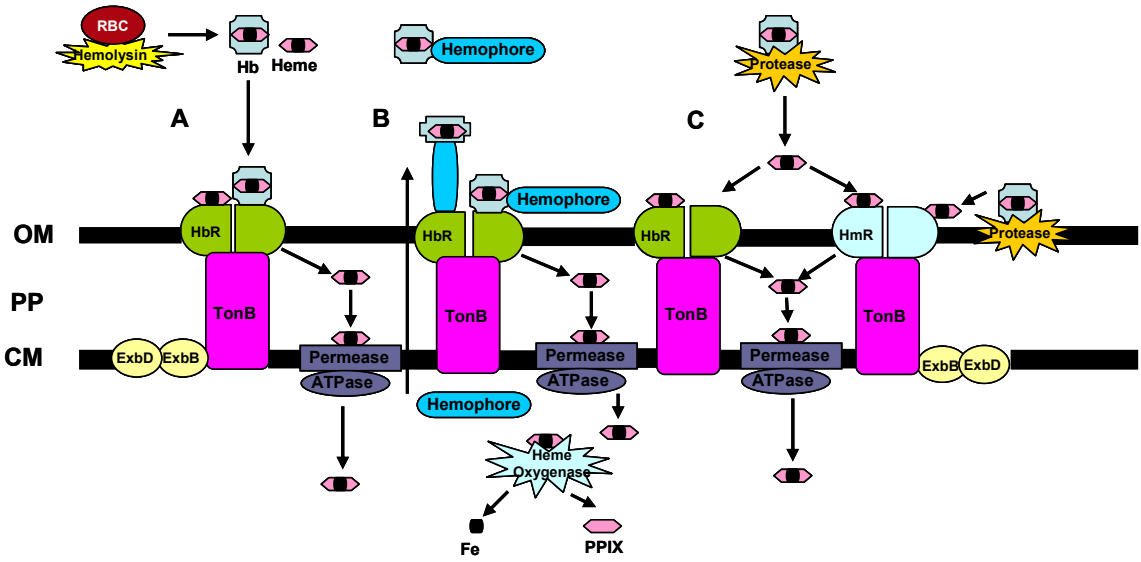

Adapted from *Molecular Microbiology, 2001. 39*

Several gram-negative bacteria secrete small extracellular proteins called hemophores. They are secreted by ABC transporters and this process involves their carboxy-terminal secretion signal [60]. Hemophores bind heme and deliver it to specific outer membrane receptors. One of the best-studied systems is the HasA-HasR mediated heme uptake in *Serratia marcescens*. While usually the role of hemophores is to bind free heme or Hb-bound heme, the hemophore, HasA, secreted by HasDEF in *S. marcescens* has been shown to extract heme from hemoproteins. The free heme is then delivered to the outer membrane receptor HasR [61, 62]. HasR can transport either free heme or heme from hemoglobin, but the presence of HasA promotes heme uptake to a greater extent. The mechanism of heme transfer to HasA from hemoglobin is not understood. It is thought that hemoglobin loses its heme moiety in solution, which is then bound by HasA [63]. Similar hemophore-mediated heme acquisition systems have been identified in *Porphyromonas gingivalis* and the human pathogenic strain of *Escherichia coli* [64, 65].

The only known bacterial system that utilizes heme bound to hemopexin (HPX) is the HuxA hemophore system found in *Haemophilus influenzae* [66]. *H. influenzae* does not make heme and the *HuxABC* gene cluster found in these bacteria allows it to utilize hemopexin, a heme-binding blood plasma protein very efficiently. HuxA is actively secreted by HuxB and has been shown to be absolutely required for the utilization of heme-HPX complexes [58].

Some gram-negative bacteria secrete proteases that degrade host hemoproteins to release heme. A heme binding protein in *E. coli* EB1 strain was shown to possess proteolytic activity, as it was able to degrade hemoglobin [66]. *Porphyromonas*

gingivalis, a gram-negative anaerobic bacterial pathogen, secretes a class of protease called gingipains [67]. Of the several gingipains, the lysine-specific cysteine protease Kgp has been shown to both bind and degrade hemoglobin, hemopexin and haptoglobin [66].

Since heme is an essential nutrient for most pathogenic bacteria, it has been shown that virulence of pathogenic bacteria can be affected by targeting heme uptake pathways. Mutations in heme-iron uptake genes in *Staphylococcus aureus* reduced its pathogenicity in the invertebrate animal model, *C. elegans* [68]. In *Bordatella pertussis*, the bacterial agent responsible for whooping cough in humans, heme utilization by the bacteria has been shown to contribute to bacterial pathogenesis in the mouse infection model [69].

While several bacterial heme uptake and transport systems have been well-characterized, only recently have proteins involved in heme uptake been identified in eukaryotes. In pathogenic yeast, *Candida albicans*, *RBT5* and *RBT51* have been identified as heme uptake genes. Rbt5 and Rbt51 are mannosylated proteins, and Rbt5 is highly induced upon iron starvation [70]. Despite 70% homology between the two genes in *C. albicans*, *RBT5* played a more important role than RBT51 in utilization of heme as an iron source. Disruptions in these genes did not reduce the virulence of *C. albicans* in murine models [71]. *C. albicans* possess a heme-oxygenase enzyme (*CaHMX1*) that shares 25% identity with the human HO and CaHMX1 has been shown to be positively regulated by both heme and hemoglobin [72]. Whether heme-iron utilization is essential for pathogenicity would be best addressed by using mutants such as *Cahmx1*Δ or *Cahmx1*Δ and *CaRbt5*Δ double mutants, that are devoid

of the ability to use the heme as an iron source [73]. Such studies have not been done yet.

In mammals, it has been proposed that heme uptake from the enterocytes occurs through a receptor-mediated endocytic pathway. A study done by Grasbeck *et al* in pigs, showed the existence of a heme-binding protein on the microvilli of the upper small intestine [74]. Evidence for such an intestinal receptor has been reported in humans [75]. It has also been shown that this high affinity binding is lost when a trypsin digestion is performed, indicating the existence of a receptor for heme [76]. Electron microscopy studies have been performed after administration of heme or hemoglobin into the duodenum from rats or dogs. These studies reported the presence of heme on the microvilli and then accumulation of heme in vesicles that were identified as secondary lysosomes [12]. Heme was absent from these vesicles 2-3 hours after the initial dose and heme was not observed in the basal region of the cells. These results provided strong evidence that heme uptake occurs via endocytosis, but the heme-binding receptor has yet to be identified [12]. Although results from this study also suggested that iron released from heme is transported out of vesicles, no such transport mechanism has been identified.

Shayegi *et al* identified SLC46A1 as a heme carrier protein and named it HCP-1[77]. *Hcp-1* was isolated from mouse duodenum using a suppression subtractive hybridization screen using hypotransferrinaemic mice [78]. *Hcp-1* encodes a protein of ~ 50 kDa that localized to the plasma membrane. Functional studies in *Xenopus* oocytes expressing *Hcp-1*, revealed a 2-3 fold increase in heme uptake with an apparent Km of 125 μM. Uptake of radiolabeled heme from duodenal

tissue was inhibited upon incubation with HCP-1 antibodies. However, recent studies have shown that SLC46A1 is in fact a folate/proton symporter and was renamed as the Proton Coupled Folate Transporter (PCFT/HCP-1) [79]. RNA interference assays of *PCFT/ HCP-1* in CaCo-2 cells reduced pH-dependent folate uptake by 60-80%. Folate transport by this protein was at least an order of magnitude higher than that observed for heme with a Km of ~1.3 at pH 5.5, suggesting that folate might be the physiological ligand for HCP-1. Interestingly, human patients with hereditary folate malabsorption carry a missense mutation in *PCFT/HCP-1* that leads to the formation of a non-functional protein. It is currently unclear whether PCFT/HCP-1 is a low affinity heme transporter.

Although the heme biosynthesis pathway and its intermediates are well characterized, the export of ALA out and the import of coproporphyrin III into the mitochondria for heme biosynthesis are unknown [80]. Recently published reports have identified potential porphyrin transporters. A mammalian ABC transporter located on the outer mitochondrial membrane, ABCB6 was shown to interact with heme and porphyrins [81]. The authors of this study demonstrated that ABCB6 transports coproporphyrin III (CPIII) from the cytoplasm into the mitochondria. The authors extrapolated their findings to suggest that ABCB6 transports coproporphyrinogen III (CPgen III), an intermediate in the heme biosynthetic pathway, from the cytoplasm into the mitochondria [81]. A major setback of this study is that the authors used a non-physiological substrate CPIII, which is a planar porphyrin, rather than the non-planar CPgen III. A parallel study by Kabe *et al* showed that the inner mitochondrial protein, oxoglutarate carrier (OGC) facilitates

uptake of 2-oxoglutarate into the mitochondria. In this study, the authors used two fluorescent non-physiological porphyrin derivatives PdTCPP and PdTAPP. These molecules accumulated in the mitochondria, and, various techniques were used to show that these porphyrin derivatives bind OGC [82]. Transport of 2-oxoglutarate was inhibited by different porphyrin derivatives including protoporphyrin IX, coproporphyrin III and hemin [82]. A major caveat in this study is that the work was performed using synthetic porphyrin derivatives, which do not resemble CPgen III and their physiological and biochemical properties have not been characterized.

Two ABC transporters have been implicated in mediating transport of components required for heme biosynthesis and hematopoiesis, although the ligands of these transporters are unknown. To identify novel GATA-1 (a transcription factor essential for normal erythropoiesis) regulated genes, Shirihai *et al.* conducted a subtractive analysis in G1E cells (an erythroid line from GATA-1 lacking embryonic stem cells) and identified ABC-me (ABC-mitochondrial erythroid) [83]. They showed that this protein localizes to the mitochondrial inner membrane and is induced during erythroid maturation. They also found that overexpression of ABC-me induces hemoglobin synthesis in erythroleukemia cells. Because of the expression pattern, mitochondrial localization and overexpression effects of ABC-me, the authors suggest that ABC-me may mediate the transport of one or more intermediates of the heme biosynthesis [83].

Pondarre *et al.* have shown that the mitochondrial ATP-binding cassette transporter Abcb7 was essential for hematopoiesis and that partial loss of function mutations in Abcb7 resulted in X-linked sideroblastic anemia with ataxia [84]. The

authors showed by chimera analysis in mice, that the zinc protoporphyrin/heme ratio in erythrocytes increased in proportion to the contribution of Abcb7^{E433K} mutant cells (a hematologically severe form of mutation in humans) suggesting that loss of function of Abcb7 alters the availability of reduced iron to synthesize heme [84].

Two heme exporters have been reported in erythroid cells. The feline leukemia virus receptor was initially identified as a cell surface protein for feline leukemia virus subgroup C [85]. Infection of cats with this virus resulted in aplastic anemia, a type of anemia in which erythroid progenitor cells failed to mature from burst-forming units to the colony-forming units-erythroid cells. This virus-induced anemia has been mapped to a region of the gene encoding the surface envelope glycoprotein region 1. The surface envelope glycoprotein region 1 binds to the host receptor, feline leukemia virus subgroup C receptor or FLVCR [86]. FLVCR, a 60kDa protein, is a member of the major facilitator superfamily. It shares amino acid sequence homology to at least five *C. elegans* proteins of unknown function. FLVCR is expressed in different hematopoietic cells and showed weak expression in the fetal liver, pancreas and kidney [85]. Quigley *et al* have shown that FLVCR can mediate efflux of zinc mesoporphyrin in rat renal epithelial and hematopoietic K562 cells. They have also shown that heme efflux mediated by FLVCR is important for erythroid differentiation [87]. Keel *et al* recently reported that FLVCR-null mice fail to undergo erythropoiesis and die at midgestation [88]. These mice also exhibit cranio-facial and limb deformities reminiscent of patients with Diamond-Blackfan anemia, a severe but rare congenital erythroid anemia that presents in infancy. By using HO-1 and ferritin as reporters for heme and iron status in macrophages, the

authors showed that FLVCR exported heme when macrophages phagocytosed senescent red blood cells. These observations confirm the results from a previous study performed by Knuston et al, which demonstrated that not all heme is broken down in the macrophage to release iron [89].

A second heme exporter, ABCG2 was identified recently [90]. ABCG2 belongs to ATP-binding cassette (ABC) transporter family and was initially identified as a protein that confers drug resistance in breast cancer cells. The role of ABCG2 in heme transport was discovered accidentally when ABCG2-null mice fed a modified diet developed skin photosensitivity [91]. This was due to the accumulation of a degradation product of chlorophyll, pheophorbide a, which is structurally similar to protoporphyrin IX. This suggested a role for ABCG2 as an exporter of protoporphyrin compounds. Expression of ABCG2 is regulated by HIF1, and it has been shown that ABCG2 transported porphyrins under hypoxic conditions [92]. The problem with the conclusions of this study is that the mice lacking the putative heme exporter ABCG2 did not have any phenotypes associated with defects in heme dependent pathways other than mild photosensitivity.

C. elegans as a model organism

A major experimental setback in identifying molecules and pathways involved in heme homeostasis has been the inability to dissociate tightly controlled heme biosynthesis and degradation from intracellular trafficking events. The need for identifying better tools and tractable model systems to study heme homeostasis led our research group to identify *Caenorhabiditis elegans*, a free-living nematode, as a

natural heme auxotroph. This round worm lacks all eight genes required to synthesize heme and acquires heme from its diet to sustain growth and development [93]. Importantly, the phylogenetically related parasitic nematodes were also found to be heme auxotrophs [93].

Helminthic infections are a huge burden to both public health and agriculture. More than two billion people are afflicted by helminthiasis, and agricultural losses due to plant-parasitic nematodes are estimated to be approximately eighty billion dollars annually [94, 95]. Drug resistance is rampant, and there is a need to find new drug targets to eliminate these infectious agents [96, 97]. Genomic analysis of heme biosynthetic enzymes has revealed that *C. elegans* lacks orthologs for these enzymes. Heme biosynthetic enzyme activity measurements confirmed that *C. elegans* lack the ability to make heme [93]. It has been shown that other free-living nematodes such as *Panagrellus redivivus, Oscheius myriophila* and *Paragordius varius* and parasitic nematodes such as *Strongyloides stercoralis*, *Ancylostoma caninum*, *Haemonchus contortus*, *Trichuris suis* and *Ascaris suum* also lack the enzymes that are required for heme biosynthesis [93]. Analysis of the genomes for these nematodes, however indicate that they encode abundant hemoproteins suggesting the possibility that they must acquire heme from their environment. Using a liquid axenic growth medium, it was demonstrated that *C. elegans* have a biphasic requirement for heme and therefore rely on exogenous heme for metabolic processes. This suggests that worms might have evolved specific mechanisms to absorb heme from their diet and transport heme to cellular compartments for incorporation into hemoproteins. It is possible that worms also have a heme storage system to store any excess heme and an intercellular

heme transport system to mobilize heme from intestinal cells, the site of absorption, to other cell types.

Reports published have suggested a role for heme in the pathogenicity of different parasitic worms. Hookworm infections due to *Ancylostoma ceylanicum* is prevalent in developing countries and is associated with iron deficiency anemia. A recent study demonstrated the importance of host iron status as a key mediator of hookworm pathogenicity [98]. Hamsters fed a normal diet or a diet with severe iron restriction, were infected with hookworms. Animals fed a diet with reduced iron had a significant reduction in the intestinal load of worms. This observation suggested that hookworms rely on host iron for their growth and development and that treatment of hookworm infection with anthelminthic drugs in combination with iron supplements might exacerbate the severity of infection. Since hookworms, like *C. elegans*, also lack the ability to make heme, another plausible explanation given by the authors was that animals fed a low-iron diet have reduced worm burden due to inadequate amounts of heme for hookworm metabolism [93, 98].

Brugia malayi, a filarial nematode, is the causative agent of lymphatic filariasis that is endemic in Asia. Analysis of the genome sequence of *Brugia malayi* revealed the absence of the heme biosynthesis enzymes in these parasites [99]. Therefore, it is highly likely that these parasites obtain heme from the host or from *Wolbachia*, an intracellular endosymbiotic bacterium. *Wolbachia* has all but one of the heme biosynthetic enzymes and is probably an important heme source for *B. malayi*. Antibiotics that eliminate the endosymbiont have inhibitory effects on the development and fertility of the parasitic nematode and have been used to treated

patients with filariasis. Since heme is important for the growth and development of the nematode another potential drug target is the heme uptake pathway in *B. malayi* or the heme biosynthesis pathway of *Wolbachia* [100].

Our observations that *C. elegans* lacks the ability to make heme and acquire heme exogenously from their diet permits its use in the interrogation of the role of heme in human nutrition and cell biological aspects of heme homeostasis. In principle, intestinal heme absorption in *C. elegans* may be similar to dietary heme uptake by the human intestine. Furthermore, the absence of intracellular heme synthesis in *C. elegans* provides a "clean" genetic background to study organismal heme trafficking pathways. *C. elegans* has been used as a model organism for over four decades [101]. The developmental fate map for every cell has been determined. The genome has been fully sequenced and more than 70% of human genes are conserved in *C. elegans* [102, 103]. These animals are genetically tractable, optically transparent and greatly amenable for genetic screens and cell biological studies. Taken together, *C. elegans*, a natural heme auxotroph, serves as a unique animal model in delineating the cellular pathways and biochemical mechanisms in heme homeostasis.

Chapter 2 Materials and Methods

Worm cultures

When control over heme was required worms were cultured with shaking at 20°C in mCeHR-2 medium supplemented with either 10 or 20 μM hemin (Frontier Scientific) [104]. When solid media was required, worms were grown on nematode growth medium (NGM) agar plates (3 g/L NaCl, 2.5 g/L peptone, 30 g/L agar, 5 mg/L cholesterol, 0.1 M $CaCl_2$, 0.1 M $MgSO_4$ and 25 mM KH_2PO_4) spotted with OP50 bacteria. For RNA-mediated interference assays, NGM plates were made as described above but also contained 50 μg/mL carbenicillin, 12 μg/mL tetracycline and 2 mM IPTG (to induce the synthesis of double stranded RNA). RNAi plates were spotted with HT115 (DE3) bacteria (an *E. coli* strain that is deficient for RNase III that normally degrades dsRNAs and takes advantage of an IPTG-inducible T7 RNA polymerase gene contained within a stable insertion of lambda prophage DE3) [105].

Synchronization of worms

Worms in liquid mCeHR-2 medium were harvested by centrifugation at 800 X *g* for 5 min [104]. The medium was aspirated and 0.1 M sodium chloride was added. The worms were allowed to settle on ice for 5 min. The supernatant was aspirated and the adult worms that settled at the bottom of the tube were bleached using a solution of 1.1 % sodium hypochlorite (Clorox bleach) and 0.55 M sodium hydroxide to harvest eggs [104]. The eggs were washed twice (800 x *g*, 45 sec) with sterile water and were

allowed to hatch overnight at 20°C in M9 buffer (86 mM NaCl, 42 mM Na_2HPO_4, 22 mM KH_2PO_4 and 1 mM $MgSO_4$).

Preparation of hemin chloride

10 mM hemin chloride was prepared by dissolving 0.1301g of hemin chloride in 20 mL of 0.3 N NH_4OH. The pH was adjusted to 8.0 using HCl, and the volume was brought up to 20 mL with 0.3 N NH_4OH, pH 8.0. The solution was filtered using a 0.22 μm filter (Millipore) and frozen for up to a week at -20°C. Zinc mesoporphyrin (ZnMP), gallium protoporphyrin IX (GaPPIX) and protoporphyrin IX were prepared as described above except these solutions were not filtered. All porphyrin compounds were obtained from Frontier Scientific.

Hemin dose response

Synchronized L1 larvae were obtained by bleaching P_0 worms grown at 20 μM hemin. 100 L1 larvae were placed in 24-well plates containing mCeHR-2 medium with different concentrations of heme. The plates were covered with foil and worms were grown at 20°C with continuous shaking. Worm growth was monitored every day. The total number of worms from two replicate samples was counted on day nine. Averages of the total number of worms from the two replicate samples were used to generate the graph.

RNA isolation and microarray analysis

Equal numbers (3000 worms/mL) of L1 larvae (F_1), which were obtained from P_0 worms grown at 20 μM hemin chloride, were inoculated in mCeHR-2 medium with 4, 20 or 500 μM hemin chloride and grown at 20°C with continuous shaking. They were grown till they were gravid adults that were bleached to obtain F_2 larvae. Synchronized F_2 larvae were obtained by hatching the eggs obtained from F_1 adults in M9 buffer containing 4, 20 or 500 μM hemin. Equal numbers (3000 worms/mL) of L1 larvae (F_2) were inoculated in mCeHR-2 medium supplemented with 4, 20 or 500 μM hemin. They were grown with continuous shaking at 20°C. The worms were harvested at the late L4 stage, flash frozen in liquid nitrogen, and stored at -80°C. Frozen worm pellets were ground into a fine powder using a mortar and pestle, and total RNA was extracted using Trizol (Invitrogen). RNA thus obtained was subjected to RNase-free DNase treatment for 1 h at 37°C and purified using the RNeasy kit (Qiagen). Total RNA from three biological replicates was hybridized to Affymetrix *C. elegans* whole genome arrays. The RNA samples were processed by the DNA microarray facility at the National Institute of Diabetes and Digestive and Kidney Diseases, NIH. The resulting data were normalized for 20-probe set data files and analyzed using MAS 5.0 (Affymetrix). Data from worms grown in mCeHR-2 medium with 4 and 500 μM hemin were compared to data from worms grown in 20 μM hemin. Microarray data were verified with the Robust Multichip Average Method (RMA, R package) [106]. Quantile normalization and background corrections were performed using PM (perfect match) probe intensities. A total of 288 heme-responsive genes were obtained using both MAS 5.0 and RMA (fold

change cut-off ≥ 1.6) analyses. Amino acid sequences for each of these 288 genes were obtained from Wormbase and further analyzed for topology (TMHMM 2.0, SOSUI), motifs (ELM, BLOCKS, Pfam), and pathway classification (KEGG). Putative human orthologs were identified by BLAST searches (E-value ≤ 10^{-4}) of the human genome databases for the 288 candidate genes. Multiple sequence alignment was performed using ClustalW (v. 1.83)

cDNA synthesis and quantitative real-time PCR

First strand cDNA was synthesized using 2 μg of total RNA using Superscript II First Strand cDNA synthesis kit (Invitrogen). Primers spanning at least one intron for quantitative real-time PCR (qRT-PCR) were designed using Primer Express (Applied Biosystems) and Beacon designer 4 (Premier Biosoft) programs. PCR was performed using the iCycler iQ Real-time PCR Detection System (BioRad) with 0.12 U/μl Taq DNA polymerase, 40 nM fluorescein (Invitrogen), and SYBR Green I Nucleic Acid Gel Stain (Invitrogen) diluted 1:10 [107]. The PCR amplification was run for 40 cycles. The PCR products were between 150 and 200 bp in length. Quality of the PCR products was determined by dissociation curve analysis and gel electrophoresis. Each experiment was performed in triplicate. Average C_T values were used for $2^{-\Delta\Delta Ct}$ calculations of relative fold changes in gene expression [108].

RNA blotting

For RNA blot analysis, 10 μg of total RNA from N2 worms grown at 4, 20 or 500 μM hemin chloride was resolved on a 1.5 % formaldehyde agarose gel, transferred to a nylon membrane (Zeta Probe, BioRad) and probed with ^{32}P-α-dCTP (Amersham

Biosciences) labeled cDNA that was generated using the random priming kit (Stratagene). The probes were hybridized to the membrane for 16 h in ULTRAHyb buffer (Ambion), washed, and analyzed after 48 h with a PhosphorImager (Molecular Dynamics).

Generation of the *hrg-1::gfp* heme-sensor strain

The putative promoter (~3 kb upstream of ATG start codon) of *C. elegans hrg-1* was cloned into the *Pst*I - *Apa*I sites of vector pPD95.67 (Fire vector kit) that contained GFP preceded by a nuclear localization signal and followed by *unc-54* 3'UTR, to create a *hrg-1::gfp* transcriptional fusion. Transgenic lines were generated by microinjection of 50 ng/μl of the *hrg-1::gfp* plasmid into wild-type N2 worms along with pRF4 plasmid (*rol-6*) for positive selection of transformants [109]. The transformant with 25 % trasmittance of GFP expression was chosen for integration. The integrated transgenic strain (IQ6011) was generated using gamma radiation (2500 rads/5 min). After gamma irradiation, worms were allowed to recover. About 100 F_1 progeny were picked singly onto NGM plates spotted with OP50 bacteria. After the F_1 worms laid progeny, about 5 F_2 worms from each of the 100 plates were picked singly and analyzed for the *Rol* phenotype. Transgenic lines with 100% transmission for *rol-6* and *hrg-1::gfp* were obtained.

RNA-mediated interference assays

C. elegans hrg-1 and *hrg-4* open reading frames were cloned into the *Pst*I- *Hind*III sites of the L4440 RNAi feeding vector and transformed into the *E. coli* HT115(*DE3*) strain. RNAi feeding bacteria were grown in LB broth supplemented with either 5 or 25 μM hemin or no added hemin (0 μM) for 5.5 h. NGM agar plates for RNAi were spotted with the RNAi feeding bacteria and the bacteria were allowed to induce for 24 h at room temperature. Equal numbers of IQ6011 synchronized F_1 L1 larvae, obtained by bleaching P_0 worms grown in mCeHR-2 medium plus 10 μM hemin, were placed on the NGM plates spotted with the RNAi feeding bacteria. After feeding on RNAi bacteria for 96 h, worms were analyzed with a Leica MZF16A fluorescence stereoscope. The fluorescence intensity measurements were quantified with SimplePCI v 6.2 (Hamamatsu). *P* values for statistical significance were calculated by using a one-way ANOVA with Student–Newman–Keuls multiple comparison test by using INSTAT version 3.06 (GraphPad, San Diego).

ZnMP uptake assays

The NGM plates for RNAi were prepared and spotted with RNAi feeding bacteria as described previously, except the bacteria were grown in LB broth without any added heme. For analysis of ZnMP (Frontier Scientific) uptake, equal numbers of IQ6011 synchronized F_1 L1 larvae, obtained by bleaching P_0 worms grown in mCeHR-2 plus 1.5 μM hemin, were exposed to the RNAi bacteria on NGM plates for 60 h. The worms were then washed with M9 buffer and transferred to mCeHR-2 medium containing 1.5 μM hemin and 10 μM ZnMP. Worms were grown at 20°C with

continuous shaking for 16 h. To measure ZnMP fluorescence intensity in the worms, images were taken using a Leica DMIRE2 epifluorescence/DIC microscope fitted with a Rhodamine filter and a CCD camera. Image intensities were quantified with SimplePCI. For the deletion strains, ZnMP uptake assays were performed as described above except regular NGM plates spotted with OP50 bacteria were used. *P* values were calculated as described previously.

GaPPIX toxicity assays

Twenty synchronized L1 larvae, obtained by bleaching P_0 worms grown in mCeHR-2 medium with 1.5 μM hemin, were placed on NGM plates spotted with RNAi bacteria grown in LB broth without any added heme. After 60 h, the worms were then transferred to NGM plates containing 1 μM GaPPIX and spotted with RNAi bacteria to sustain knock-down of the *hrgs*. After 24 h of egg-laying, the gravid mothers were picked and burned to prevent additional eggs from being laid. On day 5, the total number of surviving larvae and viable eggs that hatched was counted.

For GaPPIX toxicity measurements in the Δ*hrg-1* and Δ*hrg-4* deletion strains, ten L4 larvae from each strain were transferred to NGM agar plates spotted with OP50 bacteria. After allowing the gravids to lay eggs for 36 h, the number of surviving larvae was counted.

Biolistic transformation of *C. elegans*

Large numbers of *unc-119 (ed3)* worms were grown at 20°C with continuous shaking in 90 mL of mCeHR-2 medium in T175 cm^2 flasks containing mCeHR-2 medium with 20 μM hemin. For biolistics transformation, the worms were transferred to 50 mL conical centrifuge tubes and spun at 800 X *g* for 2 min. Worms were resuspended in M9 buffer, and the adult worms in the 50 mL tubes were allowed to settle for 15 min on ice. The supernatant was aspirated, and the washing process was repeated twice. The worms were then evenly distributed to form a confluent layer on a chilled, 10 cm, unseeded NGM agar plate.

Gold particles were prepared by weighing 30 mg of the particles into a silicon-treated 1.5 mL microcentrifuge tube. The particles were then soaked in 70% ethanol for 15 min, washed three times with sterile water and resuspended in 0.5 mL of 50% glycerol. For each transformation, 5 μg of *unc-119* rescue plasmid was mixed with 8 μg of plasmid containing either *Cehrg-1* or *hrg-4* constructs, and the total volume was brought to 50 μL with sterile water. The DNA mix was then mixed with 100 μL of the gold particles. To this mixture, 150 μL of 2.5 M $CaCl_2$ and 60 μL of 0.1 mM spermidine (Sigma) were added. The mixture was briefly spun at 6000 X *g*, and the supernatant was removed. The pellet was resuspended in 300 μL 70% ethanol and spun briefly. After removing the supernatant, 170 μL of 100% ethanol was added to the pellet and vortexed for 10 min. 20 μL of DNA-coated gold particles were spread onto each of the seven macrocarriers (BioRad) and allowed to dry.

The transformation was carried out using the PDS-1000/He particle delivery system with the Hepta adaptor (BioRad), as per manufacturer's instructions [110].

After transformation, worms were allowed to recover for 30 min and were transferred from the NGM plate to a 50 mL tube using 10 mL of M9 salt solution. Equal volume of worms (500 μL) in the M9 buffer were spread on to 20 NGM agar plates seeded with 500 μL of JM109 bacterial strain. Once the excess liquid had been absorbed by the plates, the plates were incubated at 25°C for two weeks. The plates were analyzed for wild-type animals using a Leica stereoscope. The wild-type transformants were picked out singly onto NGM plates spotted with OP50 bacteria and their progeny were examined for GFP or YFP expression.

Worm lysis and GFP measurements

IQ6011 and IQ6041 worm strains were grown at 20°C with continous shaking in mCeHR-2 medium supplemented with 2 μM hemin, 4 μM hemin, 20 μM hemin, 4 μM hemin with 20 μM protoporphyrin IX, or 4 μM hemin with 1 mM iron chloride for two generations. Worms were harvested by centrifugation at 800 X *g* for 5 min and washed twice with M9 buffer. The final worm pellet was resuspended in M9 buffer with protease inhibitor cocktail set III (Calbiochem) and lysed with FastPrep-24 (MP Bio) in the presence of Lysing Matrix D beads for 60s at the 6.5 m/s setting. The worm lysates were centrifuged twice at 16,000 X *g* for 30 min to remove worm debris, and 250 mg of the total protein, as measured by the Bradford (BioRad) method, was used to quantify GFP fluorescence. Measurements were obtained at 20º C using an ISS PC1 spectrofluorometer with a 1mm slit-width at a fixed excitation of 488 nm. Scanning emission spectra (500-600 nm) were obtained for each sample, and graphs were generated using the peak absorbance value of GFP at 506 nm.

PCR analysis using Rapid amplification of cDNA ends

The Smart™ RACE cDNA amplification kit (Clontech) was used to generate cDNA from total RNA isolated from N2 worms grown at 4 μM hemin for RACE PCR analysis. All primers have a Tm between 62ºC and 65ºC. PCR amplification of cDNA was done using Advantage® 2 PCR enzyme system (Clontech). PCR products were cloned into the pCRII vector using a TA cloning system (Invitrogen). At least 5 different clones for the 5' and 3' ends of each gene (*hrg-1* and *hrg-4*) were sequenced and analyzed.

Cloning of *C. elegans hrg-1*, *C. elegans hrg-4* and human *HRG1*

C. elegans hrg-1 and *hrg-4* cDNA was cloned by reverse transcription of total RNA isolated from worms grown at 4 μM hemin, and amplified by PCR using primers containing *Bam*HI and *Xho*I linkers, either with or without the HA epitope tag. Primers designed to amplify worm open reading frames were based either on Wormbase predictions or 5' and 3' RACE experiments. Human *HRG1* was amplified from the image clone (Open Biosystems) by PCR using primers containing *Bam*HI and *Xho*I linkers, either with or without the HA epitope tag. The PCR products were ligated into plasmids pCDNA3.1 (+) Zeo (Invitrogen) and pEGFP-N1 (Clontech) for expression in mammalian cells.

For zebrafish experiments, we cloned the *Cehrg-1* construct tagged with the HA epitope into pCS2 (+) plasmid. For *Xenopus* experiments, the *Cehrg-1, Cehrg-4* and *hHRG1* constructs tagged with the HA epitope were cloned into pT7TS plasmid.

Immunological analysis

HEK 293 cells were routinely cultured in basal growth medium composed of DMEM (GIBCO/BRL) and 10 % bovine serum (Atlanta Biologicals) supplemented with penicillin / streptomycin / glutamine. The pCDNA3.1 (+) Zeo and pEGFP-N1 plasmids expressing CeHRG-1, hHRG1 or CeHRG-4 either with or without the HA tag were transiently transfected into cultured adherent monolayers of HEK 293 cells using Lipofectamine 2000 (Invitrogen). The pCS2 (+) and pT7TS plasmids expressing CeHRG-1, hHRG1 or CeHRG-4 with HA tag were also transiently transfected into HEK 293 cells. Cells were harvested 48 h post-transfection by cell lysis buffer (20 mM HEPES, pH 7.4, 0.5 % Triton X-100 and 150 mM NaCl) supplemented with protease inhibitor cocktail set III on ice for 15 min and cell lysates were clarified by centrifugation for 10 min at 10,000 X *g* at 4ºC. The Bradford method was used to determine the protein concentration of the supernatant from all samples. For immunoblotting, lysates were mixed with Laemmli Sample Buffer containing 100 mM DTT without heat denaturation, resolved by SDS-PAGE, and transferred to nitrocellulose membranes. The membranes were blocked for 1 h in 5 % blotto (5 % dry milk in 1X PBS/ 0.05 % Tween-80). After blocking, the membranes were incubated overnight at 4ºC in 5 % blotto containing rabbit polyclonal antibody against HA epitope at 1:5000 dilution (Sigma) or GFP at 1:2000 dilution (Qiagen). The membranes were washed three times at room temperature (10 min per wash) with 1X PBS/ 0.05 % Tween-80 and incubated for 30 min at room temperature in 5 % blotto containing horseradish peroxidase-conjugated secondary antibody at 1:10,000

dilution (Pierce). The membranes were washed as previously described. The detection was done using the SuperSignal West Pico Chemiluminescence kit (Pierce).

Immunofluorescence assays

For immunofluorescence experiments, HEK 293 cells grown on glass coverslips were transiently transfected with pEGFP-N1 plasmids either containing *Cehrg-1*, *hHRG1* or *Cehrg-4* along with the organelle markers using FuGene 6 (Roche). 24 hours post-transfection, the cells were fixed for 20 min at room temperature in freshly prepared 4% paraformaldehyde and washed three times (5 min per wash) with 1X PBS. The fixed cells were incubated for 2 min in 1X PBS containing DAPI (1:50,000 dilution) and washed three times with 1X PBS. Coverslips were then mounted on microscope slides using ProLong Antifade (Molecular Probes). Confocal studies were performed using a laser scanning Zeiss LSM 510 confocal microscope with Argon (458 and 488nm) and HeNe (543 and 633nm) lasers. A planApo 100X oil immersion objective lens was used. For labeling the plasma membrane, cells grown on coverslips were incubated with Alexa633-conjugated wheat germ agglutinin (Molecular Probes) for 5 min at 37º C prior to fixation. Lysosomal (LAMP1::YFP) and endosomal (Rab7::CFP and Rab11::YFP) markers were generously given to us by Dr. Jennifer Lippincott-Schwartz.

`Heme / Iron depletion and MEL cell hemoglobinization studies

HEK293 cells were treated with heme-depleted medium (DMEM, 10 % heme-depleted FBS, 1% PSG, 0.5 mM succinyl acetone) for 20 h. Heme-depleted serum was generated by treatment with 10 mM ascorbic acid for about 7 h [111]. For iron

chelation, 100 μM desferroxamine (Sigma) was added to the cells 6 h after addition of the heme-depleted medium. A 50 μM heme-replete medium was generated by mixing 10 mM hemin chloride and 1 mg/mL BSA stock solution with tissue culture medium and incubating overnight at 4°C. For iron stock solution, 5 mM ferric citrate was mixed with 5 mM SIH (salicylaldehyde isonicotinoyl hydrazone) in a 1:2 ratio to generate Fe-SIH [112]. After 14 h incubation of the cells, the heme-depleted medium was replaced with medium containing DMEM, 10 % heme-depleted FBS, 1 % PSG, 0.5 mM succinyl acetone (Sigma), and either 50 μM heme or 100 μM Fe-SIH. Cells were allowed to incubate in the fresh medium for an additional 3 h. After a single wash with PBS, total RNA was extracted using Trizol. Extracted RNA samples were treated with TurboDNase (Ambion). Total RNA (2 μg) from each sample was used for cDNA synthesis (iScript cDNA synthesis kit, BioRad). qRT-PCR was performed using primers for *hHMOX1*, *hTfR1* and *hHRG1*. Fold change was calculated using the $2^{-\Delta\Delta Ct}$ method. SIH was a generous gift from Dr. Prem Ponka.

Mouse erythroleukemia cells (DS19 clones) were cultured in DMEM, 10 % FBS, 1 % PSG, and 1% non-essential amino acids (Invitrogen). The cells were induced with 1.5 % DMSO (Sigma) to simulate erythroid maturation. After 4 days of induction, the cells were harvested. For the time-course study, cells were harvested every 12 h for the 72 h period after induction with DMSO. The cell pellets for RNA extraction were flash frozen in Trizol. Total RNA was extracted from all samples and treated with TurboDNase. qRT-PCR was performed on cDNA synthesized (First strand cDNA synthesis kit, Invitrogen) using 2 μg of total RNA from each of the

samples. Quantitative analysis was performed using the $2^{-\Delta\Delta Ct}$ method. Dr. Barry Paw generously gave us the MEL cells (DS19 clones).

PCR genotyping worm deletion strains

Single worms were lysed in a buffer containing 50 mM KCl, 10 mM Tris-HCl, 2.5 mM $MgCl_2$, 0.45% NP-40, 0.45% Tween-20, 0.01% gelatin and freshly prepared proteinase K at a final concentration of 1 mg/mL. The lysis was performed at -80°C for 2 hours, 65°C for 1 hour and 95°C for 30 min. PCR primers were designed to detect a 650 bp fragment of *hrg-1* in the Δ*hrg-1* strain (*tm3199*) and a 450 bp fragment of *hrg-4* in the Δ*hrg-4* strain (*tm2994*).

Brood size assay and morphology assessment of the deletion strains

Ten L4 larvae from each strain of worms were placed individually on NGM agar plates spotted with OP50 bacteria. After allowing them to lay progeny for 2 days, the gravid worms were transferred to a new plate and the progeny from the previous plate were counted. This process was repeated twice and the total number of progeny was calculated.

For examining the morphological defects, worms were transferred to agar pads on microscope slide with ~ 20 μL of 10 mM levamisole. After placing a cover slip on the agar pad, the worms were analyzed using Leica DMIRE2 epifluorescence/ DIC microscope fitted with a 40X objective lens. Images were obtained using a CCD camera fitted to the Leica DMIRE2 microscope. The "percentage defects" was calculated by dividing the number of worms with defects by the total number of worms analyzed for each strain and multiplying by 100.

Chapter 3 Genome-wide analysis of genes involved in regulation of heme homeostasis

Summary

Heme is a prosthetic group of proteins that perform a wide variety of cellular functions [113]. Heme synthesis occurs via a multistep pathway with defined intermediates that are highly conserved among most eukaryotes [93]. Even though the pathways of heme biosynthesis and degradation have been well-characterized, the molecular mechanisms that are involved in intracellular heme trafficking in eukaryotes are unknown. One of the major setbacks in identifying the molecules and pathways that mediate heme homeostasis has been the inability to dissociate the tightly regulated processes of heme biosynthesis and degradation from intracellular trafficking events [80]. *C. elegans* lacks the ability to make heme, despite containing numerous hemoproteins associated with a variety of metabolic processes [93]. Furthermore, it has been demonstrated that worms utilize heme from their diet for incorporation *in toto* into hemoproteins [93]. Because hemes are hydrophobic macrocycles and free heme can cause cell injury due to its peroxidase activity, we rationalized that worms must regulate heme uptake. To understand the molecular mechanisms of heme homeostasis in eukaryotes, we conducted genome-wide microarray analysis using Affymetrix *C. elegans* genome arrays on RNA samples extracted from worms that were grown in mCeHR medium supplemented with 4, 20 or 500 μM heme. Using two different methods (Microarray Suite software 5.0, MAS 5.0 and Robust Multichip Average, RMA), a total of 288 heme-responsive genes

(*hrgs)* were identified. The 288 *hrgs* were either up or down regulated by at least 1.6 fold at 4 and/or 500 μM heme compared to control samples at 20 μM hemin. There were 121 *hrgs* that had homologs in humans, suggesting that results from studies conducted in *C. elegans* can be useful to understand heme metabolism in humans. Of the 288 genes, 46 *hrgs* have been predicted to contain at least one transmembrane domain indicating that some of the *hrgs* could be membrane transporters involved in heme uptake or trafficking. The genome-wide microarray analysis provided the first comprehensive catalog of heme-responsive genes in any animal and whose products are strong candidates for molecules involved in eukaryotic heme homeostasis.

Results

We have previously demonstrated that *C. elegans* lacks the highly conserved genes for heme biosynthesis [93]. To determine whether *C. elegans* requires heme for growth, worms were cultured in liquid axenic mCeHR medium in the presence of different amounts of heme. Worms responded in a biphasic manner to heme levels in the medium (Fig. 1). The optimal concentration for worm growth was 20 μM heme, and, at this concentration, the worms took about 3.5 days to reach the gravid stage from L1 larvae. The worms continued to grow and reproduce at concentrations ranging from 1.5 μM to 500 μM heme. At heme concentrations other than 20 μM, it took longer for the L1 larvae to reach the gravid adult stage and the brood size was smaller. Worms grown in the absence of exogenous heme arrested at the L4 larval stage, and the development of worms grown in ≥ 800 μM heme was arrested at the L2/L3 larval stages. This arrest was probably due to toxicity from excess heme.

Our observations that worms can grow to the L4 larval stage in the absence of exogenous heme suggested that either there were trace amounts of heme in the growth medium or that maternal heme stored in the eggs during embryogenesis was sufficient to sustain larval development. We found that L1 larvae, when obtained from worms grown in CeHR medium containing 500 μM heme and transferred to CeHR medium lacking any exogenous heme, developed to the young adult stage. The progeny obtained from worms grown at 1.5 μM heme and transferred to CeHR medium lacking any exogenous heme were arrested at the L2/L3 larval stages (A.U.R and I.H. unpublished results). These results support our hypothesis that hermaphrodites stored heme in the eggs that was sufficient for early embryogenesis and post-embryonic development.

To demonstrate that a heme uptake system exists in *C. elegans*, labeling experiments using a fluorescent heme analog, zinc mesoporphyrin IX (ZnMP), revealed that worms accumulate ZnMP and that the fluorescence of ZnMP can be competed by heme. Moreover, worms grown at concentrations at or below 20 μM heme showed an uptake of ZnMP that was much more robust than that of worms that were grown at concentrations greater than 100 μM heme [93]. These results suggested that heme uptake was stimulated when worms were grown under limiting conditions of heme and heme uptake was down regulated when worms were grown at high heme concentrations. Taken together, these findings reveal that heme homeostasis in *C. elegans* is regulated in accordance with the metabolic requirements of the animal. Physiologically, this conclusion is reasonable because heme homeostasis necessitates maintaining a balance to ensure levels of heme are high

enough to perform all necessary biological functions but low enough to avoid toxicity due to excess heme. However, these data do not reveal whether heme regulation occurs at the transcriptional or post-transcriptional level. As a first step toward understanding heme homeostasis, we performed a genome-wide analysis using Affymetrix *C. elegans* whole genome arrays to identify genes that are regulated by heme at the transcriptional level.

Worms were grown at 4, 20 or 500 μM heme in axenic CeHR medium. Worms grown at 20 μM heme were used as control samples because the heme dose response analysis showed that 20 μM heme was the optimal heme concentration, for growth and development (Fig. 1). Worms grown at 4 and 500 μM heme exhibited a 16 h growth delay but were morphologically indistinguishable from worms grown at 20 μM heme. In order to eliminate genes to eliminate the maternal load of heme as a variable, wild-type N2 worms were grown in mCeHR medium containing 4, 20 or 500 μM heme for two generations (Fig. 2). F_2 worms were harvested at the late L4 stage for RNA isolation. RNA was extracted, treated with RNase-free DNase and purified using Qiagen RNeasy column. Each experiment was performed three independent times to account for experimental variations and to allow for proper sampling.

Figure 1. *C. elegans* requires heme for growth and reproduction.

Biphasic response of *C. elegans* cultured in the presence of increasing amounts of heme (μM). One hundred larvae at the L1 stage were grown for 9 days in mCeHR medium in a 24-well plate with each well containing an increased concentration of heme (μM). The total numbers of worms in each well were counted on day 9. Each data point represents the mean (± SD) from three separate experiments performed in triplicate. The red circle represents the hemin concentrations at which the worms had similar growth rates.

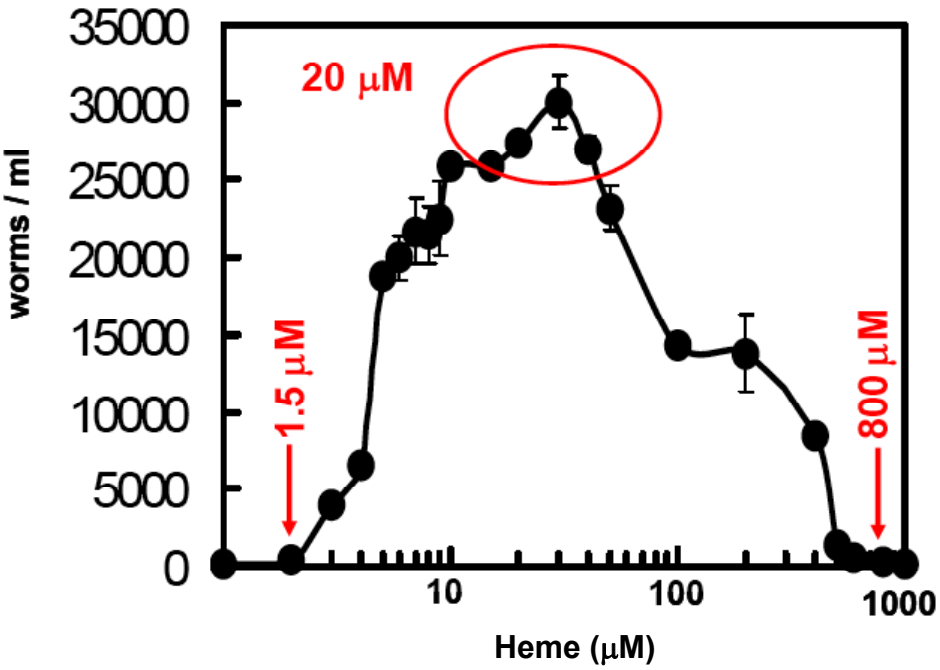
35000
30000
25000
20000
15000
10000
5000
0
worms / ml
20 μM
1.5 μM
800 μM
10
100
1000
Heme (μM)

The statistical analyses of the microarray data were initially performed using the Affymetrix MAS 5.0 Suite software. Of the 22,627 probe sets, 835 probe sets revealed changes at either 4 or 500 μM heme compared to the control data from 20 μM heme. Using the cut-off of ≥ 1.6, we identified 288 genes from MAS 5.0 analysis.

The experiment was designed to minimize both the maternal effect of heme and the changes in genes that might be involved in heme regulation at the embryonic stage. In order to check if there were any germline genes that were transcriptionally regulated by heme, we compared results from our heme microarrays with the germline gene expression microarrays and identified 58 genes that were involved in worm developmental processes [114].

The MAS 5.0 software uses the mismatch probe sets for background correction, and it has been reported to yield a significant number of false-positives [106]. We therefore also analyzed the microarray results using the Robust Multichip Average method (RMA from R package) which provides the users with the option of using only the perfect match probes for background correction [106, 115]. The disadvantage of the RMA method is that it compresses the fold change estimates by 10-20% thereby, leading to a modest loss of accuracy and generation of false-negatives [116]. Therefore, we used a lower threshold of ≥ 1.2 fold change in gene expression and identified a total of 82 genes. From these initial analyses using MAS 5.0 (fold-change cut-off ≥ 1.6) and RMA (fold change cut-off ≥ 1.2), we obtained 370 candidate genes.

After eliminating the genes that were duplicated, increasing the fold change cut-off for RMA analysis to ≥ 1.6, and using the average fold change of the replicates,

there were 266 genes identified using MAS 5.0 and 22 additional genes using the RMA method. A total of 288 genes, including 8 previously identified germline genes, showed a ≥ 1.6-fold change in gene expression profiles at 4 or 500 μM heme compared to the control at 20 μM. A heat map for the 288 heme-responsive genes (*hrgs*) generated using Gene Spring version 5.0 revealed that the overall quality of the microarray data was consistent across the three biological replicates with the exception of one sample from worms grown at 4 μM heme which showed significant variability in comparison to the other two replicates (Fig. 3). We therefore excluded this particular sample from further analysis.

The 288 heme-responsive genes (*hrgs*) were categorized based on whether the signal was up, down or unchanged in samples obtained from worms grown in 4 or 500 μM heme as compared to the 20 μM reference samples. There were 80 genes that were upregulated at 4 μM heme and 75 genes that were upregulated at 500 μM heme (Table 1). We conducted quantitative real-time PCR (qRT-PCR) analysis on 30 genes to confirm the changes revealed by microarray analysis. 26 of the 30 genes were confirmed by qRT-PCR. A representative set of genes that have been confirmed are shown in Figure 4. Clustering analysis revealed that the majority of *hrgs* were clustered on chromosome V in the *C. elegans* genome (Fig. 5). Chromosome V has an increased number of *hrgs* that were upregulated at 4 μM heme.

Using protein sequences obtained from Wormbase for these 288 *hrgs*, we performed BLAST and reciprocal BLAST searches to identify human homologs (Table 2) [117]. These searches revealed that there were 121 *hrgs* that showed sequence similarity between *C. elegans* and humans with an E-value cut-off ≥ 10^{-4}.

Characterization of the *hrgs* common to both worms and humans might provide insights into the heme homeostasis pathways in mammals.

We have previously demonstrated that parasitic nematodes also lack the ability to synthesize heme and rely on exogenous heme supply [93]. We therefore reasoned that genes, which are essential for heme homeostasis that is nematode-specific, could be used as therapeutic drug targets for helminthic infections. Interestingly, analyses of the genome of *Trypanosoma brucei* suggested that the trypanosomes lack the genes encoding for heme biosynthesis enzymes [118]. With the help of our collaborator Dr. Najib El-Sayed (Maryland Pathogen Research Institute, University of Maryland), we were able to identify homologs in the parasites *Schistosoma mansoni*, T*rypanosoma brucei*, *Trypanosoma cruzi* and *Leishmania major* (Table 2). As shown in Figure 6a, of the 288 genes there were 12 heme auxotroph-specific *hrgs*, 37 *hrgs* that had homologs only in humans and 84 that were common to both. There were a total of 96 *hrgs* common between *C. elegans* and the parasites. This constitutes ~ 33% of the *hrgs* identified from the microarray analysis. Among the 109 genes upregulated at 4 μM heme, there were only 9 human-specific and 5 heme auxotroph-specific *hrgs* (Fig. 6b). Of the 104 genes that showed increased gene expression at 500 μM heme, 12 had human-specific homologs and 4 *hrgs* were found in the parasite genomes (Fig. 6c). Altogether, these results reveal that *hrgs*, identified from our microarray experiment in *C. elegans*, have homologs in humans and in parasites that are heme auxotrophs.

Figure 2. Schematic representation of the genome-wide analysis.

Three independent sets of worms were grown at 4, 20 or 500 μM heme in mCeHR medium for two generations. Worms were harvested at the late L4 stage. RNA was isolated and hybridized to Affymetrix *C. elegans* whole genome array containing 22,627 probe sets per chip. Affymetrix MAS 5.0 software and RMA were utilized to analyze the data. Data from worms grown at 4 and 500 μM heme were compared to control data from worms grown at 20μM heme. The expression of 288 genes was either increased or decreased in response to heme by at least 1.6 fold.

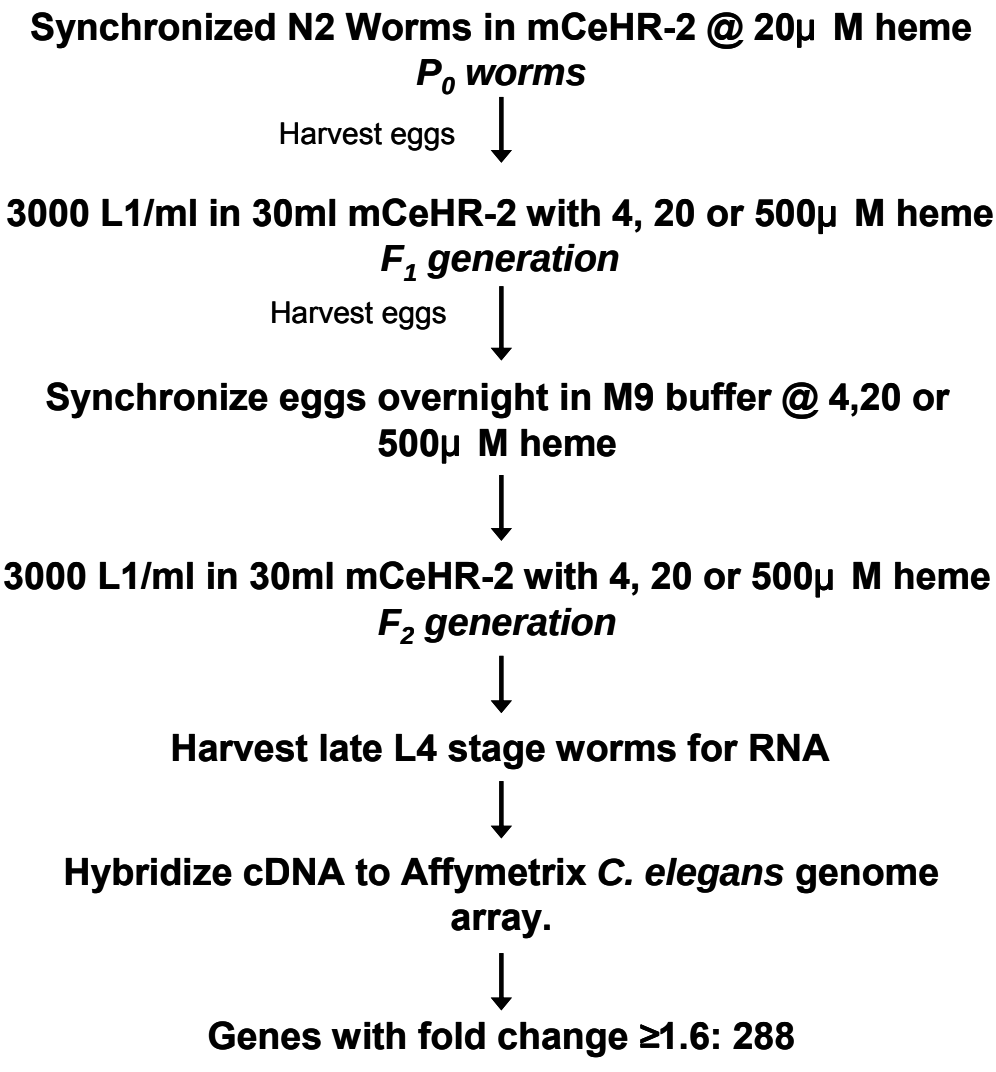
Synchronized N2 Worms in mCeHR-2 @ 20µ M heme
P_0 worms
Harvest eggs
3000 L1/ml in 30ml mCeHR-2 with 4, 20 or 500µ M heme
F_1 generation
Harvest eggs
Synchronize eggs overnight in M9 buffer @ 4,20 or 500µ M heme
3000 L1/ml in 30ml mCeHR-2 with 4, 20 or 500µ M heme
F_2 generation
Harvest late L4 stage worms for RNA
Hybridize cDNA to Affymetrix C. elegans genome array.
Genes with fold change ≥1.6: 288

Figure 3. Heat map for the heme microarrays.

A heat map generated using Gene Spring version 5.0 for the 288 *hrgs* shows that the overall quality of the microarray data was good. Data from all nine chips are represented. The up and down arrows indicate upregulation or downregulation in 4 or 500 μM heme when compared to 20 μM heme. The data from the first replicate sample from 4 μM heme, indicated with an asterisk, were inconsistent with the data from the other two replicates. Yellow represents no change in signal intensity, blue indicates a decrease, and red indicates an increase in signal intensity.

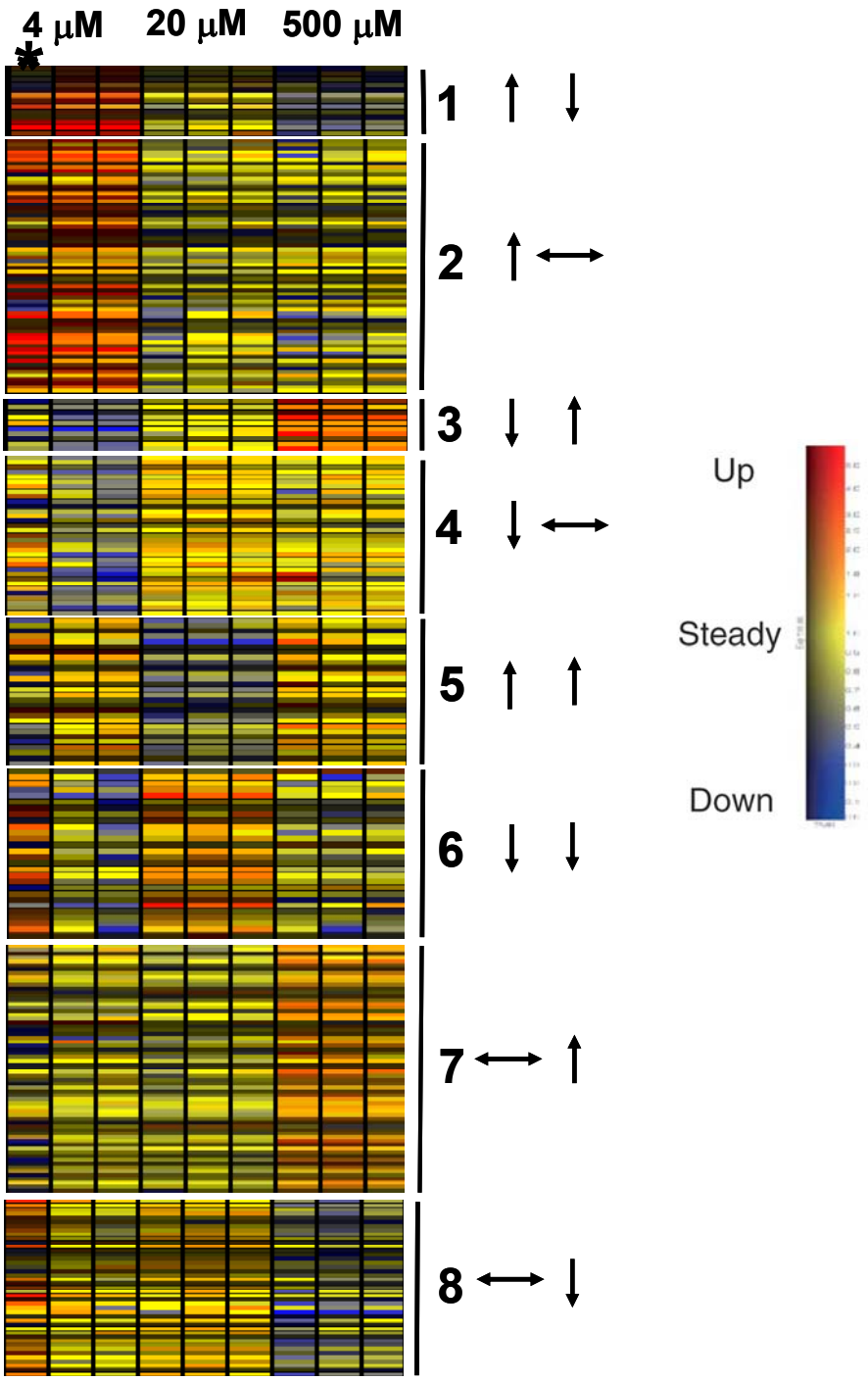
4 μM
20 μM
500 μM
1
2
3
4
5
6
7
8
Up
Steady
Down

Figure 4. Validation of microarray results by real-time PCR.

Validation of microarray data by qRT-PCR on RNA from worms grown in mCeHR-2 medium supplemented with 4, 20 or 500 μM heme. RNA from 20 μM heme was used as the reference sample. Data were compared to internal *gpd-2* control and the fold change was obtained using $2^{(-\Delta\Delta Ct)}$ method.

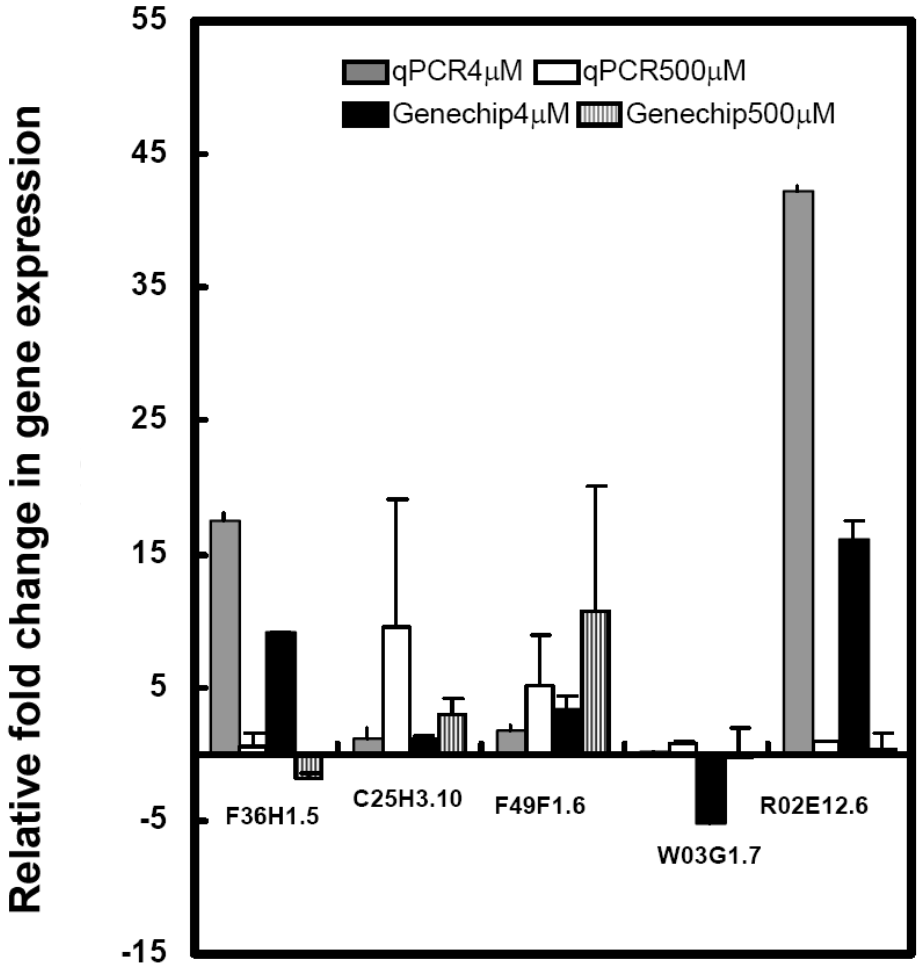
Relative fold change in gene expression
55
45
35
25
15
5
-5
-15
qPCR4μM
qPCR500μM
Genechip4μM
Genechip500μM
F36H1.5
C25H3.10
F49F1.6
W03G1.7
R02E12.6

Table 1. List of 288 genes identified from the microarray analysis.

Description	Gene name	4μM	500μM	4μM	500μM
C04H5.7		2.80	5.78	up	up
C24F3.3	nas-12	3.05	1.83	up	up
C32H11.10	dod-21	2.42	7.04	up	up
C34H4.2		1.81	1.86	up	up
F02D8.4		1.76	1.70	up	up
F08F8.5	numr-1	7.66	8.23	up	up
F21H7.1	gst-22	1.63	2.42	up	up
F35C5.9	clec-66	1.93	2.08	up	up
F49F1.6		3.32	10.71	up	up
F54E2.1		2.22	1.70	up	up
F58E6.7		71.25	1.66	up	up
K01D12.14	cdr-5	72.08	3.79	up	up
K02E2.4	ins-35	1.63	3.09	up	up
K08B4.3	ugt-19	2.93	2.11	up	up
K11H12.4		1.93	1.71	up	up
M02F4.7	clec-265	2.16	2.86	up	up
R10D12.9		1.64	2.48	up	up
R186.1		2.81	1.70	up	up
T05B4.3	phat-4	1.81	1.70	up	up
T24A11.3	toh-1	1.80	1.63	up	up
Y26D4A.10		1.75	2.20	up	up
Y38E10A.5	clec-4	2.00	2.10	up	up
Y40B10A.2		1.63	1.84	up	up
Y40B10A.6		4.04	7.74	up	up
Y51A2D.4	hmit-1.1	2.00	1.87	up	up
Y54G2A.11		2.32	2.16	up	up
Y75B8A.28		2.75	1.70	up	up
ZC443.6	ugt-16	3.28	1.91	up	up
C08F11.11		1.62	-2.02	up	down
C15C8.3		16.57	-2.25	up	down
C44B7.5		3.78	-2.14	up	down
EEED8.3		2.00	-5.55	up	down
F36H1.5	hrg-4	9.19	-1.81	up	down
F57C2.4		2.94	-2.64	up	down
F58E6.8		12.73	-2.40	up	down
F58G6.3		2.75	-1.80	up	down
F59D8.1	vit-3	4.35	-1.74	up	down
K09F5.2	vit-1	1.65	-1.80	up	down
W07B8.1		5.86	-1.91	up	down
Y62H9A.6		2.83	-8.36	up	down
ZK813.1		3.74	-3.37	up	down
C01G6.3		3.62	-0.34	up	
C04F6.1		1.74	-0.47	up	
C05E7.2		1.74	1.35	up	
C08B6.1		1.84	0.19	up	
C10G8.4		4.20	1.51	up	
C16C4.4	math-14	36.92	-1.33	up	
C25A1.8	clec-87	2.15	0.35	up	
C29E4.7	gsto-1	12.15	-1.32	up	
C31C9.1	tag-10	4.59	-0.49	up	
C33A12.6	ugt-21	2.87	1.14	up	
C33H5.13		1.62	1.39	up	
C42D4.3		1.93	1.39	up	
C42D8.2		2.62	-0.71	up	
C44B12.1		3.14	-1.03	up	
C50H11.15	cyp-33C9	2.94	1.26	up	
C54D10.1	cdr-2	1.66	1.53	up	
C54F6.14	ftn-1	1.66	0.88	up	
D1054.10		3.28	-1.44	up	
F07C4.2	clec-45	3.51	0.48	up	
F07C4.9	clec-46	2.93	0.53	up	
F07F6.5	dct-5	1.68	1.35	up	
F11G11.3	gst-6	1.88	1.59	up	
F14F4.3	mrp-5	3.48	0.38	up	
F15B9.6		4.78	1.49	up	
F17E9.4		3.78	-0.79	up	
F18A12.4		10.87	0.15	up	
F26F12.1		1.72	-0.54	up	
F32H5.1		3.14	0.36	up	
F32H5.3		2.00	1.49	up	
F35B3.4		2.14	1.48	up	
F36A2.3		1.93	0.33	up	

Description	Gene name	4μM	500μM	4μM	500μM
F38A3.1	col-81	1.68	-0.48	up	
F41F3.4	col-139	1.61	-0.25	up	
F42G2.2		2.30	1.18	up	
F44G3.2		1.80	-1.18	up	
F47C10.2	btb-21	2.07	1.39	up	
F48E3.4		1.80	-0.79	up	
F52E1.1	pos-1	2.00	-0.44	up	
F58E6.4		2.20	0.13	up	
F59D6.3		2.22	-0.66	up	
F59D8.2	vit-4	5.80	-1.34	up	
H23N18.1	ugt-13	1.77	-0.17	up	
K01D12.9		2.07	0.85	up	
K02B9.1	meg-1	3.07	-1.10	up	
K07H8.6	vit-6	4.45	-0.88	up	
K10B2.2		2.84	0.25	up	
K10D11.1	dod-17	1.68	0.62	up	
M02H5.4	nhr-202	2.30	1.24	up	
R02E12.6	hrg-1	16.04	0.33	up	
R06C7.4	cpg-3	1.87	0.20	up	
R193.2		2.82	-0.35	up	
T02G5.11		1.96	0.33	up	
T04G9.7		2.94	-0.63	up	
T05A1.2	col-122	1.81	-0.74	up	
T11F9.3	nas-20	1.87	-0.88	up	
T18H9.1	grd-6	1.87	1.86	up	
T21C9.13		2.94	-0.54	up	
T21F4.1		1.80	1.43	up	
T28C12.6		1.80	1.57	up	
W02G9.4		1.68	0.33	up	
W03G11.1	col-181	1.71	-0.51	up	
Y37D8A.19		4.45	-0.68	up	
Y54G11A.7		3.62	0.36	up	
Y62H9A.4		4.66	0.66	up	
Y73F8A.9	pqn-91	1.74	0.59	up	
ZC373.2		4.01	-0.77	up	
ZK1193.1	col-19	2.28	-0.22	up	
ZK742.3		2.55	1.55	up	
B0218.8	clec-52	-14.84	2.10	down	up
C17F4.7		-1.91	1.82	down	up
F08G5.6		-2.07	4.33	down	up
F21F8.4		-2.65	1.70	down	up
F55G11.4		-1.88	4.98	down	up
T24B8.5		-3.22	5.59	down	up
Y46C8AL.2	clec-174	-1.76	3.69	down	up
Y46C8AL.5	clec-72	-1.69	2.04	down	up
Y46D2A.2		-1.76	2.05	down	up
ZK666.6	clec-60	-3.49	2.73	down	up
C04G2.5		-1.70	-1.97	down	down
C14C6.3		-2.32	-2.20	down	down
E01G4.6		-2.62	-2.17	down	down
E03A3.4	his-70	-2.39	-2.07	down	down
F01G10.9		-1.78	-2.03	down	down
F08H9.5	clec-227	-1.68	-2.10	down	down
F09G2.3		-1.63	-4.62	down	down
F10C2.7		-10.83	-4.26	down	down
F15E11.12		-10.20	-4.21	down	down
F15E11.15		-10.58	-3.85	down	down
F22A3.6	ilys-5	-2.49	-1.87	down	down
F22B5.4		-1.81	-2.79	down	down
F28C6.5		-1.63	-1.64	down	down
F44E5.4		-7.21	-4.14	down	down
F44E5.5		-5.25	-4.16	down	down
F55C10.4		-1.87	-2.31	down	down
F56H6.5	gmd-2	-2.35	-4.15	down	down
F57G8.7		-2.22	-2.70	down	down
F58B3.2	lys-5	-2.07	-1.83	down	down
K06H6.1		-2.67	-2.22	down	down
K06H6.2		-4.67	-2.28	down	down
T22B7.3		-2.39	-1.80	down	down
W03F11.5		-1.68	-1.71	down	down
W07A12.6	oac-54	-2.07	-2.42	down	down
W07A12.7	rhy-1	-2.02	-2.37	down	down

Table 1, continued from previous page

Description	Gene name	4µM	500µM	4µM	500µM
F56A6.1	sago-2	-1.15	1.63		up
H20E11.1		1.12	1.68		up
K02G10.7	aqp-8	0.00	2.01		up
K08E7.9	pgp-1	0.00	2.15		up
M28.8		1.28	1.83		up
R09D1.8		0.44	2.53		up
R13A5.10		0.13	1.61		up
T01C3.4		-1.28	2.60		up
T05E12.6		1.23	1.96		up
T10B10.4		1.23	1.63		up
T10H4.12	cpr-3	1.28	2.17		up
T19C4.5		-0.08	1.77		up
T19C9.8		1.53	2.54		up
T21C9.8	ttr-23	1.47	2.17		up
W08E12.3		1.42	1.68		up
Y105C5B.15		-1.37	1.89		up
Y34F4.4		1.46	1.72		up
Y39D8C.1	abt-4	0.00	1.63		up
Y39G8B.7		-1.46	2.25		up
Y46C8AR.1	clec-76	1.53	1.75		up
Y47H9C.1		-1.07	2.73		up
Y48A6B.7		-1.11	1.72		up
Y48E1B.8		-0.04	1.87		up
Y50D4A.1		1.58	4.91		up
ZC443.5	ugt-18	1.21	2.37		up
ZK6.10	dod-19	1.15	2.44		up
B0286.3		-0.12	-1.97		down
B0393.5		-1.53	-1.67		down
C05C10.4		-1.28	-2.14		down
C06B3.7		1.21	-2.21		down
C07E3.10		-1.57	-1.69		down
C09D4.3		-1.24	-1.67		down
C24G7.2		-0.04	-1.70		down
C27D6.3		-0.21	-2.07		down
C33F10.1		0.12	-1.80		down
C34D4.3		1.37	-3.61		down
C50B6.7		1.23	-2.53		down
C55F2.1		-0.43	-2.17		down
F17C8.7		-0.30	-1.91		down
F26B1.1		1.35	-2.42		down
F26C11.1		-1.28	-10.56		down
F26H11.2	nurf-1	-1.17	-1.79		down
F28D1.5	thn-2	-1.28	-3.51		down
F32B6.4		-0.09	-1.66		down
F36A4.2		0.04	-2.75		down
F37B1.8	gst-19	1.39	-2.30		down
F38B6.4		-1.07	-2.03		down
F47C10.6	ugt-32	-1.46	-2.11		down
F47D12.7		-0.04	-3.49		down
F59C6.6	nlp-4	-1.52	-2.23		down
H25K10.1		-1.57	-1.74		down
K01A2.3		-1.11	-2.62		down
K01A2.4		-1.37	-11.35		down
K05F1.7	msp-63	1.49	-1.80		down
K07C6.4	cyp-35B1	-1.55	-6.77		down
K07E3.3	dao-3	-1.37	-1.73		down
K09C6.8		-0.40	-8.49		down
M02D8.4		-1.42	-1.75		down
T09F5.1		-1.52	-1.71		down
T09F5.9	clec-47	1.57	-8.01		down
Y11D7A.5		-1.53	-1.72		down
Y53F4B.32	gst-29	0.04	-1.97		down
Y59H11AM.3		1.57	-4.39		down
Y67A6A.2		-1.37	-1.75		down
Y71G12B.17		0.00	-1.73		down
Y71H2AM.16		-1.52	-2.15		down
ZK105.1		-0.16	-1.71		down
ZK520.5	cyn-2	-0.08	-4.81		down
ZK970.7		-0.08	-1.67		down
C45B2.5	gln-1	1.32	1.68		up
R03G8.3		1.39	1.79		up
T03F7.7		1.42	1.64		up

Description	Gene name	4µM	500µM	4µM	500µM
Y105C5B.7		-3.14	-14.34	down	down
Y43D4A.5		-2.77	-1.78	down	down
Y71G12B.18		-12.25	-2.15	down	down
D1086.3		-1.87	-1.41	down	
F28H7.3		-1.68	0.52	down	
F32A5.5	aqp-1	-1.74	-1.30	down	
F46B6.8		-2.94	0.49	down	
F47G9.3	cutl-18	-1.94	-1.29	down	
F49E12.9		-1.87	1.37	down	
F54D5.8	dnj-13	-1.68	-1.42	down	
F54F3.3		-3.26	1.60	down	
F58B3.3	lys-6	-2.00	-1.02	down	
F59B10.5		-1.62	-1.39	down	
H40L08.2		-2.23	0.38	down	
K07E3.1		-1.68	-1.23	down	
K10C2.3		-3.14	-1.49	down	
M60.2		-2.02	0.36	down	
R09B5.4	fpn-1.2	-1.88	-0.46	down	
R13H4.3		-1.62	0.36	down	
T07C4.4	spp-1	-1.80	-0.44	down	
T08A9.8	spp-4	-1.80	-0.41	down	
T10E9.8		-1.63	-1.49	down	
T16G1.7		-2.07	-0.36	down	
W03G1.7		-5.25	-0.10	down	
W04E12.8	clec-50	-1.68	1.13	down	
Y19D10B.7		-2.01	-0.31	down	
Y37A1A.2		-2.02	-0.55	down	
Y37D8A.4		-1.75	-1.52	down	
Y46G5A.29		-1.75	-1.58	down	
Y46H3A.2	hsp-16.41	-1.80	-0.08	down	
Y46H3A.3	hsp-16.2	-1.74	-0.09	down	
Y51H4A.5		-11.33	-0.74	down	
Y54F10AM.6		-1.75	-0.64	down	
Y5H2A.1		-2.02	-1.40	down	
ZK377.1	wrt-6	-1.96	-1.59	down	
ZK455.4	asm-2	-1.80	1.13	down	
C03H5.1	clec-10	1.16	2.82		up
C13D9.9	ugt-7	1.49	2.40		up
C14C6.5		-1.23	3.12		up
C17H12.6		1.28	1.90		up
C25H3.10		1.15	2.99		up
C30G7.1	hil-1	1.23	1.87		up
C31H5.6		0.04	1.80		up
C32D5.6		1.23	1.75		up
C34H4.1		1.46	2.27		up
C45E5.4		1.32	1.65		up
C48B4.1		-1.20	1.66		up
E03H4.10	clec-17	1.16	2.73		up
F01D5.1		-1.11	2.56		up
F01D5.3		-1.52	2.10		up
F01G10.3	ech-9	-0.04	3.26		up
F08F3.3	rhr-1	1.12	1.98		up
F09C8.1		-1.47	2.38		up
F10A3.2	fbxa-88	-1.11	1.66		up
F20G2.1		1.29	2.01		up
F22A3.1		-0.22	1.67		up
F27C8.4	spp-18	-1.52	1.96		up
F27E5.1		1.28	1.67		up
F35C5.7	clec-64	0.43	3.37		up
F35C5.8	clec-65	1.32	1.87		up
F36G9.14	fbxa-99	1.00	1.71		up
F37B1.5	gst-16	1.37	1.77		up
F39E9.1		1.37	3.13		up
F44C8.1	cyp-33C4	0.28	2.28		up
F44G3.10		1.58	3.49		up
F46E10.11		1.19	1.62		up
F48G7.5		1.11	3.02		up
F48G7.8		0.16	3.07		up
F49F1.5		-1.28	2.87		up
F49H6.13		0.12	1.88		up
F49H6.3		1.19	2.10		up
F53A9.2		1.21	2.02		up

To identify potential heme transporters among *hrgs*, we analyzed the 288 proteins for putative transmembrane domains [58, 119-123]. Predictions using TMHMM 2.0 revealed that 41 of the 288 genes encoded for proteins that had at least one putative transmembrane domain (TMD) (Table 3) [124]. Interestingly, among these 41 genes were aquaglyceroporin-related proteins (*aqp-1* and *aqp-8* with 6 and 4 TMDs respectively) that transport small molecules such as glycerol, urea and water; a cytochrome P450 family member *cyp-33C9* (one TMD) predicted to bind heme and a permease (R02E12.6), with four transmembrane domains [125-127].

Gene ontology analysis indicated that the *hrgs* identified from our microarray study were involved in a variety of processes such as embryonic development, electron transport, lipid metabolism and iron-sulfur cluster assembly (Table 4) [128]. There was no significant over representation of *hrgs* in any particular gene ontology term (biological process or molecular function) likely because heme is a cofactor for proteins that perform diverse biological functions. Of the 288 *hrgs* whose expression changed significantly in response to heme, only 63 (21%) have been assigned to any known biological processes.

While GO analysis is useful for functional analysis of biological processes, current GO annotation for *C. elegans* is insufficient to make any functional predictions for the *hrgs*. The Kyoto Encyclopedia of Genes and Genomes (KEGG) is another tool that is frequently used to analyze complex microarray data and make functional predictions [129]. As shown in Table 5, analysis of the 288 *hrgs* revealed that only 10 *hrgs* (~3%) have been mapped to KEGG pathways. A majority of heme-

responsive genes are novel and therefore have not been assigned to any known biological pathway.

Several genome-wide RNA-mediated interference (RNAi) experiments have been performed in *C. elegans* and the data from all these experiments are available on Wormbase [130-134]. We found that several RNAi phenotypes have been reported for 46 (`15%) of the 288 *hrgs* (Table 6). Of the 46 *hrgs* with RNAi phenotypes, 13 were upregulated at 4 μM heme and 5 were down regulated at 4 μM heme. RNAi of most *hrgs* resulted in developmental defects such as embryonic lethality and sterility. This observation is physiologically significant because heme is essential for the reproduction of *C. elegans*, and, therefore, depletion of mRNA for genes involved in heme homeostasis will result in defects in animal growth and developmental [135]. These results are consistent with our studies which revealed that absence of any exogenous heme in the growth medium results in worm growth arrest at early larval stages (Fig. 1).

Figure 5. Chromosome clustering

Clusters of heme-responsive genes whose transcript levels were altered at 4 μM (open bars) and/ or 500 μM heme (black bars). Genes that were upregulated are in red, and *hrgs* that were down regulated are in green. Chromosomes are represented as horizontal bars.

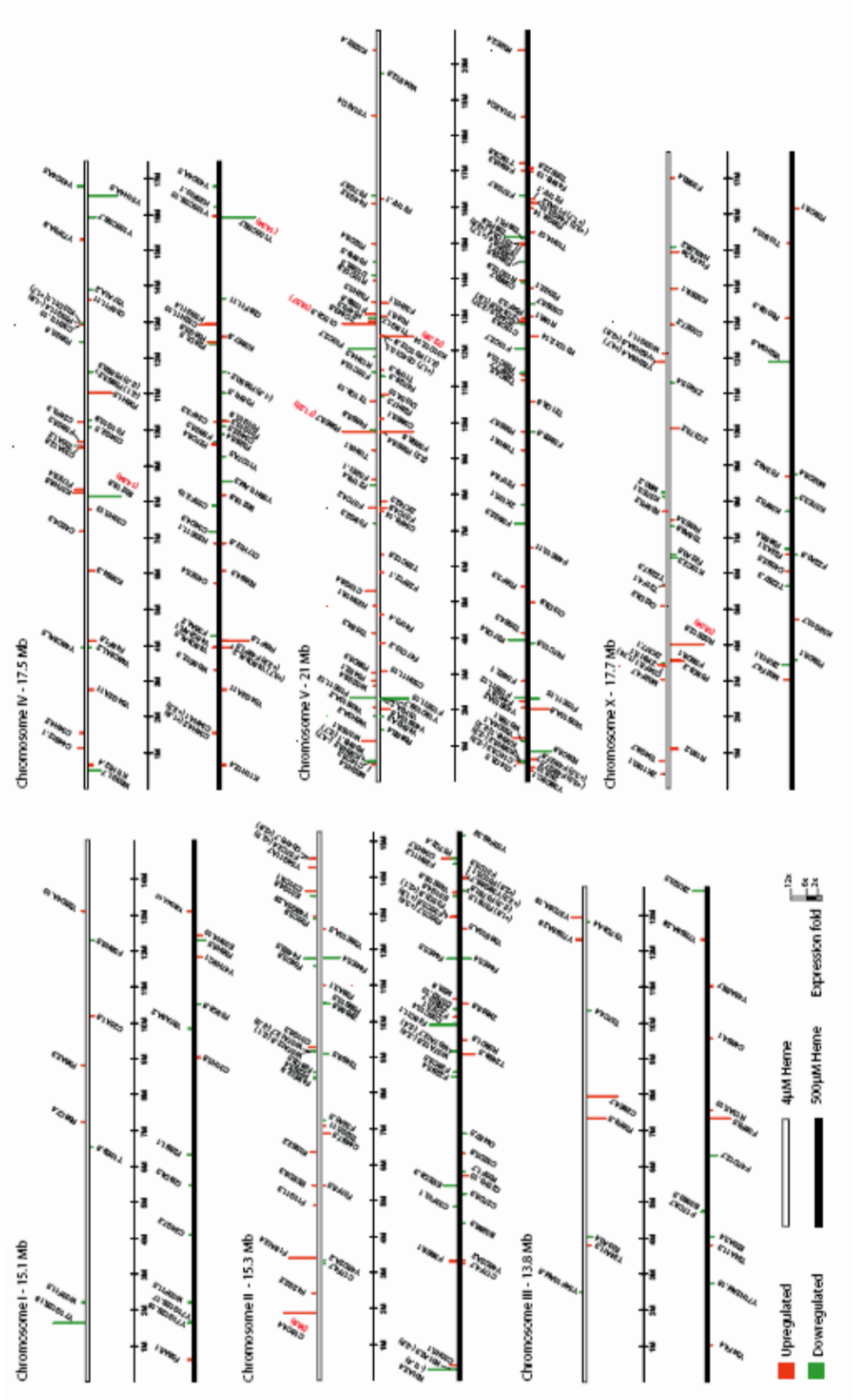
Chromosome I - 15.1 Mb
Chromosome II - 15.3 Mb
Chromosome III - 13.8 Mb
Chromosome IV - 17.5 Mb
Chromosome V - 21 Mb
Chromosome X - 17.7 Mb
Upregulated
Downregulated
4µM Heme
500µM Heme
Expression fold

Table 2. Heme-dependent changes in gene expression from *C. elegans* microarray.

The 288 genes were categorized based on whether they were upregulated, down regulated or showed no change at 4 or 500 μM heme concentrations when compared to control data from 20 μM heme. *C. elegans* protein sequences for the 288 genes were used to perform BLAST and reciprocal BLAST searches to identify human homologs (E-value cut-off ≥ 10^{-4}). Putative homologs were also identified in the parasitic helminth *Schistosoma mansoni* and protozoan parasites *Trypanosoma brucei*, *Trypanosoma cruzi* and *Leishmania major*.

Category	Heme		Total genes	Orthologs in humans	*S. mansoni*	*T. brucei*	*T. cruzi*	*L. major*
	4μM	500μM						
1	↑	↓	13	3	2	1	2	2
2	↑	↔	67	28	19	9	8	9
3	↓	↑	10	3	3	1	1	0
4	↓	↔	33	15	10	3	5	3
5	↑	↑	29	13	8	3	4	3
6	↓	↓	28	10	10	5	5	5
7	↔	↑	65	26	16	7	7	10
8	↔	↓	43	23	13	3	3	3
Total			288	121	81	32	35	35

Figure 6. Comparative analysis of the 288 *hrgs* across human and parasitic genomes

Protein sequences for the *hrgs* obtained from Wormbase were used to search for homologs in the human genome and genomes of *Schistosoma mansoni, Trypanosoma brucei, Tryoanosoma cruzi and Leishmania major*. **a)** All 288 amino acid sequences were utilized to identify homologs in the indicated genomes. (**b)** and **(c)** Amino acid sequences for *hrgs* upregulated at either 4 or 500 μM heme were used to perform homology searches.

a

Total of heme sensitive genes: 288

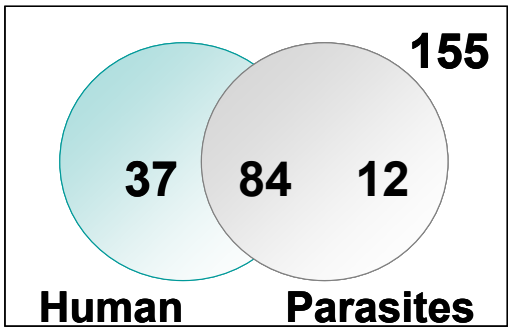

b

4 μM upregulated genes: 109

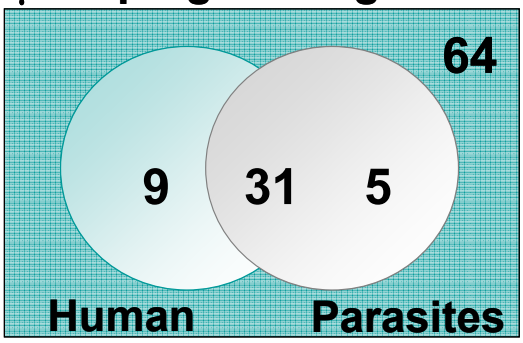

c

500 μM upregulated : 104

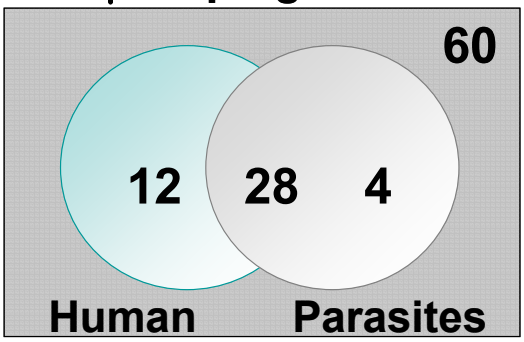

Table 3. List of genes with predicted transmembrane domains

Worm protein sequences obtained from Wormbase were analyzed using TMHMM 2.0 to identify putative hydrophobic regions and transmembrane domains (TMDs). The 41 genes with putative TMDs have been sorted based on the number of TMDs. The fold changes at 4 and 500 mM heme have been indicated. Negative fold change implies down regulation.

Description	Gene name	4 μM fold change	500 μM fold change	TMDs
Y39D8C.1	abt-4	0.00	1.63	15
F08F3.3	rhr-1	1.12	1.98	12
F10C2.7		-10.83	-4.26	12
F14F4.3	mrp-5	3.48	0.38	12
Y37A1A.2		-2.02	-0.55	12
K08E7.9	pgp-1	0.00	2.15	11
W07A12.7	rhy-1	-2.02	-2.37	11
Y51A2D.4	hmit-1.1	2.00	1.87	10
F09G2.3		-1.63	-4.62	9
R09B5.4	fpn-1.2	-1.88	-0.46	9
W07A12.6	oac-54	-2.07	-2.42	9
R10D12.9		1.64	2.48	8
F32A5.5	aqp-1	-1.74	-1.30	6
M28.8		1.28	1.83	5
F36H1.5	hrg-4	9.19	-1.81	4
F44G3.10		1.58	3.49	4
F49H6.13		0.12	1.88	4
F49H6.3		1.19	2.10	4
K02G10.7	aqp-8	0.00	2.01	4
K07E3.1		-1.68	-1.23	4
R02E12.6	hrg-1	16.04	0.33	4
T10E9.8		-1.63	-1.49	4
T21C9.13		2.94	-0.54	4
C13D9.9	ugt-7	1.49	2.40	3
F58G6.3		2.75	-1.80	3
K01A2.3		-1.11	-2.62	3
C24G7.2		-0.04	-1.70	2
C33F10.1		0.12	-1.80	2
F49E12.9		-1.87	1.37	2
F58E6.7		71.25	1.66	2
F58E6.8		12.73	-2.40	2
K01A2.4		-1.37	-11.35	2
K08B4.3	ugt-19	2.93	2.11	2
Y51H4A.5		-11.33	-0.74	2
B0393.5		-1.53	-1.67	1
C27D6.3		-0.21	-2.07	1
C50H11.15	cyp-33C9	2.94	1.26	1
C54D10.1	cdr-2	1.66	1.53	1
F22B5.4		-1.81	-2.79	1
R03G8.3		1.39	1.79	1
Y54G2A.11		2.32	2.16	1

Table 4. List of genes with known GO terms

Biological processes and molecular functions associated with the 288 heme-responsive genes that were identified from the microarray.

Description	Molecular function	Biological Process	GO group*
B0286.3	Phosphoribosylamidoimidazole activity	De novo IMP biosynthetic pathway	IEA
B0393.5	Calcium ion binding	Cell-matrix adhesion	IEA
C01G6.3		Embryonic development	IMP
C05C10.4	Acid phosphatase activity		IEA
C09D4.3	Protein kinase activity	Amino acid phosphorylation	IEA
C15C8.3	Pepsin A activity	Proteolysis	IEA
C24G7.2	Sodium channel activity	Sodium ion transport	IEA
C27D6.3		Locomotory behaviour	IMP
C29E4.7	Glutathione transferase activity	Positive regulation of growth, embryonic development	IEA, IMP
C31H5.6	Palmitoyl-CoA hydrolase activity	Lipid metabolism	IEA
C32D5.6		DNA repair	IMP
C34D4.3	Structural molecule activity		IEA
C44B12.1		Embryonic development	IMP
C48B4.1	Acyl-CoA oxidase activity	Electron transport	IEA
C50B6.7	Catalytic activity	Carbohydrate metabolism	IEA
EEED8.3	Lipid binding	Transport and embryonic development	IEA, IMP
F01D5.3	Receptor activity		IEA
F01G10.9		Reproduction	IMP
F02D8.4	Carboxypeptidase A activity	Proteolysis	IEA
F08G5.6		Defense response	IMP
F08H9.5	Sugar binding		IEA
F09C8.1	Hydrolase activity	Lipid metabolism	IEA
F09G2.3	Inorganic phospohate transporter activity	Phosphate transport	IEA
F10C2.7	Transporter activity	inorganic anion transporter activity	IEA
F18A12.4	Metallopeptidase activity and zinc ion binding	Proteolysis, neprilysin acitvity	IEA
F20G2.1	Oxidoreductase activity	Fatty acid biosynthesis	IEA
F21F8.4	Aspartic-type endopeptidase	Proteolysis	IEA
F26C11.1	Acid phosphatase activity		IEA
F28C6.5		Embryonic development	IMP
F28H7.3	Triacylglycerol lipase activity	Lipid metabolism	IEA
F32H5.1	Cysteine-type peptidase activity	Positive regulation of growth	IEA, IMP
F36A2.3	Oxidoreductase activity	Oviposition and locomotory behaviour	IEA, IMP
F38B6.4	Catalytic activity	Biosynthetic process	IEA
F44E5.4	ATP binding, unfolded protein binding	Iron-sulfur cluster assembly, Protein folding	IEA
F44E5.5	ATP binding, unfolded protein binding	Iron-sulfur cluster assembly, Protein folding	IEA
F44G3.2	Kinase activity		IEA
F46B6.8	Carboxylic ester hydrolase	Lipid metabolism	IEA
F46E10.11		Positive regulation of growth , larval development	IMP
F47C10.2	Protein binding		IEA
F47D12.7	Protein binding		IEA
F48E3.4	Serine-type endopeptidase	Proteolysis	IEA
F48G7.5		Reproduction, gamete generation	IMP
F49E12.9	Catalytic activity	Metabolic process	IEA
F53A9.2	Metallopeptidase activity and zinc ion binding	Proteolysis	IEA
F54F3.3	Carboxylic ester hydrolase	Lipid metabolism	IEA
F58G6.3	Copper ion binding activity	Copper ion metabolism	IEA
F58G6.7	Copper ion binding activity	Copper ion metabolism	IEA
F59D6.3	Pepsin A activity	Proteolysis	IEA
H25K10.1	Hydrolase activity		IEA
K09C6.8	Protein kinase activity	Serine/Threonine kinase activity	IEA
K10C2.3	Protein kinase activity	Serine/Threonine kinase activity	IEA
M02F4.7	Sugar binding		IEA
M28.8		Metabolic process	IEA
M60.2		Defense response	IMP
R09D1.8	Chitinase activity	Chitin catabolic process	IEA
R13A5.10	Zinc ion binding, hydrolase activity		IEA
R13H4.3	Acid phosphatase activity		IEA
R186.1		Embryonic development	IEA
R193.2		Positive regulation of growth	IMP
T01C3.4	Lipase activity	Lipid catabolic process	IEA
T02G5.11	RNA binding and zinc ion binding		IEA
T04G9.7		Embryonic development	IMP
T09F5.1	Galctosyl transferase	Protein amino acid glycosylation	IEA
T19C4.5	Iron, Oxygen and heme binding		IEA
T21F4.1	Arginase activity	Arginine catabolic process	IEA
W07A12.6	Transferase activity	Oviposition	IMP
W07B8.1	Cysteine-type peptidase activity	Proteolysis	IEA
W08E12.3	Electron carrier activity	Electron transport	IEA
Y105C5B.15	Hydrolase activity		IEA
Y105C5B.7	Hydrolase activity		IEA
Y26D4A.11	Chromatin binding	Chromatin assembly or disassembly	IEA
Y37D8A.19		Larval development	IMP
Y37D8A.4		Intracellular signaling cascade	IEA
Y40B10A.2	O-methyl transferase activity		IEA
Y40B10A.6	O-methyl transferase activity		IEA
Y46C8AL.2	Sugar binding		IEA
Y46D2A.2	Transcriptional elongation regulation activity	Regulation of transcription	IEA
Y46G5A.29	Calcium ion binding		IEA
Y48A6B.7	Zinc binding, hydrolase activity		IEA
Y51H4A.5	Triacylglycerol lipase activity	Lipid metabolism	IEA
Y54G11A.7	Binding	Embryonic development	IEA
Y71G12B.17		Transport	IEA
Y71H2AM.16	Acid phosphatase activity		IEA
ZK742.3	Oxidoreductase activity	Electron transport	IEA
ZK813.1		Multicellular organismal development	IEA

* IEA, Inferred by Electronic Annotation; IMP, Inferred from Mutant Phenotype

Table 5. List of genes with KEGG descriptions

Description	Gene name	KEGG pathway
C45B2.5	gln-1	Glutamate metabolism
F01G10.3	ech-9	Fatty acid metabolism
F14F4.3	mrp-5	Multidrug resistance protein
F32A5.5	aqp-1	Aquaglyceroporin related protein
F52E1.1	pos-1	Posterior segregation
F56H6.5	gmd-2	Fructose & mannose metabolism
F58B3.2	lys-5	Lysozyme
K07E3.3	dao-3	Lysozyme
T11F9.3	nas-20	Astacin protease
ZK455.4	asm-2	Sphingolipid metabolism

Table 6. List of genes with known RNAi phenotypes

Description	Gene name	RNAi phenotype*
C01G6.3		Ste,Emb
C04G2.5		increased fat content
C27D6.3		Unc
C29E4.7	gsto-1	Unc,Emb,Rup,Pvl,Egl,Gro,Chr segregation a
C30G7.1	hil-1	Egl,Spontaneous mutn rate increased, Unc
C32D5.6		Spontaneous mutn rate increased
C32H11.10	dod-21	Age
C33A12.6	ugt-21	fat content inceased
C44B12.1		Ste,Emb,Emb
C55F2.1		Ste
EEED8.3		Emb
F01G10.9		Ste
F08F3.3	rhr-1	Emb
F08G5.6		Esp
F08H9.5	clec-227	increased fat content, extended life span
F14F4.3	mrp-5	Lvl,Gro,Bli,Ric,Clr,Slu
F22A3.6	ilys-5	Emb
F22B5.4		Unclassified
F26H11.2	nurf-1	Stp,Gro
F28C6.5		Emb
F32A5.5	aqp-1	Age
F32H5.1		Gro
F35C5.7	clec-64	Unc,Him
F36A2.3		Emb,Unc
F46E10.11		Prl, Lvl,Gro
F48G7.5		Ste, stp, Sck
F52E1.1	pos-1	Emb,intestinal development abnormal
F54E2.1		reduced brood size
F56A6.1	sago-2	Emb
F56H6.5	gmd-2	prl,Lvl,Unc,Lva,Bmd,Egl
F59D8.1	vit-3	Emb, Gro
F59D8.2	vit-4	Emb, Gro
H25K10.1		fat content reduced
K05F1.7	msp-63	sec:fat increased, Emb, fat reduced
K07C6.4	cyp-35B1	Age, fat content reduced
K07E3.3	dao-3	Age
K10D11.1	dod-17	Age
M60.2		Esp, transgene expression increased
R186.1		Emb
T04G9.7		Emb
T07C4.4	spp-1	Age
T10H4.12	cpr-3	Emb
W07A12.6	oac-54	Egl
W07A12.7	rhy-1	Egl
Y37D8A.19		Lva
Y54G11A.7		Emb
ZK6.10	dod-19	Age

***** Embryonic lethal (Emb), maternal sterile (Ste), abnormal body morphology (Bmd), larval arrest (Lva), larval lethal (Lvl), protruding vulva (Pvl), slow growing (Gro), sterile progeny (Stp), abnormal life span (Age), abnormal egg laying (Egl), uncoordinated movement (Unc), blisters (Bli), clear (Clr), aldicarb resistance (Ric), abnormal feeding behavior (Eat)

Discussion

We postulated that specific molecules exist for the uptake and transport of heme within cells because free heme is hydrophobic and cytotoxic. A major impediment in the identification of heme uptake and transport pathways has been the inability to disassociate the tightly regulated processes of heme biosynthesis and degradation from heme transport. We have identified *C. elegans* as a unique animal model for interrogating the pathways involved in heme homeostasis because worms do not make heme but rather rely solely on exogenous heme for their growth and development (Fig. 1) [93]. Once worms absorb heme from the diet through the intestinal apical surface, we hypothesize that heme must be trafficked to different cellular compartments for incorporation into hemoproteins. It is also possible that in worms, there are specific molecules to transport heme from the intestine to other cell types. Unlike other organisms that make heme, *C. elegans* is unique, as it does not synthesize heme and thereby, for the first time, allows for external control of heme levels in an intact animal solely by dietary means.

Using the Affymetrix *C. elegans* whole genome array, we performed a transcriptional profiling experiment to identify genes in worms that were regulated by heme at the transcriptional level. While the Affymetrix *C. elegans* whole genome array has been widely used since it was introduced in 2002, our study is the first of its kind as we have used the microarrays to study nutrient-gene interactions by growing worms in liquid culture [114, 136-139]. From our microarray analysis we identified 288 genes that showed ≥ 1.6 fold change in gene expression at 4 or 500 μM. We confirmed the gene expression profiles for about 26 of the 288 genes. Among these

were aquaglyceroporin-like proteins (*aqp-1* down regulated at 4 μM heme and *aqp-8* upregulated at 500 μM heme), cytochrome P450 family member (*cyp-33C9*) upregulated at low heme concentration and several genes of unknown function. Glutathione transferases (GST) are detoxifying enzymes that have been proposed to be heme-binding proteins in parasitic nematodes [140]. A recent proteomic analysis has identified GST-19 as highly heme-responsive. The authors have shown that it is produced under high heme levels and have proposed that GST-19 might be involved in processing heme compounds thereby indirectly influencing heme trafficking when there is an excess of intracellular heme concentrations [140]. Interestingly, there were three glutathione transferases (*gst-22*, *gst-29* and *gst-16*) identified from our microarray analysis. It is possible that these genes might also play a role in maintaining intracellular heme levels. Gene ontology and KEGG pathway analysis showed that *hrgs* span across different biological process and there were only a few *hrgs* that are known heme enzymes or hemoproteins. This finding was surprising because it suggests that the heme homeostasis machinery is under transcriptional control by heme rather than the target proteins. The vast majority of *hrgs* are of unknown function, and, therefore, do not have any biological processes or pathways attributed to them. Furthermore, RNAi phenotypes reported for 46 of the 288 *hrgs* revealed that knockdown of the *hrgs* resulted in growth and developmental defects. Taken together, our findings are physiologically relevant because hemoproteins perform diverse functions ranging from miRNA processing (DGCR8) to gas sensing (hemoglobin) to regulation of gene expression (Bach1) and knockdown of genes

involved in maintaining heme homeostasis would result in severe phenotypes such as lethality [80, 141-145].

Although heme is an important cofactor of proteins that perform a wide variety of functions, the molecular mechanisms underlying the uptake and intracellular trafficking of heme in eukaryotes remain poorly understood. The results from our microarray analysis give us insights into heme homeostasis in eukaryotes at a global level. Observations made in *C. elegans* could also be extrapolated to heme homeostasis in humans as more than 40% of the worm *hrgs* have homologs in humans and may therefore have functionally conserved roles in various heme dependent pathways. Of these 288 *hrgs,* approximately 37 have homologs in humans but are absent in parasites suggesting a conserved role for some of these *hrgs* in regulating heme homeostasis in vertebrates. Presumably, of the 84 *hrgs* common to worms and humans there may be some that play an important role in heme uptake and trafficking in both worms and humans.

Parasitic worm infections are a huge burden to public health since more than two billion people world-wide are afflicted by helminthic infections [146]. Annual crop losses due to plant-parasitic nematodes are estimated to be around eighty billion dollars [94]. There is an urgent need to find new drug targets to tackle helminthic infections because drug resistance is already prevalent in these parasites [96, 97]. We showed that parasitic nematodes lack the ability to make heme and rely on exogenous heme for their growth and development [93]. A recent study conducted by Held *et al.* has demonstrated that the infectivity of hookworms, which feed on blood in the host, was significantly lower in hamsters fed a low-iron diet [98]. This observation

revealed the importance of host heme and iron status in the survival of parasitic nematodes. Interestingly, protozoan parasites such as Trypanosomes, the causative agents of diseases such as sleeping sickness (*Trypanosoma brucei*), Chagas disease (*Trypanosoma cruzi*) and leishmaniasis (*Leishmania major*), also seem to lack the ability to make heme and therefore utilize exogenous heme [118, 147, 148]. Homology searches of the 288 heme-responsive genes identified from our microarray study in the genomes of the parasitic trematode *S. mansoni* and protozoans such as *T. brucei*, *T. cruzi* and *L. major* showed that of the 288 *hrgs*, 12 were specific to heme auxotrophs. This finding is significant because it indicates the existence of heme auxotroph-specific genes that may encode for proteins involved in heme uptake and transport pathways. These heme auxotroph-specific genes could potentially be used as novel drug targets against parasitic infections.

Since membrane transporters have transmembrane domains, we analyzed the 288 *hrgs* using TMHMM 2.0 and found that 41 of the 288 *hrgs* had at least one predicted transmembrane domain. It is possible that of the 41 *hrgs*, there might be some genes that encode proteins involved in heme transport. We have previously shown that gallium protoporphyrin IX (GaPPIX) is a highly toxic heme analog [93]. Thus depleting heme transport genes responsible for heme uptake may result in resistance to GaPPIX [93]. To test if any of these 41 *hrgs* were involved in heme uptake, we performed RNAi assays and looked for resistance against GaPPIX. Six of the 41 genes showed different levels of resistance against GaPPIX toxicity (A.U.R and I.H. unpublished results). Among these were *pgp-1* (P- glycoprotein related protein, a member of ABC transporter superfamily), *hmit-1.1* (proton-dependent myo-

inositol transporter) and *mrp-5* (multidrug resistance protein) [149]. Interestingly, there were ~ 247 genes that encoded for proteins without any predicted transmembrane domain. It has been demonstrated from iron and copper transport studies that soluble proteins such as chaperones (Atox1, a copper chaperone that delivers copper to Menkes ATPase) and storage proteins (Ferritin, an iron storage protein) play an important role in regulating the intracellular levels of toxic yet essential trace metals [150, 151].

Although we have identified the heme-responsive genes in worms, it is important to characterize these genes in order to understand their role in regulating heme homeostasis. A powerful and a high-throughput approach to accomplish this goal, is to perform RNA-mediated interference assays. Using the *hrg-1::gfp* "heme-sensor" strain generated in our laboratory, Dr. Severance in our research group conducted RNAi assays for all the *hrgs* identified from the microarrays. He found 53 genes that caused aberrant regulation of GFP in the heme sensor strain. It is therefore possible that some of these genes might be involved in the heme homeostasis pathway.

The results from the microarray analysis in *C. elegans* will help in providing molecular insights into heme homeostasis pathways in eukaryotes. In the present study, we report the identification of a novel catalog of genes that are regulated by heme at the transcriptional level. Further characterization of these genes is important to elucidate their biological roles in organismal heme homeostasis.

Chapter 4 Characterization of *C.elegans hrg-1* and *hrg-4*

Summary

We performed a transcriptional profiling experiment using Affymetrix *C. elegans* whole genome array and identified 288 heme-responsive genes. We postulated that expression of genes encoding for heme transporters might be higher at lower heme concentrations for maximum uptake of dietary heme. Therefore, we sorted the proteins encoded by the 80 *hrgs* that were upregulated at low heme into categories based on whether algorithms predicted the proteins to have transmembrane domains, transport functions and/or heme or metal binding motifs. We identified two genes, *hrg-1* and its paralog *hrg-4*, that were highly heme responsive. *Cehrg-1* has homologs in vertebrates, while *Cehrg-4* is worm-specific. Using transcriptional GFP reporter constructs, we show that *hrg-1* and *hrg-4* localize to the intestinal cells of the worms. Depletion of *hrg-4* in worms by RNA-mediated interference (RNAi) results in decreased ZnMP fluorescence in the gut and resistance to GaPPIX toxicity. In contrast, knock-down of *hrg*-1 by RNAi leads to an increased ZnMP fluorescence in the gut but causes no effects on animal viability using GaPPIX toxicity assays. Transient knockdown of *hrg-1* in zebrafish results in hydrocephalus, yolk tube malformations and, most strikingly, anemia. Worm HRG-1 fully rescues all the phenotypes observed due to knock-down of *hrg-1* in zebrafish. Ectopic expression in mammalian cells showed that HRG-4 localizes to the plasma membrane. Human and worm HRG-1 proteins localize together to the endo-lysosomal compartments.

CeHRG-1 and hHRG1 bind heme at lower pH and CeHRG-4 binds heme over a broader pH range. Studies conducted in *Xenopus* oocytes reveal that all three proteins transport heme. These results reveal an evolutionarily conserved role for HRG-1 proteins. The work described here lays the foundation for delineating the molecular mechanisms for heme transport in metazoans using *C. elegans* as the animal model.

Results

Seeking to identify molecules involved in heme homeostasis, we conducted a genome-wide analysis using Affymetrix *C. elegans* whole genome array using RNA isolated from worms grown in mCeHR-2 medium containing 4, 20 or 500 μM heme and identified 288 heme-responsive genes (*hrgs*). We reasoned that in order to maximize heme uptake from the diet, the expression of genes that encode for putative heme transporters might be upregulated in heme-limiting conditions. There were 80 *hrgs* that showed greater expression at 4 μM heme but were either down regulated or unchanged at 500 μM heme, compared to reference samples at 20 μM heme. From the microarray experiment, expression of F36H1.5 was upregulated greater than 10-fold under low heme conditions but was undetectable at 500 μM heme. This gene was named heme-responsive gene-4 (*hrg-4*). RNA blotting and qRT-PCR analyses revealed that the *hrg-4* mRNA level was significantly increased at 4 μM heme but was undetectable at 20 and 500 μM heme (Fig. 1a, b). We identified three putative paralogs in *C. elegans*, which we termed *hrg-1* (R02E21.6), *hrg-5* (F36H1.9) and *hrg-6* (F36H1.10) with 27 %, 35 % and 39 % identity at the amino acid level, respectively (Fig. 2). Both *hrg-1* and *hrg-4* were highly heme responsive (Fig. 1a). The magnitude of upregulation of these genes at 1.5 μM heme and the response to

high heme concentrations, however, were markedly different (Fig. 1b and inset). Two paralogs, *hrg-5* and *hrg-6*, did not show any heme-dependent changes in their level of expression. While *hrg-4*, *hrg-5* and *hrg-6* are nematode-specific genes, *hrg-1* has putative homologs with ~ 25% amino acid sequence identity in vertebrates. The multiple sequence alignment obtained using Clustal W showed several conserved residues between worm HRG-1 and its vertebrate homologs (Fig. 3). The HRG-1 proteins have conserved tyrosine (YxxØ) and acidic-dileucine based sorting signal (D/ExxxLL) in the cytoplasmic carboxy terminus [152]. The YxxØ motif is involved in rapid internalization of the proteins from the plasma membrane. This sorting motif has also been implicated in the targeting of transmembrane proteins to the lysosomes and sorting of proteins to the basolateral membrane in polarized cells [152]. The dileucine-based sorting signal plays an important role in sorting many type I, type II and multispanning membrane proteins. Like the tyrosine motif, D/ExxLL motif is also involved in internalization of proteins from the plasma membrane and targeting of proteins to the lysosomes.

Topology modeling of HRG-1 and HRG-4 identified four predicted transmembrane domains (TMDs) (Fig. 4). We also identified residues that could potentially either bind heme directly such as the invariant histidine (H90 of HRG-1) in TMD2 or the FARKY (Y[A/S]HRY in vertebrates) motif in the C-terminus tail that could interact with the side chains of the heme moiety (Fig. 2-4). Studies in gram-negative bacteria have suggested an important role for histidine residues in the delivery of heme for cytochrome *c* biogenesis [153]. The invariant H90 of HRG-1 in TMD2 is substituted with a tyrosine (Y63) in HRG-4. Tyrosine heme ligand differs

from the histidines in that it has a lower redox potential and the coordination stabilizes heme from carrying out oxidative chemistry [154]. The tyrosine moiety in soluble guanylate cyclase has been shown to be involved in coordinating the propionate side chains in heme [153, 155, 156]. Based on the studies mentioned above, we postulate that the histidine in HRG-1 and tyrosine in HRG-4 may be involved in binding of heme by these proteins.

To study the temporo-spatial expression patterns of *hrg-1* and *hrg-4*, we generated transcriptional fusion constructs with GFP reporters to create integrated transgenic lines of *C. elegans*, either by gamma irradiation (IQ6011, *hrg-1::gfp*) or biolistics (IQ6041, *hrg-4::gfp*). Both these genes were expressed specifically in the intestinal cells in larvae and adults (Fig. 5a, b). The expression of GFP in transgenic worms with the *hrg*-4 transcriptional reporter was very weak. This can be attributed to the fact that biolistic transformation of *C. elegans* results in low-copy-number integrated lines [157]. As shown in Fig. 5, the levels of GFP expression can be modulated in a single generation of worms, by changing the amount of exogenous heme, suggesting that these worms can sense the amount of organismal heme. The expression of both *hrg-1* and *hrg-4* was regulated by exogenous heme and repression of these genes was specific to heme. Unlike the dramatic down regulation of GFP expression at 20 μM heme in the IQ6011 strain, there was only a modest decrease in GFP expression at 20 μM heme in the IQ6041 strain. This is consistent with the results from qRT-PCR data which showed that at a concentration of 15 μM heme where *hrg-1* is already down regulated *hrg-4* shows about 3-fold upregulation.

Neither protoporphyrin IX nor iron altered the expression of GFP in the IQ6011 or IQ6041 strains (Fig. 6a, b).

We then assessed the effect of depletion of *hrg-1* and *hrg-4* in worms by RNA-mediated interference using the following assays: first, the expression of GFP in the *hrg-1::gfp* heme-sensor strain; second, the accumulation of fluorescent heme analog (ZnMP) and third, the sensitivity of animals to toxic heme analog, gallium protoporphyrin IX (GaPPIX), a toxic heme analog [93]. RNAi of *hrg-1* resulted in a significant increase in GFP expression only at low heme levels in the heme sensor strain, but knockdown of *hrg-4* resulted in the expression of GFP in the *hrg-1::gfp* worms at concentrations of heme that are usually sufficient to repress GFP expression (Fig. 7a). *hrg-4* RNAi resulted in no accumulation of ZnMP in worms that were grown in 1.5 μM heme, a concentration sufficient for a robust uptake of heme in worms (Fig. 7b). Consistent with these observations, progeny of *hrg-4* RNAi worms were resistant to GaPPIX toxicity (Fig. 7c). In contrast, *hrg-1* depleted animals showed increased levels of ZnMP fluorescence when compared to control (Fig. 7b), and there was no discernable effect on animal viability using the GaPPIX toxicity assays (Fig. 7c). The GaPPIX toxicity assay was performed by Anita Rao (Hamza lab). The observed RNAi phenotypes of *hrg-4* and *hrg-1* suggest that HRG-4 is involved in uptake of heme into the worm intestinal cells whereas HRG-1 mediates heme homeostasis through an intracellular compartment.

Figure 1. *Cehrg-4* and *Cehrg-1* are upregulated at low heme concentrations

a) Northern blot analysis of *hrg-4* and *hrg-1* expression in response to 4 and 20 μM heme in mCeHR-2 medium. The blot was stripped and reprobed with glyceraldehyde 3-phosphate dehydrogenase (*gpd-2*) as a loading control **b)** Expression of *hrg-4* (circles) and *hrg-1*(squares) mRNA estimated by quantitative RT-PCR from total RNA obtained from worms grown at indicated heme concentrations. Each data point represents mean ± S.D and the results are representative of three experiments. Inset shows mRNA levels at higher heme concentrations.

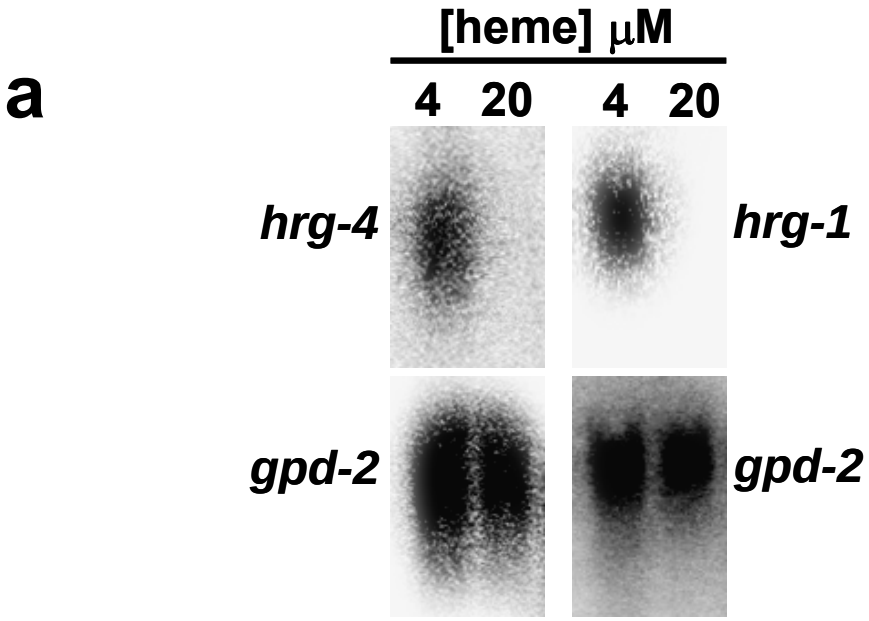
a
[heme] μM
4 20 4 20
hrg-4
hrg-1
gpd-2
gpd-2

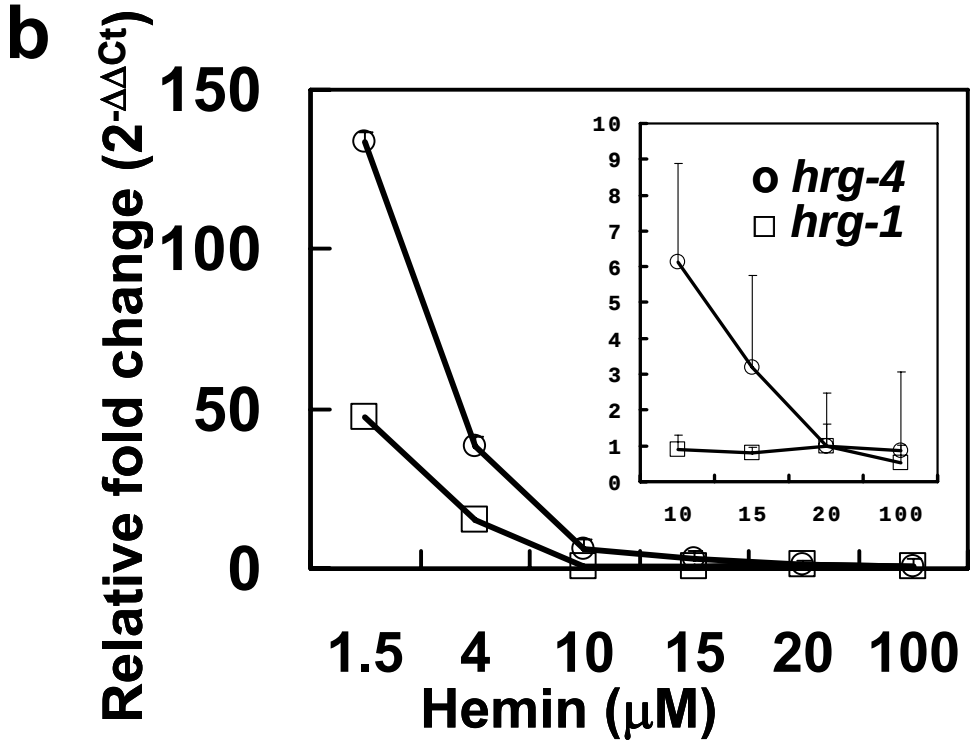
b
Relative fold change (2-ΔΔCt)
150
100
50
0
o hrg-4
□ hrg-1
10
9
8
7
6
5
4
3
2
1
0
10 15 20 100
1.5 4 10 15 20 100
Hemin (μM)

Figure 2. CeHRG-4 paralogs in the *C. elegans* genome

Multiple sequence alignment of CeHRG-1, -4, -5 and -6 paralogs obtained using ClustalW (v. 1.83). Identical amino acids and conservative changes are indicated by reversed and shaded characters, respectively. Asterisk indicates conserved histidines in HRG-1 that are replaced by tyrosines in HRG-4 and HRG-6. Boxed residues denote the four putative transmembrane domains based on predictions from HRG-1. C-terminus tyrosine (YxxØ) and di-leucine (D/ExxxLL) based sorting motifs in HRG-1 are indicated.

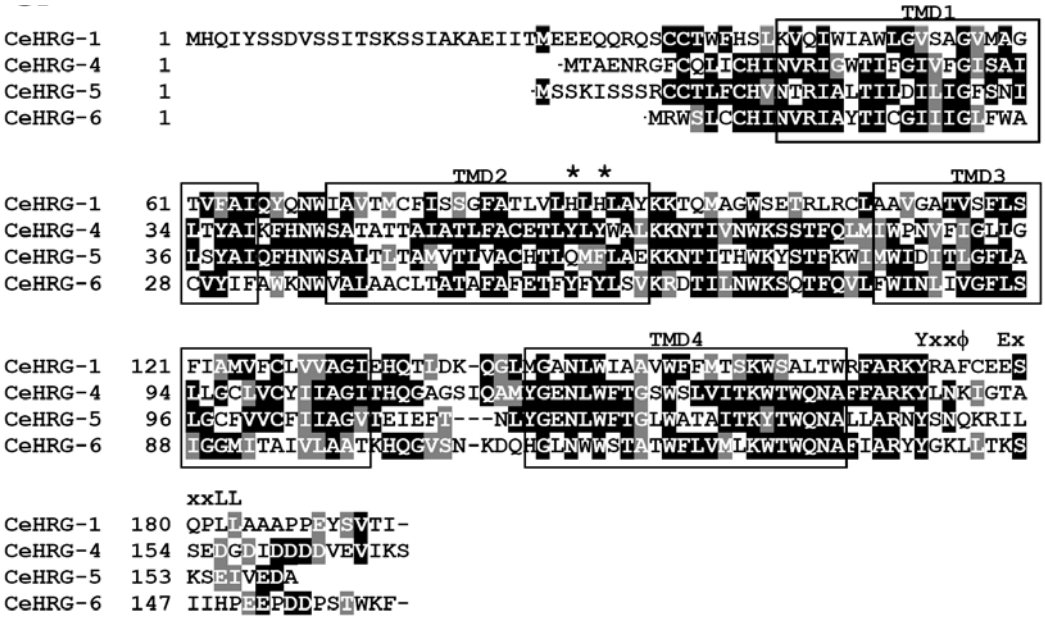
TMD1
CeHRG-1 1 MHQIYSSDVSSITSKSSIAKAEIITMEEEQQRQSCCTWFHSLKVQIWIAWLGVSAGVMAG
CeHRG-4 1 -MTAENRGFCQLICHINVRICWTIFGIVFGISAI
CeHRG-5 1 -MSSKISSSRCCTLFCHVNTRIALTILDILIGFSNI
CeHRG-6 1 -MRWSICCHINVRIAYTICGIIIGLFWA
TMD2
TMD3
CeHRG-1 61 TVFAIQYQNWIAVTVCFISSGFATLVLHLHLAYKKTQMAGWSETRLRCLAAVGATVSFLS
CeHRG-4 34 LTYAIKFHNWSATATTAIATLFACETLYLYWALKKNTIVNWKSSTFQLMIWPNVFIGLLG
CeHRG-5 36 LSYAIQFHNWSALTLTAMVTLVACHTLQMFLAEKKNTITHWKYSTFKWIMWIDITLGFLA
CeHRG-6 28 CVYIFAWKNWVALAACLTATAFAFETFYFYLSVKRDTILNWKSQTFQVLFWINLIVGFLS
TMD4
Yxxϕ
Ex
CeHRG-1 121 FIAMVFCLVVAGIFHQTIDK-QGLMCANLWIAAVWFFMTSKWSALTWRFARKYRAFCEES
CeHRG-4 94 LLGCLVCYIIAGITHQCAGSIQAMYGENLWFTCSWSLVITKWTWQNAFFARKYLNKIGTA
CeHRG-5 96 LGCFVVCFIIAGVTEIEFT---NLYGENLWFTGLWATAITKYTWQNALLARNYSNQKRIL
CeHRG-6 88 IGGMITAIVLAATKHQGVSN-KDQHGLNWWSTATWFLVMLKWTWQNAFIARYYGKLITKS
xxLL
CeHRG-1 180 QPLLAAAPPEYSVTI-
CeHRG-4 154 SEDGDIDDDDVEVIKS
CeHRG-5 153 KSEIVEDA
CeHRG-6 147 IIHPEEPDDPSLWKF-

Figure 3. CeHRG-1 has homologs in vertebrates

Multiple sequence alignment of *C. elegans* HRG-1 with human (AAH65033.1), zebrafish (AAH53186.1), mouse (NP_080629.1), chicken (NP_001026574.1) and Xenopus (AAH82899.1) using ClustalW W (v. 1.83). Identical amino acids and conservative changes are indicated by reverse and shaded characters. Asterisk, histidine (H90); circles, aromatic amino acids; box, putative transmembrane domains; YxxxØ, C-terminal tyrosine motif; D/ExxxLL, di-leucine motif.

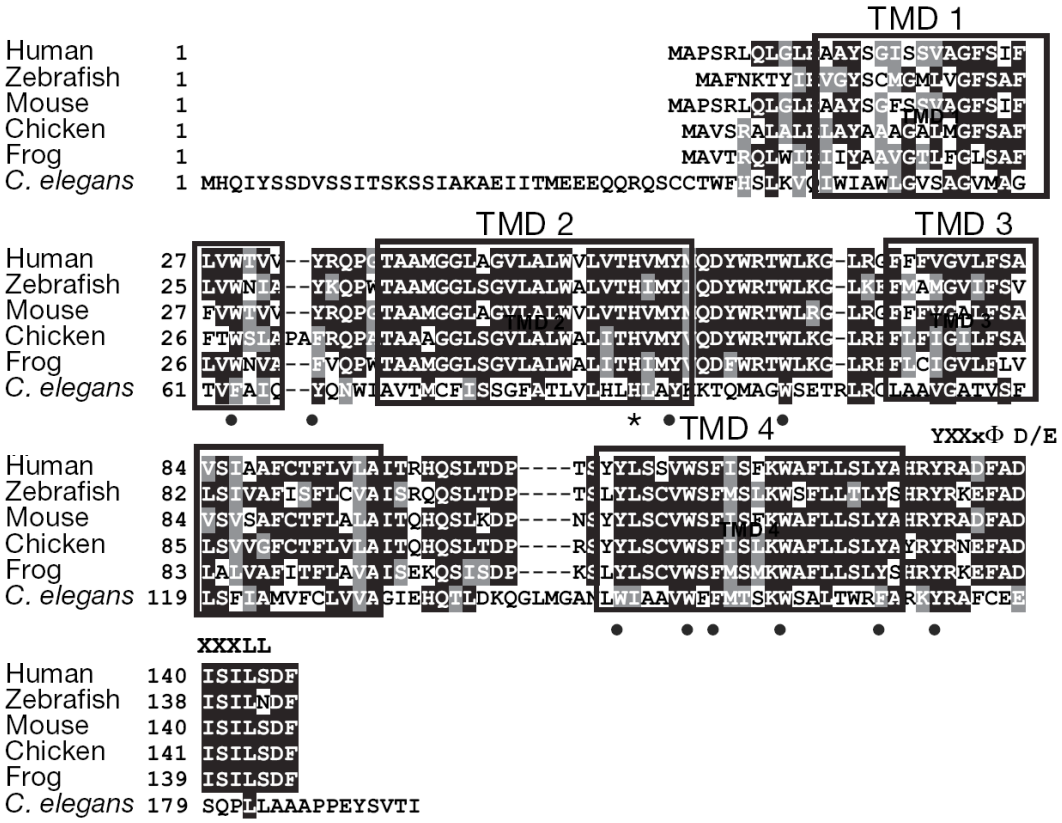
TMD 1
TMD 2
TMD 3
TMD 4
YXXxΦ D/E
XXXLL
Human
Zebrafish
Mouse
Chicken
Frog
C. elegans

Figure 4. Predicted topology of *C. elegans* HRG-1 and HRG-4

Putative topology of **(a)** *C. elegans* HRG-1, **(b)** hHRG1 and **(c)** *C. elegans* HRG-4 predicted by TMHMM 2.0 and SOSUI. The amino and carboxy-termini are cytoplasmic, E1 and E2 are the exoplasmic loops and C1 is the cytoplasmic loop. Amino acids shaded red are potential heme binding residues and those in green and blue (CeHRG-1) are important for the intracellular localization of the protein. HRG-1 proteins share certain characteristics with tetraspanin proteins, including polar residues (gray), and cysteines (orange) within TMDs that serve as putative palmitoylation sites. A potential N-linked glycosylation site (NWS) is also indicated in HRG-4.

.

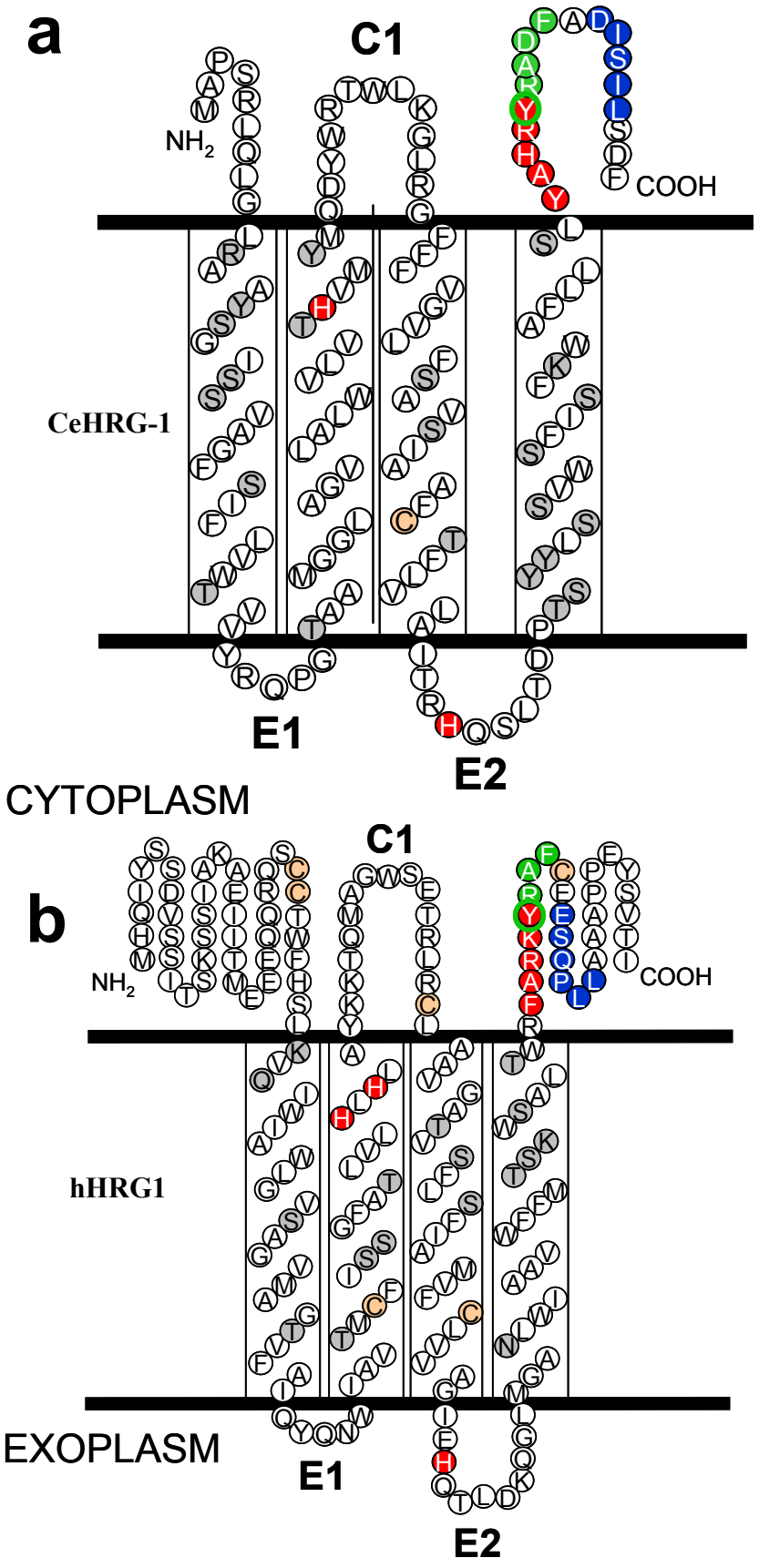
a
C1
NH2
COOH
CeHRG-1
E1
E2
CYTOPLASM
b
C1
NH2
COOH
hHRG1
EXOPLASM
E1
E2

C

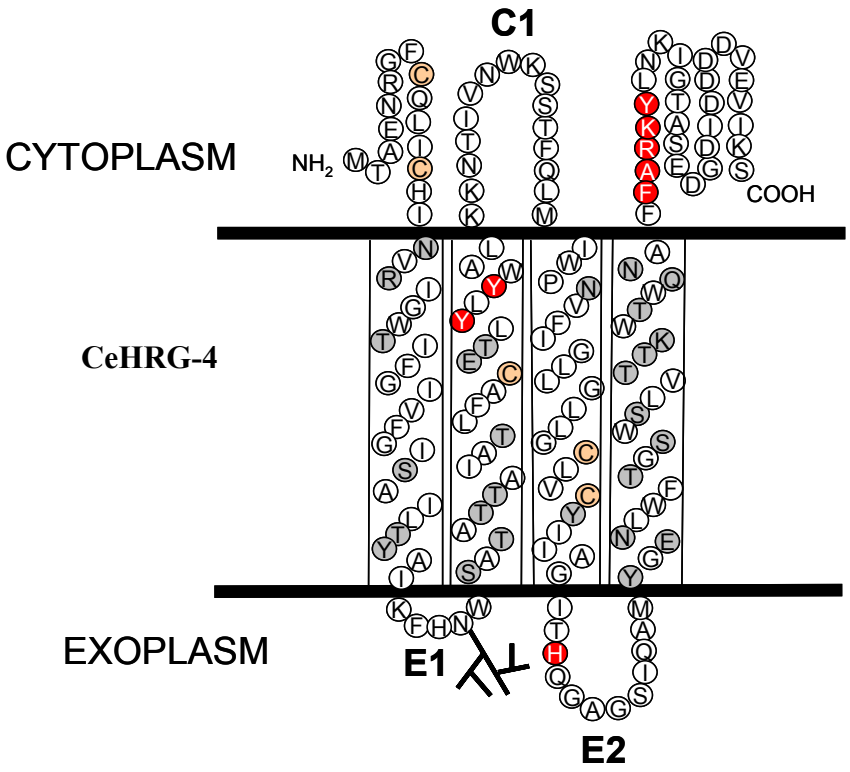

Figure 5: IQ6011 *hrg-1::gfp* and IQ6041 *hrg-4::gfp* heme-sensor responds to exogenous heme

L1 larvae of stable integrated transgenic line were sequentially exposed to mCeHR medium containing 2 μM heme (left and right panels) and 200 μM heme (center) **a)** *hrg-1* promoter (3kb) was cloned into pPD95.67 plasmid that contained GFP preceded by a nuclear localization signal (NLS) and followed by the 3' UTR from *unc-54* to create a *hrg-1::gfp* transcriptional fusion. A stably integrated transgenic worm (IQ6011) was generated by injection of the *hrg-1::gfp* fusion construct followed by gamma irradiation **b)** 3kb promoter region of *hrg-4* was fused to GFP preceded by a nuclear localization signal (NLS) and followed by the 3' UTR from *hrg-4* using Gateway Multisite recombination kit to create a *hrg-4::gfp* transcriptional fusion. A stably integrated transgenic worm (IQ6041) was generated by bombarding the *hrg-4::gfp* fusion construct along with gold particles into *unc-119* temperature sensitive mutant strain.

a

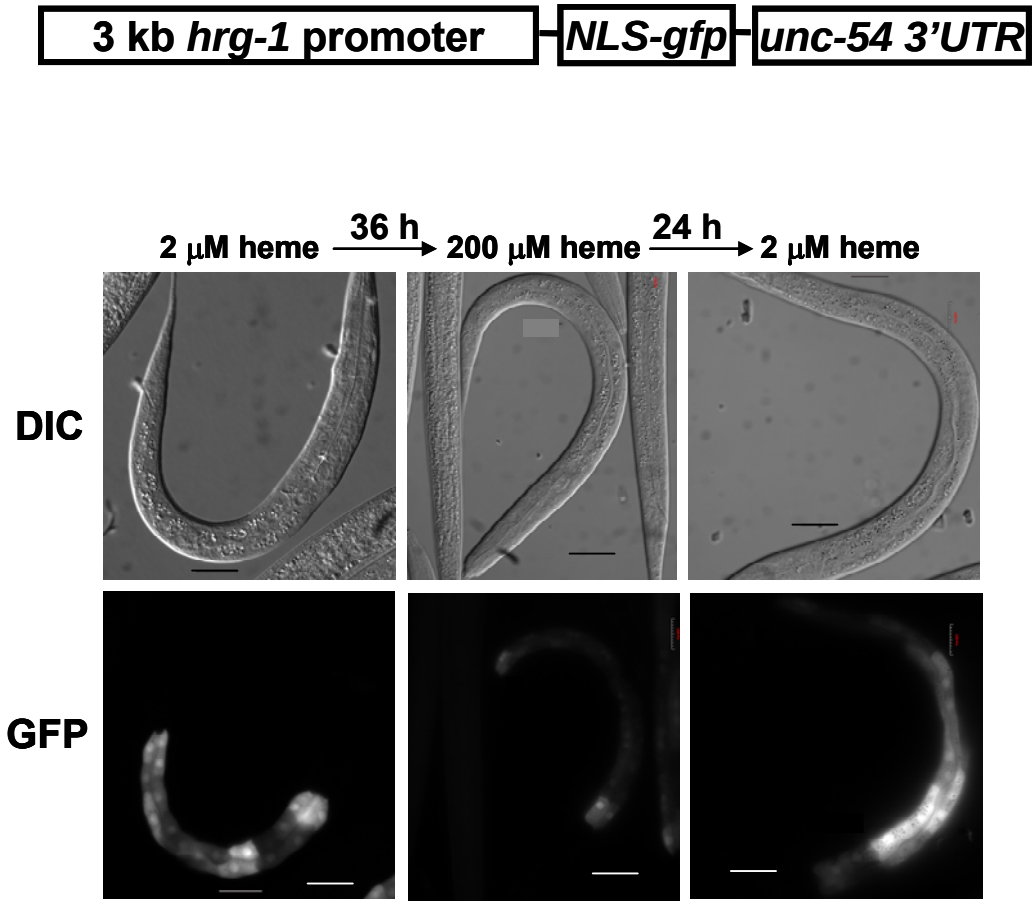
3 kb hrg-1 promoter
NLS-gfp
unc-54 3'UTR
2 μM heme
36 h
200 μM heme
24 h
2 μM heme
DIC
GFP

b

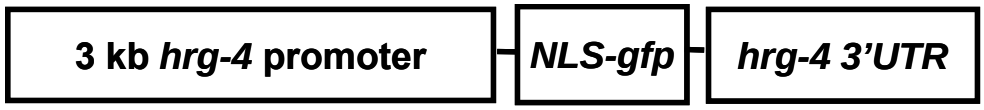
3 kb *hrg-4* promoter
NLS-gfp
hrg-4 3'UTR

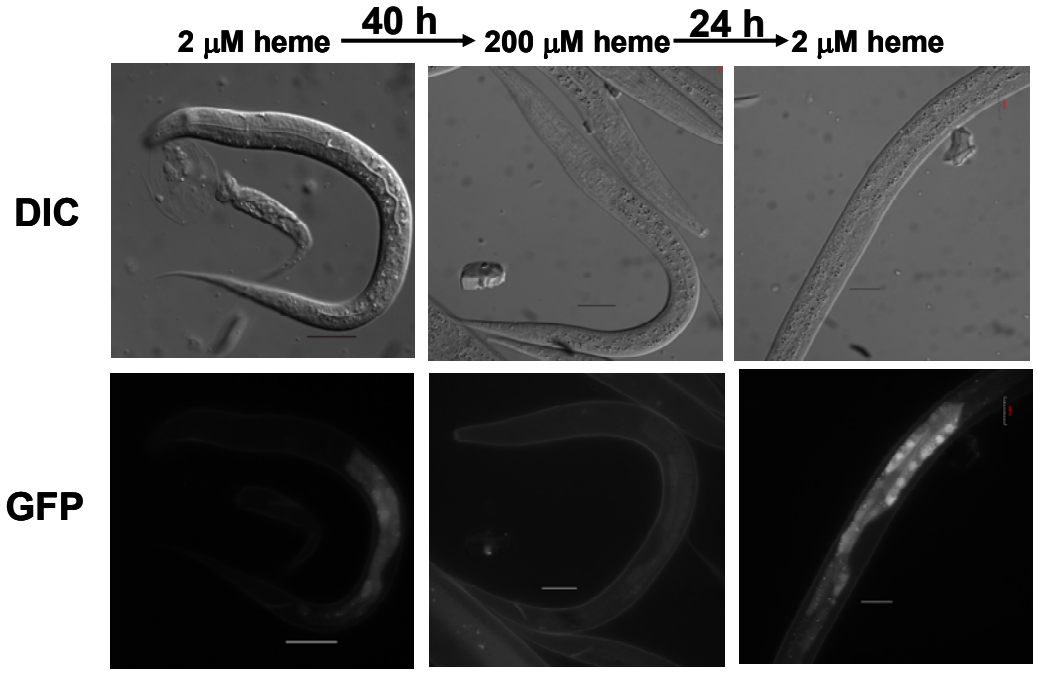
2 μM heme
40 h
200 μM heme
24 h
2 μM heme
DIC
GFP

Figure 6. Spectrometric analysis of GFP expression

a) *hrg-1::gfp* (IQ6011) and **b)** *hrg-4::gfp* (IQ6041) worms were grown in mCeHR medium in the presence of indicated amounts of either heme, or heme supplemented with 20 μM protoporphyrin IX or 1 mM iron for two generations. Mixed population of worms from each treatment was harvested, and GFP fluorescence was quantified with a spectrofluorometer.

a

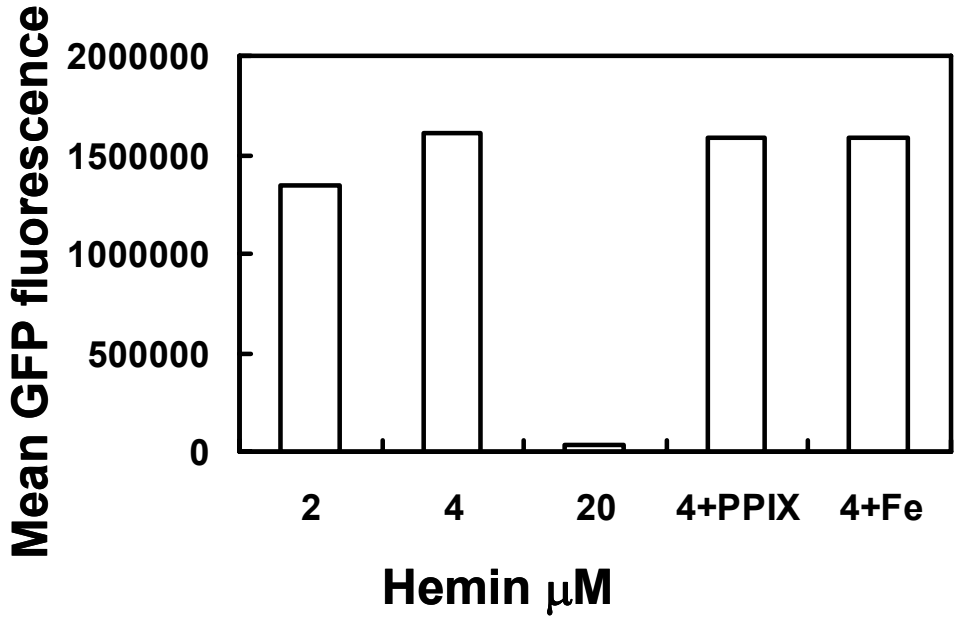
Mean GFP fluorescence
2000000
1500000
1000000
500000
0
2
4
20
4+PPIX
4+Fe
Hemin μM

b

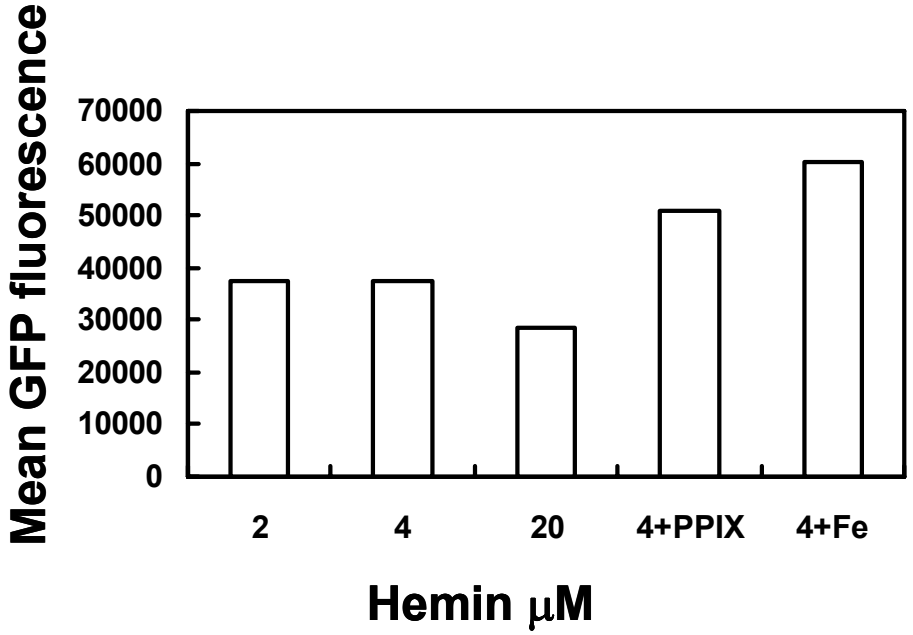
Mean GFP fluorescence
70000
60000
50000
40000
30000
20000
10000
0
2
4
20
4+PPIX
4+Fe
Hemin μM

BLAST searches revealed a homologous gene on zebrafish (*Danio rerio*) chromosome 6 (GenBank accession number BC053186) that shared approximately 21% amino acid identity with *C. elegans* HRG-1. We used zebrafish to delineate the function of HRG-1. We reasoned that disruption in heme homeostasis would be manifested as hematological defects, which can be visualized by analyzing aberrant circulating erythroid cells in the transparent fish embryos [158]. Using whole-mount *in situ* hybridization, we show that zebrafish *hrg-1* mRNA is expressed throughout the embryo including the central nervous system, at the 15-somite stage and 24 h post fertilization (See Appendix A). To knockdown *hrg-1* in zebrafish, anti-sense morpholinos (MO) were designed at the splice junction of intron 2 with either exon 1(MO1) or exon 2 (MO2) to induce mis-splicing and degradation of *hrg-1*mRNA. Embryos injected with MO1 exhibited mild anemia. By contrast, embryos injected with MO2 had severe anemia as discerned by the lack of *o*-dianisidine-positive erythroid cells (See Appendix A). MO2 morphants also showed other developmental defects, including hydrocephalus and a curved body with shortened yolk tube. The underlying cause of these discrepancies in phenotypes between MO1 and MO2 were revealed by RT-PCR which showed that MO2 caused exon-skipping resulting in a 100 bp deletion in the open reading frame, while MO1 resulted in the reduction in mRNA levels due to mis-splicing (See Appendix A). We cloned the *Cehrg-1* construct into pCS2 (+) plasmid and confirmed its expression by transfecting into HEK 293 cells and checking on a SDS-PAGE gel. These constructs were sent to Dr. Barry Paw at Brigham Women's Hospital for the rescue experiment. Despite only a

21% sequence identity between *C. elegans* and zebrafish HRG-1, co-injection of MO2 in the presence of *C. elegans hrg-1* cRNA resulted in complete rescue of anemia phenotype and the developmental defects in hydrocephalus and curved body with shortened yolk tube (see Appendix A). The phenotypes resulting from knock-down of zebrafish *hrg-1* was restricted specifically to the erythroid lineage and not to other hematopoietic- myeloid and thromboid lineages [127]. These studies suggest that both *C. elegans* and zebrafish HRG-1 are functionally equivalent and play a conserved role in maintaining heme homeostasis [127].

To further delineate the role of HRG-1 in vertebrates, we examined its gene expression, intracellular localization and biochemical properties in mammalian cells. BLAST search identified a gene in the human genome database that is homologous to *Cehrg-1*, which we refer to as *hHRG1* (SLC48A1). It is located on human chromosome 12q13 and is about 3.2 megabases from *DMT1*, the gene encoding for the primary ferrous iron transporter in mammals [159, 160]. RNA blotting in human adult tissues and cell lines detected two transcripts approximately 1.7 and 3.1 kilobases in size (Fig. 8a, b). *hHRG1* was highly expressed in the brain, kidney, heart and skeletal muscle (Fig 8a, c). *hHRG1* was abundant in cell lines derived from duodenum (HuTu80), kidney (ACHN, HEK 293), bone marrow (HEL, K562) and brain (M17, SY5Y) (Fig. 8b, d).

We examined the effects of heme and iron status on h*HRG1* gene expression. HEK 293 cells were grown for 14 h in heme-depleted medium with 500 μM succinyl acetone (SA) to inhibit heme synthesis and 100 μM desferroxamine (DFO) to chelate iron. Heme/iron depletion was followed by addition of 50 μM heme or 100 μM Fe-

SIH to the cells for a period of 3 h. Cells were harvested and total RNA was isolated. We performed qRT-PCR assays and found that the levels of h*HRG1* mRNA were unaltered. There was significant upregulation of *HMOX1* (gene encoding for heme oxygenase) under heme-replete conditions and *Tfr1* (gene encoding for transferring receptor 1) during iron-starvation (Fig 9a). To determine whether m*Hrg-1* gene expression was regulated at the transcriptional level by heme during erythroid maturation when the demand for heme is enormous, we used Friend mouse erythroleukemia (MEL) cells. MEL cells can be induced with 1.5 % DMSO to produce hemoglobin thereby simulating erythroid maturation. Induction of hemoglobin production in MEL cells resulted in the expected increase of *globin* and *Alas-2* mRNA but did not alter *Hrg-1* mRNA expression (Fig. 9b, c). These results revealed that unlike the worm homolog, *hHRG1* does not respond to changes in heme status at the transcriptional level. However, these findings do not exclude the possibility that HRG-1 may be regulated at the post-transcriptional level.

To examine the localization and function of HRG-1 proteins, we made fusion constructs of *CeHRG-1*, *hHRG1* and *CeHRG-4* with either the hemagglutinin (HA) epitope or GFP variants at the N and C-terminus and transiently transfected these constructs into HEK 293 cells.

Figure 7. *hrg-1* and *hrg-4* are essential for heme homeostasis in *C. elegans*

a) Equal numbers of synchronized L1 larvae from IQ6011 worms were grown in mCeHR-2 medium supplemented with 10 μM heme and plated on NGM agar plates spotted with RNAi feeding bacteria that was grown in the presence of either 5 or 25 μM heme. After 96 h of exposure to double-stranded RNA from the control vector, *hrg-1* or *hrg-4*, images were captured and the relative GFP fluorescence intensities were estimated using Simple PCI. Within each treatment, values with different letters are significantly different (P<0.001), as determined by using a one-way ANOVA with Student–Newman–Keuls multiple comparisons test. Each data point represents the mean ± SEM and the results are representative of five separate experiments (n= 35-45 worms per treatment). **b)** RNAi feeding was performed for 72 h using N2 worms initially grown in 10 μM heme containing mCeHR-2 medium. Following RNAi, worms were washed and incubated in mCeHR-2 medium containing 1.5 μM heme and 10 μM ZnMP for 16 h. Fluorescence images were captured using a Rhodamine filter and relative ZnMP fluorescence intensities from ~ 50 worms from each treatment were estimated using SimplePCI. **c)** Worms were first subjected to the indicated bacteria for RNAi and subsequently transferred to fresh NGM agar plates containing 1 μM GaPPIX plus RNAi bacteria. The total number of eggs that resulted in viable larvae was estimated after 5 days of exposure to GaPPIX. Each data point represents the mean ± SD and the results are representative of four separate experiments (n= 30 P_0 worms per treatment).

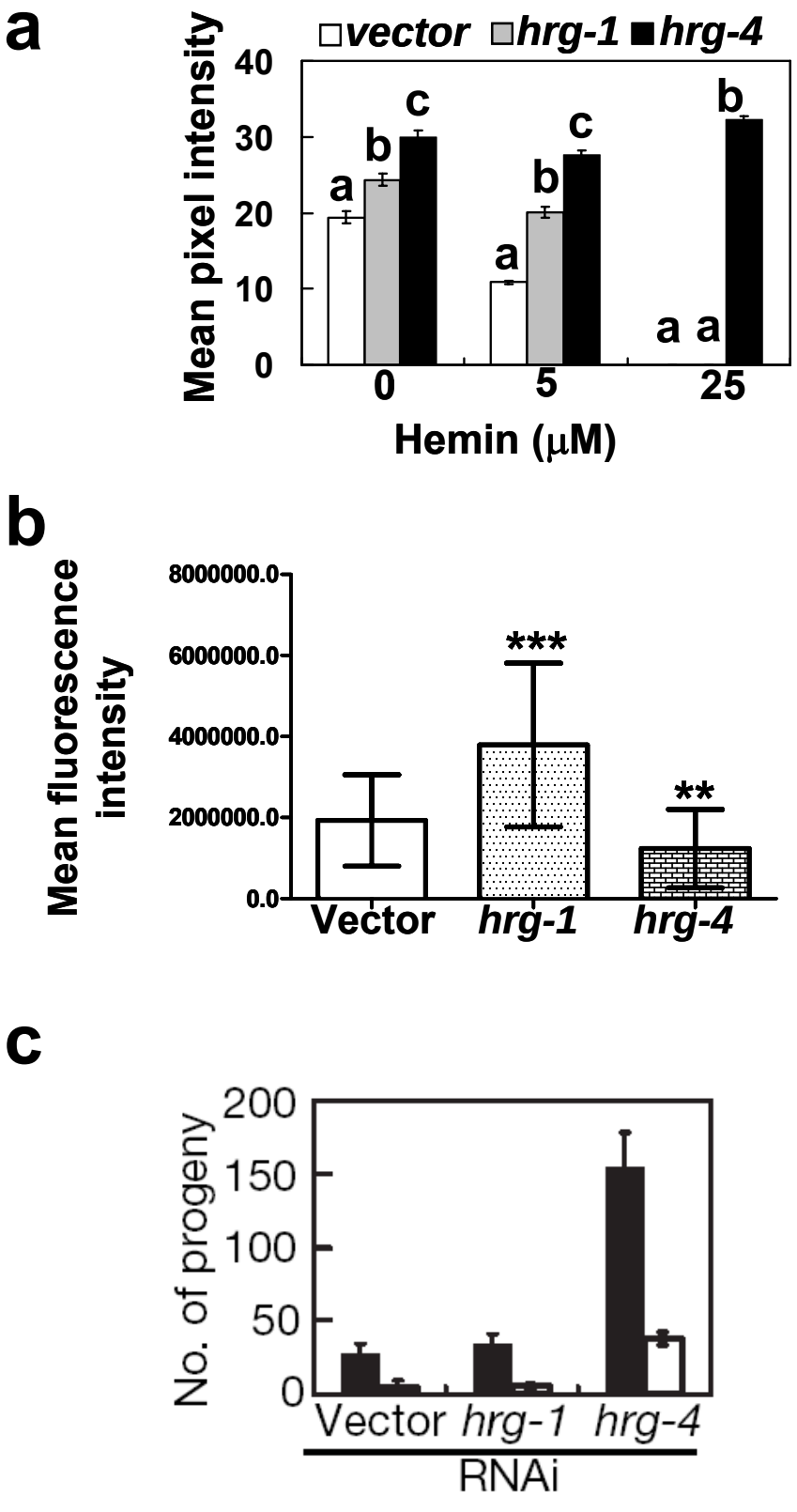
a
vector
hrg-1
hrg-4
Mean pixel intensity
40
30
20
10
0
a
b
c
a
b
c
a a
b
0
5
25
Hemin (μM)
b
Mean fluorescence intensity
8000000.0
6000000.0
4000000.0
2000000.0
0.0
***
**
Vector
hrg-1
hrg-4
c
No. of progeny
200
150
100
50
0
Vector
hrg-1
hrg-4
RNAi

While the proteins tagged with HA or GFP at the N-terminus were unstable, C-terminally tagged proteins were stable. On the SDS-PAGE gel, all three proteins migrated as monomers and other slowly migrating oligomers (Fig. 10). *In vitro* transcription and translation experiment of CeHRG-1, hHRG1 and CeHRG-4 conducted by Caitlin Hall (Hamza lab), revealed a single band on the SDS-PAGE corresponding to the monomer for each of the three proteins suggesting that the oligomerization did not occur in solution either due to overexpression of these proteins or after cell lysis (Fig. 10) [127]. To examine the intracellular localization of these proteins, we performed confocal microscopy studies with cells expressing fluorescently tagged proteins. These studies revealed that HRG-4 was on the periphery of the cells and it localized with the plasma membrane marker wheat germ agglutinin conjugated with Alexa Fluor 633. CeHRG-1 and hHRG1 were primarily distributed in an intracellular compartment throughout the cytoplasm, with the remaining approximately 10% of the total fluorescence on the cell surface (Fig. 11a). CeHRG-1 and hHRG1 colocalized to the same intracellular regions in cells. Studies with organelle markers localized these proteins with LAMP1 (a 120kD lysosomal membrane glycoprotein) and to a lesser extent with Rab 7 (a Rab GTPase involved in transport of proteins from early endosomes to late endosomes) and Rab11 (a Rab GTPase involved in the export of membrane proteins from the golgi through the endosomes and apical and basolateral endocytic recycling) (Fig. 11b) [161, 162]. Because the worm and human HRG-1 proteins localize to a low pH, endo-lysosomal compartment, we conducted heme-binding studies at pH 6.0 and 8.5. Heme-binding to CeHRG-1 and hHRG1 was greatly increased at the lower pH range (See Appendix

B). CeHRG-4, however, bound heme across a broader pH range. These findings are consistent with the intracellular localization of the HRG-1 proteins. Worm and human HRG-1 co-localize to an acidic endo-lysosomal compartment and, therefore, it makes physiological sense that binding of HRG-1 to heme was significantly improved by lowering the pH, as compared to CeHRG-4 which localizes to the plasma membrane and binds heme over a broader pH range.

To investigate whether HRG-1 proteins are heme transporters, we cloned *Cehrg-1*, *Cehrg-4* and *hHRG1* into pT7Ts plasmid for expression in *Xenopus laevis* oocytes. These constructs were sent to Dr. M. Matthew to conduct electrophysiological studies in *Xenopus* oocytes. Oocytes were injected with cRNA for all three constructs and currents were monitored under a two-electrode voltage clamp at pH 7.5. Significant heme-induced inward currents were observed only in the presence of 20 μM hemin for oocytes injected with cRNA for CeHRG-1, hHRG1 and CeHRG-4 but none in control oocytes that were injected with the human potassium channel (hKv1.1). These results are indicative of heme-dependent transport across membranes, (See Appendix C) [127].

Figure 8. Expression of human *HRG1*

a) mRNA expression of human *HRG1* in multiple adult human tissues (PBL, peripheral blood leukocytes) **b)** mRNA expression of human *HRG1* in tissue-derived cell lines. The blots were stripped and reprobed with β-actin as loading control. Relative *hHRG1* mRNA levels by RNA blots of human tissues **(c)** and cell lines **(d)** quantified by ImageQuant v 2.2. *hHRG1* mRNA was normalized to the loading control β-actin.

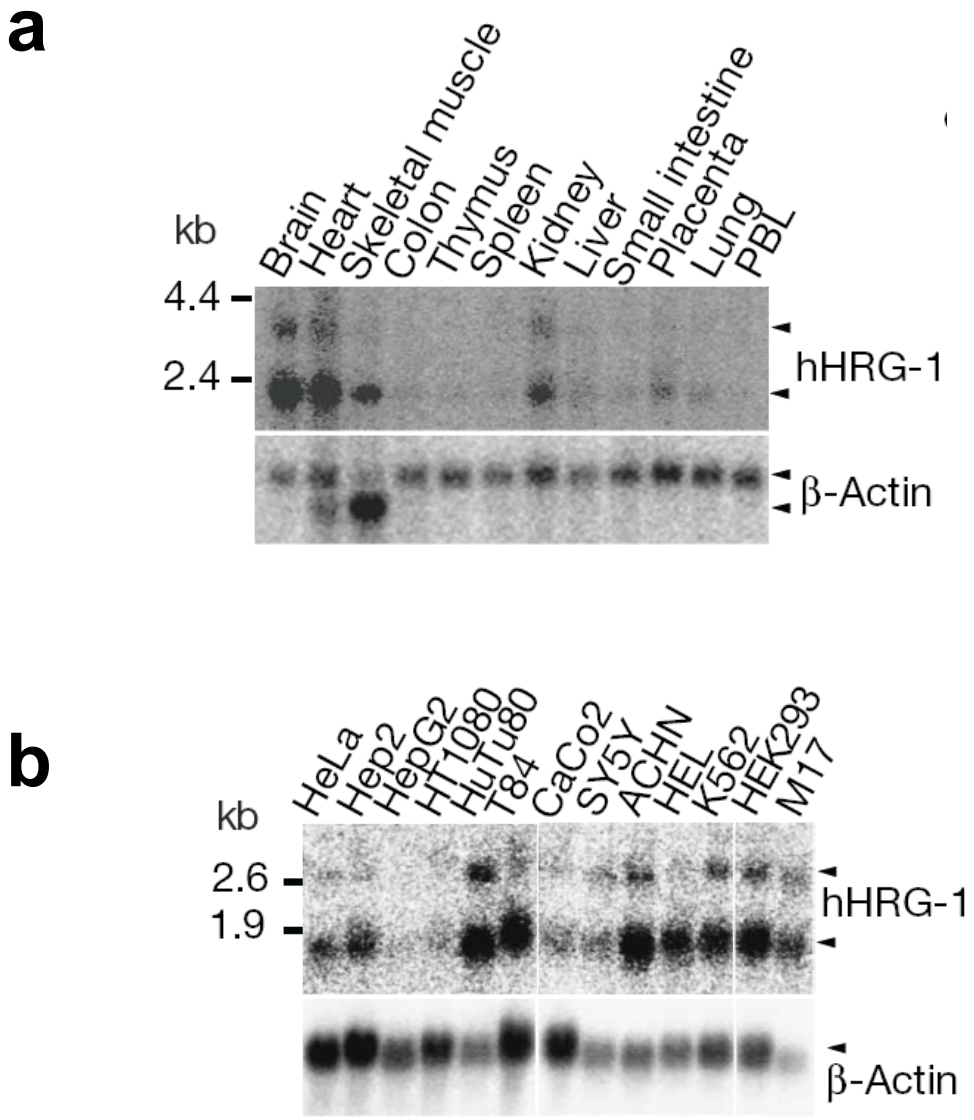
a
kb
Brain
Heart
Skeletal muscle
Colon
Thymus
Spleen
Kidney
Liver
Small intestine
Placenta
Lung
PBL
4.4
2.4
hHRG-1
β-Actin
b
kb
HeLa
Hep2
HepG2
HT1080
HuTu80
T84
CaCo2
SY5Y
ACHN
HEL
K562
HEK293
M17
2.6
1.9
hHRG-1
β-Actin
c
hHRG-1 mRNA
hHRG-1 / β-actin
Brain
Heart
Sk. muscle
Colon
Thymus
Spleen
Kidney
Liver
Sm. intestine
Placenta
Lung
PBL
Human Tissue
d
hHRG-1 mRNA
hHRG-1 / β-actin
HeLa
HEp-2
Hep G2
HT-1080
HuTu 80
T84
Caco-2
SH-SY5Y
ACHN
HEL
K562
HEK293
M17

Figure 9. Expression pattern of *HRG-1* in cultured cells.

a) *hHRG1* mRNA levels were unaltered by heme or iron depletion in cultured HEK293 cell lines. Cells were either grown in basal growth medium or in the presence of heme-depleted medium (HD), 500 μM succinyl acetone (SA) to inhibit heme synthesis, and 100 μM desferroxamine (DFO) to chelate iron. After 14 h of heme/iron depletion, cells were exposed to either 50 μM heme or 100 μM iron-SIH for 3 h. Total RNA was extracted from cells and processed for qRT-PCR using primers designed to amplify cDNA for *hHRG1*, heme oxygenase (*HMOX1*) and the transferrin receptor (*TfR1*). Gene-specific fold induction was quantified by normalizing to *GAPDH* as the loading control. (***, $P < 0.001$ and *, $P < 0.05$ between basal conditions and the indicated treatment). Mean values were calculated and differences were compared by using the Student–Newman–Keuls multiple comparison test and one-way ANOVA. **b)** *mHrg-1* mRNA is not induced during erythroid maturation in cultured mouse erythroleukemia (MEL) cells. MEL cells (DS19 clones) were induced with 1.5 % DMSO (v/v) which results in appearance of *o*-dianisidine positive cells, a marker of hemoglobinization. *mHrg-1* mRNA was unaltered in MEL cells 72 h post differentiation compared with *α-globin* (*Hba-a1*), *β-globin* (*Hbb-b1*), and *Alas-2* mRNA. **c)** Time-dependence of mRNA expression as a function of erythroid maturation in MEL cells. *mHrg-1* expression does not vary during MEL cell differentiation. Total RNA obtained from MEL cells harvested at the specific time points after induction with DMSO were quantified for *Hrg-1* mRNA expression using qRT-PCR and normalized to *Gapdh* as the loading control. Each data point represents the mean ± SEM and the results are representative of two separate experiments.

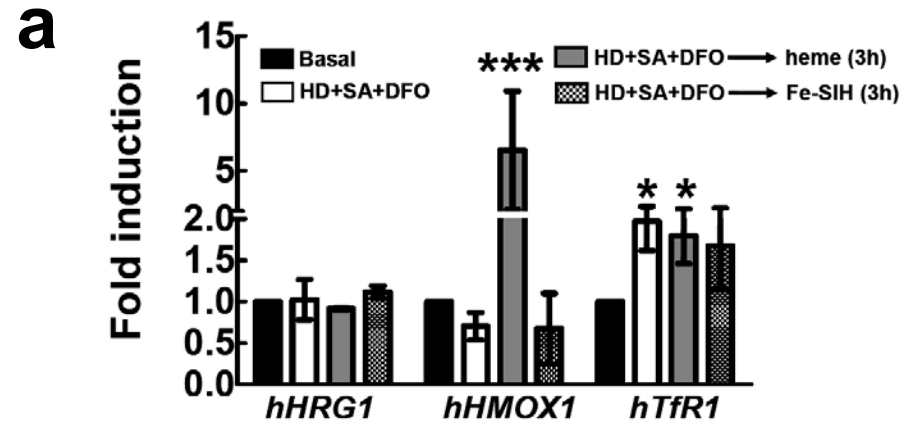
a
Fold induction
15
10
5
2.0
1.5
1.0
0.5
0.0
Basal
HD+SA+DFO
***
HD+SA+DFO → heme (3h)
HD+SA+DFO → Fe-SIH (3h)
*
*
hHRG1
hHMOX1
hTfR1

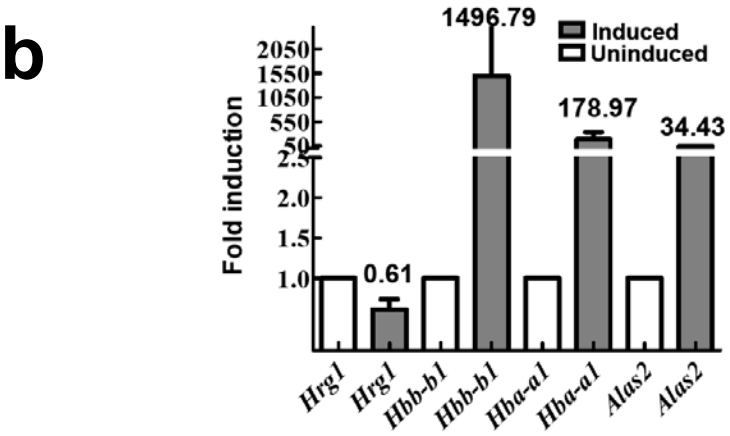
b
Fold induction
1496.79
Induced
Uninduced
178.97
34.43
2050
1550
1050
550
50
2.5
2.0
1.5
1.0
0.61
Hrg1
Hrg1
Hbb-b1
Hbb-b1
Hba-a1
Hba-a1
Alas2
Alas2

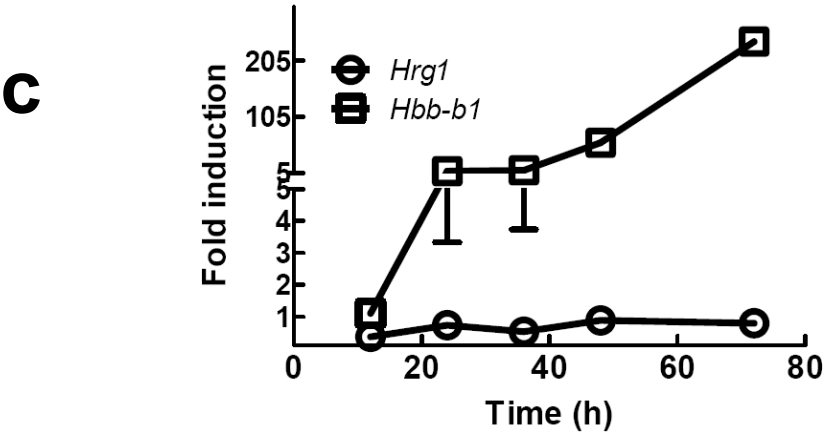
c
Fold induction
205
105
5
4
3
2
1
Hrg1
Hbb-b1
0
20
40
60
80
Time (h)

Figure 10. Expression of HRG-1 proteins in HEK 293 cells

Cell lysates from HEK 293 cells transfected with C-terminally tagged *CeHRG-1*, *hHRG1* and *CeHRG-4* were resolved by SDS-PAGE, and the proteins were detected by immunoblotting with antibodies against HA (lanes 1-3, 50 μg) and GFP (lanes 4-6, 25 μg) or by ^{35}S fluorography using an *in vitro* cell-free wheat germ expression system (lanes 7-9, 1/5th of total extract).

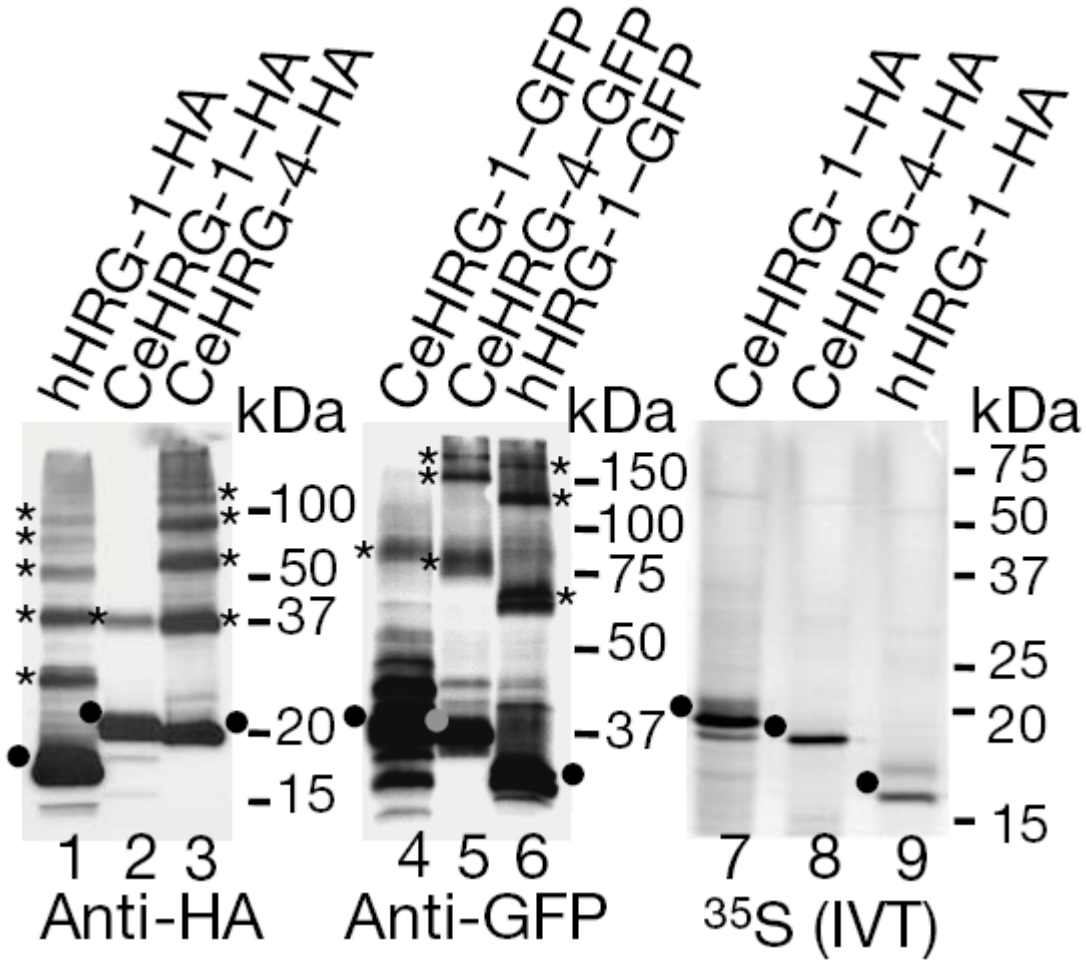
hHRG-1–HA
CeHRG-1–HA
CeHRG-4–HA
CeHRG-1–GFP
CeHRG-4–GFP
hHRG-1–GFP
CeHRG-1–HA
CeHRG-4–HA
hHRG-1–HA
kDa
kDa
kDa
100
50
37
20
15
150
100
75
50
37
75
50
37
25
20
15
1 2 3
4 5 6
7 8 9
Anti-HA
Anti-GFP
35S (IVT)

Figure 11. Localization of HRG-1 proteins in HEK 293 cells

a) Cellular localization of C-terminally tagged fluorescent proteins in transfected HEK 293 cells by confocal microscopy. The plasma membrane (PM) was identified using wheat germ agglutinin. **b)** Localization of CeHRG-1 with organelle markers as described in the text. (Scale bar = 20 μM)

a

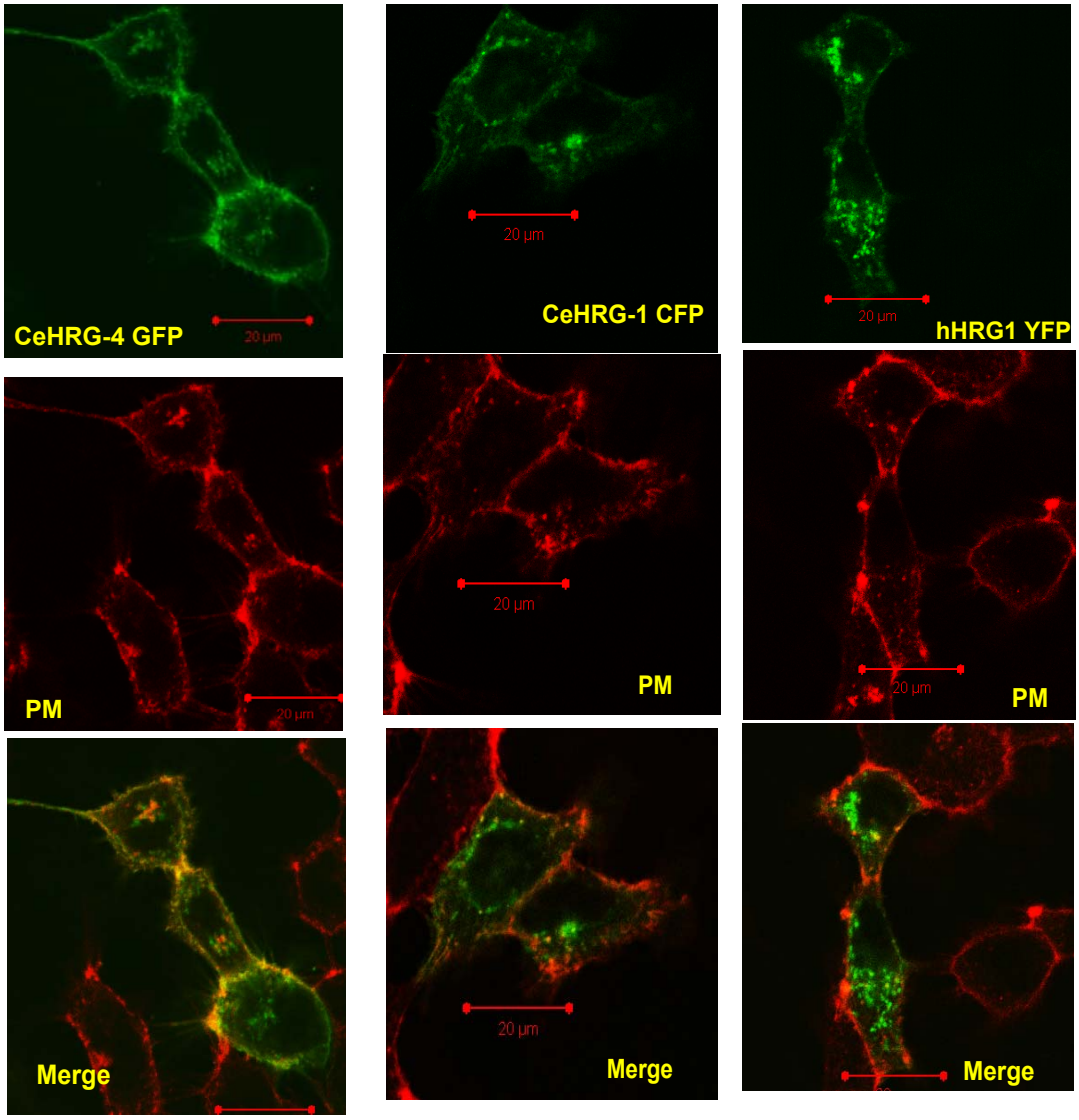
CeHRG-4 GFP
20 µm
CeHRG-1 CFP
20 µm
hHRG1 YFP
20 µm
PM
20 µm
PM
20 µm
PM
20 µm
PM
Merge
20 µm
Merge
Merge

b

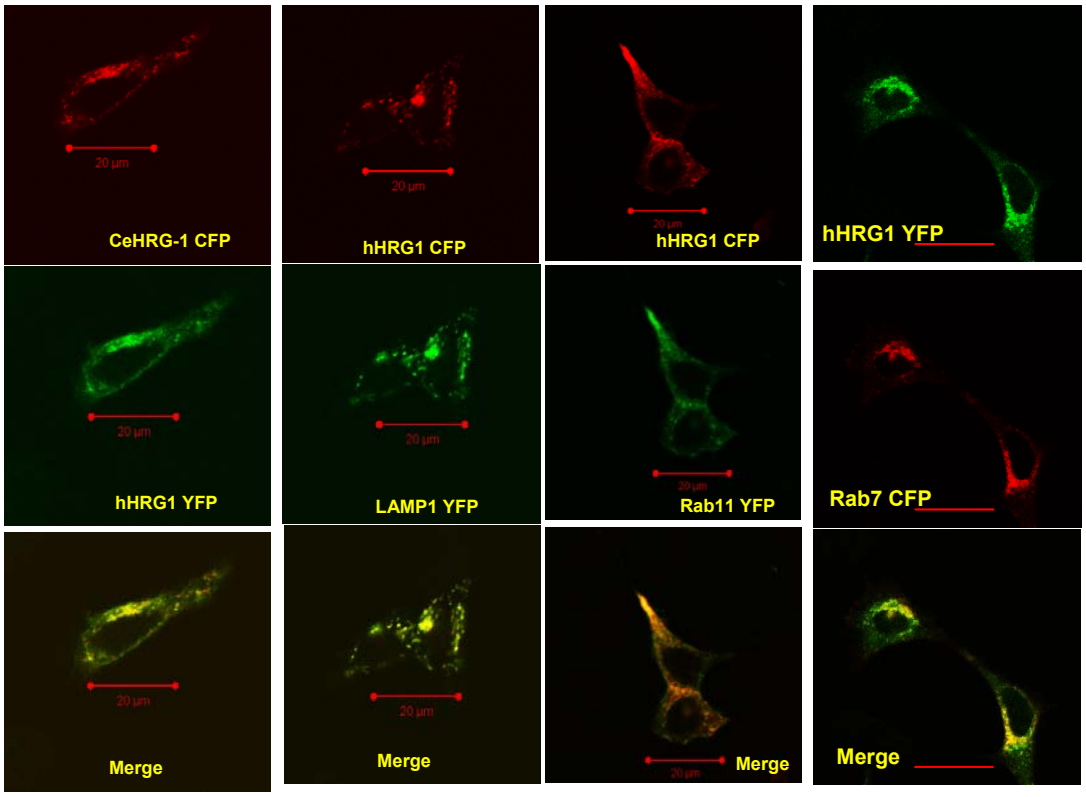
CeHRG-1 CFP
hHRG1 CFP
hHRG1 CFP
hHRG1 YFP
hHRG1 YFP
LAMP1 YFP
Rab11 YFP
Rab7 CFP
Merge
Merge
Merge
Merge

Discussion

Our results show that HRG-1 and HRG-4 are involved in mediating heme homeostasis in *C. elegans*, an organism that relies on exogenous heme for its growth and development [93]. Using cell biological and biochemical approaches in *C. elegans* and zebrafish, we have identified and established HRG-1 as a conserved protein with an important role in heme metabolism. Studies in zebrafish reveal that HRG-1 is important for the maintenance of hematopoietic cells and for specification of the central nervous system during embryonic development. The mild anemia exhibited by MO1 morphants suggests that lowering of HRG-1 levels in tissues such as developing erythrocytes that have a greater requirement of heme, results in a tissue-specific phenotype and, therefore, can be useful in understanding the role of HRG-1 in hematopoiesis. The complete phenotypic rescue of zebrafish MO2 morphants by worm HRG-1 shows that these proteins are functional orthologs with conserved roles in heme homeostasis.

We hypothesize, that because *C. elegans* relies solely on exogenous heme, there might be compensatory mechanisms to maintain heme homeostasis. This is a physiologically reasonable argument because, unlike knock-down of HRG-1 in zebrafish that results in severe phenotypes, depletion of *hrg-1* or *hrg-4* by RNA-mediated interference in worms does not result in any obvious effect on growth and development. The worm genome encodes for four paralogs (*hrg-1*, *-4*, *-5* and *-6*) that might play overlapping roles since these proteins have conserved amino acids and similar putative membrane topology. Further studies need to be done to examine whether HRG-1 paralogs play functionally conserved roles in heme metabolism.

The amino acid sequence and the predicted topology of these proteins provide clues as to how HRG-1 proteins function in heme homeostasis. While HRG-1 has tyrosine-based and acidic-dileucine based motifs that have been shown to be involved in the sorting of membrane proteins to endosomes and lysosome-related organelles, HRG-4 lacks these residues [152]. Interestingly, HRG-1 has a histidine residue at position 90 in the second transmembrane domain, and this histidine is replaced by a tyrosine in HRG-4. Since HRG-4 localizes to the plasma membrane it is more likely to encounter heme in an oxidized form. It has been shown that replacing the histidine residue with a tyrosine heme-binding ligand in proteins mitigates the reactivity of heme, possibly due to the ability of Tyr to stabilize oxidized forms of heme [163]. It is reasonable to speculate that the Tyr and His residues in TMD2 of HRG-4 and HRG-1, respectively, are important determinants of the function of these proteins.

Moreover, HRG-1 proteins share some of the features found in tetraspanins including polar residues within the transmembrane domains and cysteines within TMDs that serve as membrane-proximal palmitoylation sites [164]. Tetraspanins have been shown to organize laterally in tetraspanin-enriched microdomains (TEM). A biochemical feature of the TEM is that the tetraspanin proteins and their partners tend to remain associated under non-stringent detergent conditions [164]. Cholesterol has also been shown to associate physically and functionally with TEMs. This is particularly interesting because HRG-1 proteins migrate as oligomers on an SDS-PAGE gel under non-heat denatured conditions and it is possible that these oligomers are, in fact, heterodimers of HRG-1 and other interacting proteins. It will

be interesting to test the effects of cholesterol-depletion and the putative palmitoylation-site mutations on the localization, oligomerization and function of HRG-1 proteins.

Based on the RNAi phenotypes, sub-cellular localization, biochemical assays, and amino acid sequence analysis of the HRG-1 proteins, we propose that HRG-4 mediates heme uptake from the plasma membrane in *C. elegans* and HRG-1 modulates intracellular heme availability through a vesicular compartment (Fig. 12). Our model is physiologically reasonable because heme-limiting conditions would induce uptake and sequestration of the essential but toxic molecule through the coordinated functions of HRG-1 and HRG-4. Although HRG-4 appears to be specific to worms, the zebrafish studies demonstrate that regulation of heme homeostasis by HRG-1 is conserved in animals that synthesize heme. Since reduced levels of HRG-1 in MO1 morphants results in anemia, we speculate that hypomorphic alleles of *hrg-1* on human chromosome 12q13 might be an important determinant in congenital types of anemias.

The discovery of *hrg-1* and *hrg-4* as heme transporters provides molecular insights into eukaryotic heme homeostasis. Further studies need to be done in order to fully understand how organisms delicately balance intracellular levels of heme-an essential but toxic macrocycle.

Figure 12. Proposed model of heme homeostasis in *C. elegans*

Expression of *hrg-1* and *hrg-4* is upregulated under heme-limiting conditions. HRG-4 is localized on the plasma membrane and HRG-1 is found in an intracellular endo-lysosomal compartment. The expression *hrg-1* and *hrg-4* is down regulated at high heme, possibly preventing uptake of the toxic macrocycle, heme, under heme-replete conditions.

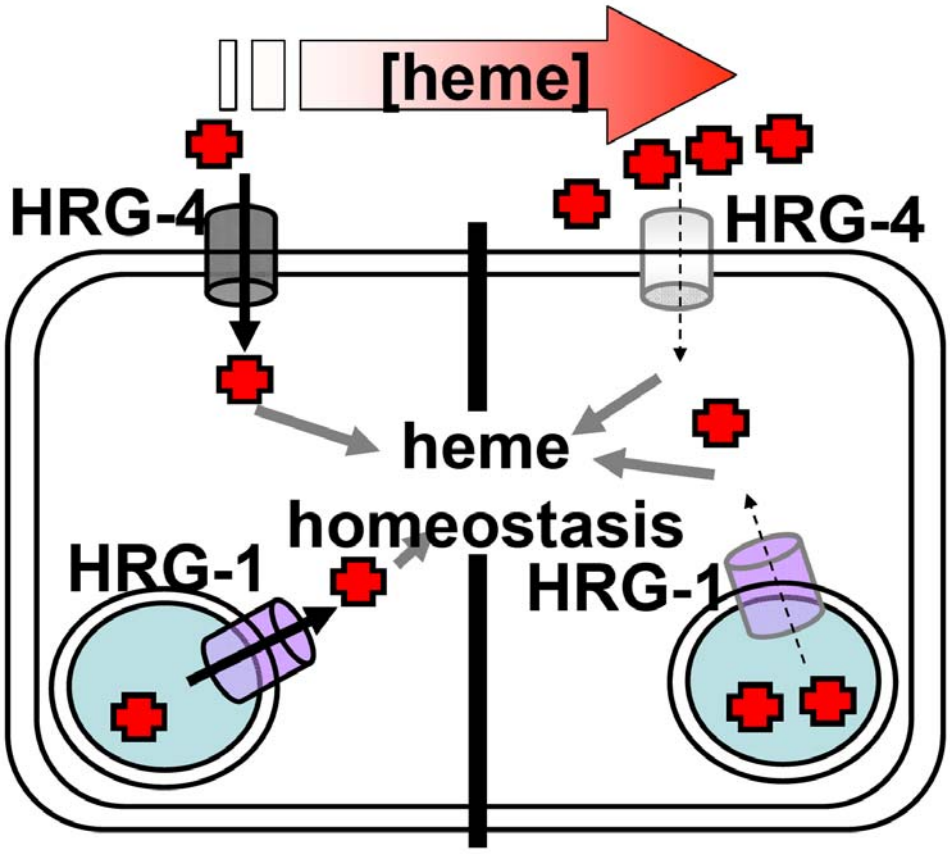
[heme]
HRG-4
HRG-4
heme
homeostasis
HRG-1
HRG-1

Chapter 5 Characterization of the role of HRG-1 proteins in worms

Summary

We have previously demonstrated that HRG-1 and its worm-specific paralog HRG-4 are heme transporters in worms [127]. Here we show that, in worms, HRG-1 and HRG-4 are expressed in worm intestinal cells albeit with different localization patterns. HRG-4 localizes to the plasma membrane of polarized intestinal cells, while HRG-1 localizes to an intracellular compartment with the fluorescent heme analog ZnMP. To better understand *hrg-1* and *hrg-4* functions, we characterize the deletion mutants of *hrg-1* and *hrg-4*. While the Δ*hrg-1* (*tm3199*) strain is a null mutant, we found that Δ*hrg-4* (*tm2994*) is not a null strain. The Δ*hrg-1* worms have decreased ZnMP fluorescence in their gut and increased resistance to GaPPIX, whereas the Δ*hrg-4* animals show increased ZnMP fluorescence uptake and sensitivity to GaPPIX. These findings are diametrically opposite to the previous observations made by depleting *hrg-1* and *hrg-4* using RNA-mediated interference. Nearly 80% of the Δ*hrg-1* animals exhibit defects in embryogenesis concomitant with a decrease in brood size. We observe a similar decrease in brood size in the Δ*hrg-1* brood mate control animals. In contrast, the Δ*hrg-4* worms appear normal. We speculate that the deletion strains may have developed mechanisms to compensate for the lack of *hrg-1* and *hrg-4*. Results from qRT-PCR analysis reveal aberrant gene expression profiles

of the *hrg-4* paralogs, *hrg-5* and *hrg-6*, in the homozygous deletion animals and their brood mate controls. Since these findings are preliminary, further characterization is needed to determine how useful these deletion strains will be in delineating the *in vivo* function of *hrg-1* and *hrg-4* in heme metabolism.

Results

We have demonstrated that HRG-1 proteins (CeHRG-1 and CeHRG-4) are heme transporters and have a conserved role in regulating heme homeostasis. To elucidate the function of these proteins *in vivo*, we synthesized *Cehrg-1* and *Cehrg-4* transcriptional constructs by fusing the ~3 kb promoter region of these genes with GFP containing a nuclear localization signal and an *unc-54* 3'UTR. We generated transgenic worms stably expressing the transcriptional constructs by injection followed by gamma irradiation (*Cehrg-1)* or by biolistics (*Cehrg-4)*. Analysis of these transgenic worms revealed that both *Cehrg-1* and *Cehrg-4* are expressed specifically in the intestinal cells (Chapter 4, Fig. 5)

While the transcriptional fusion reporters are useful for studying the spatial expression patterns of these genes, they do not provide any information on the *in vivo* localization of the proteins. In order to make translational reporter constructs, we first confirmed the predicted exon-intron boundaries and the 5' and 3' untranslated regions of both *Cehrg-1* and *Cehrg-4*. Using the 5' RACE reaction, we identified 3 different transcripts including one SL1 transcript, for *Cehrg-1*. The 5' RACE reaction for *hrg-4* was performed at least four times but we were not successful in identifying the transcriptional start site. We therefore used a PCR based approach using the *hrg-4*

primer with SL1 or SL2 primers and found a SL1 transcript for *Cehrg-4*, which was about ~ 777 bp in length (Fig. 1). The 3'-UTRs identified using 3' RACE reactions were ~190 bp and ~60 bp for *Cehrg-1* and *Cehrg-4*, respectively.

To construct a translational fusion, we used the Gateway technology using Multisite recombination (Invitrogen). The 3 kb promoter region of the *hrg-1*, *Cehrg-1* genomic region (exons and introns) and the gene for GFP (from the Fire vector kit plasmid pPD95.75) fused to the 3' *unc-54* UTR were cloned into three separate plasmids by recombination. All three entry plasmids were assembled by multisite recombination. The process was repeated for *Cehrg-4,* but, instead of GFP and *unc-*54 3' UTR, we used the gene for YFP fused with *hrg-4* 3' UTR. These plasmids were bombarded into *unc-119* strain along with the *unc-119* rescue plasmid to generate three stably expressed lines for *hrg-1* and two stably expressed lines for *hrg-4*. Analysis of the transgenic lines stably expressing the HRG-1 and HRG-4 constructs using Zeiss 510 confocal microscope revealed that both proteins were found in the intestinal cells. These results are consistent with the expression pattern for *hrg-1* and *hrg-4* in the transgenic worms (IQ6011 and IQ6041) stably expressing the transcriptional reporter constructs for these genes. Although both proteins were expressed in the intestinal cells, HRG-1 localized to an intracellular compartment while HRG-4 was expressed on the lumenal surface (Figs. 2 and 3). To further delineate the difference in localization, the transgenic worms were incubated for 16 hours in axenic mCeHR-2 medium containing 2 μM heme and 10 μM ZnMP, the fluorescent heme analog. ZnMP localized within the vesicles that were expressing

HRG-1::GFP and there was no colocalization of ZnMP with HRG-4::YFP (Fig. 2 and 3).

The transcriptional and translational reporter constructs revealed the spatial expression patterns of *hrg-1* and *hrg-4*, but to understand the *in vivo* functions of the HRG-1 proteins, we obtained deletion alleles *tm3199* (Δ*hrg-1*) and *tm2994* (Δ*hrg-4*) from the National Bioresource Project (Japan). As shown in Figure 4, Δ*hrg-1* (*tm3199*) has a 341 bp deletion in *hrg-1* that removed exon 1 (including ~ 60 bp of the *hrg-1* promoter upstream of the ATG start codon), intron 1 and a portion of exon 2. The Δ*hrg-4* (*tm2994*) is missing 202 bp from intron 1, exon 2 and intron 2 (Fig. 4a). Both the Δ*hrg-1* and Δ*hrg-4* strains were backcrossed eight times with the wild type N2 strain to generate homozygous deletion strains (Δ*hrg-4*, IQ6910; Δ*hrg-1*, IQ6912). Because deletion strains may have multiple deletions that can be difficult to outcross, we used brood mates that were wild-type for *hrg-1* and *hrg-4* as the "wild-type" controls (IQ6909 and IQ6911). To confirm the presence of the deletion, we isolated the genomic DNA and total RNA from these worms for PCR analysis. Using the primers that were designed around the deleted regions in *hrg-1* and *hrg-4*, we performed PCR analysis followed by agarose gel electrophoresis. PCR analysis of the genomic DNA obtained from the Δ*hrg-1*and Δ*hrg-4* showed a 341 bp and 202 bp deletion in *hrg-1* and *hrg-4* respectively (Fig. 4b). To determine if either of these strains were null mutants, we synthesized cDNA using total RNA isolated from the two strains. Using PCR, we observed a very faint product ~ 650 bp in the Δ*hrg-1* strain and ~450 bp product in the Δ*hrg-4* strain. Since the product in the Δ*hrg-1* strain was barely visible after 40 cycles of amplification using PCR, it is highly likely that

Δ*hrg-1* (*tm3199*) is a null mutant. But our results from the PCR analysis of *hrg*-4 using total RNA isolated from the Δ*hrg-4* strain suggests that Δ*hrg-4* (*tm2994*) is not a null strain (Fig. 4c). The predicted amino acid sequence for HRG-4 in the Δ*hrg-4* mutant animals is shown in Fig. 4d. If the mRNA is translated, then a truncated HRG-4 protein with the first two transmembrane domains will be synthesized in the Δ*hrg-4* animals.

We have previously shown that depletion of *hrg-1* and *hrg-4* by RNAi in worms resulted in aberrant heme homeostasis [127]. To test if the *hrg-1* and *hrg-4* deletion strains phenocopy the RNAi results, we used heme analogs, ZnMP and GaPPIX. We found that the Δ*hrg-1* strain showed a decreased ZnMP fluorescence and the Δ*hrg-4* worms had increased ZnMP when compared to N2 or the wild-type brood mates (Fig. 5). When these worms were fed the toxic heme analog, GaPPIX, we found that Δ*hrg-4* animals (IQ6910) were more sensitive than the brood mate control worms (IQ6909). The Δ*hrg-4* worms laid fewer progeny than IQ6909 worms at 1 μM GaPPIX (Fig. 6). By contrast, Δ*hrg-1* worms (IQ6912) showed resistance to GaPPIX in that these animals laid more progeny than the brood mate controls (IQ6911). While our results suggest that there is dysregulation of heme homeostasis in deletion strains, these findings are not consistent with the phenotypes that were observed for the knock-down of *hrg-1* and *hrg-4* by RNA- mediated interference in either N2 or IQ6011 heme-sensor strain.

Figure 1. Genomic structure of *hrg-1* and *hrg-4*

(a) RACE PCR analysis of *Cehrg-1* revealed (1) a SL1 transpliced transcript ~ 900 bp, (2) ~ 2890 bp transcript (3) ~8 kb transcript. All three transcripts had a ~ 190 bp 3' UTR**. (b)** *Cehrg-4* has one transcript, a SL1 spliced transcript that was determined to be 777 bp long by PCR analysis. 3' RACE PCR was used to determine that *Cehrg-4* has a 3' UTR of ~ 60 bp. Exons are indicated by open boxes and introns are indicated by lines. 3' UTRs are represented as gray block arrows.

a *Cehrg-1*

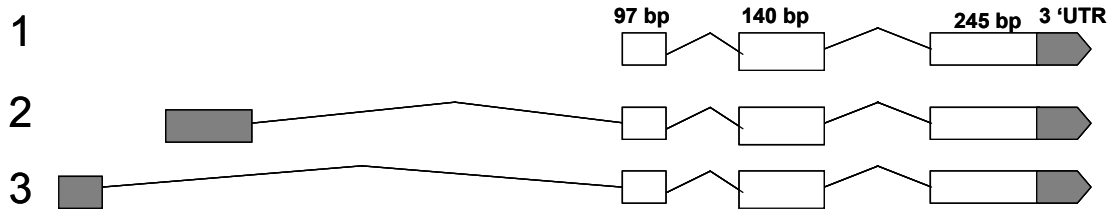

b *Cehrg-4*

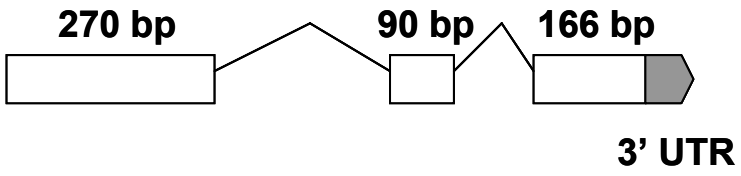

Figure 2. HRG-1 localizes to vesicular compartments in the intestine.

(a) Schematic representation of the *hrg-1::gfp* translational construct. **(b)** In the transgenic worms (IQ6111) stably expressing the HRG-1::GFP translational fusion construct, fluorescent heme analog ZnMP (red) and HRG-1::GFP (green) localize to a vesicular compartment in intestinal cells. **(c)** For clarity, the boxed region in the merge image has been enlarged. Images were obtained with a Zeiss 510 confocal microscope. (Scale Bar = 10 μm)

a

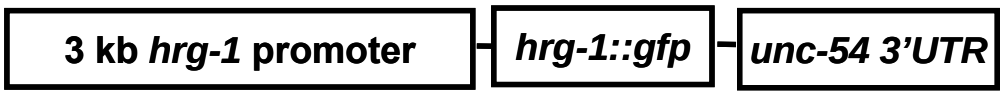
3 kb hrg-1 promoter
hrg-1::gfp
unc-54 3'UTR

b

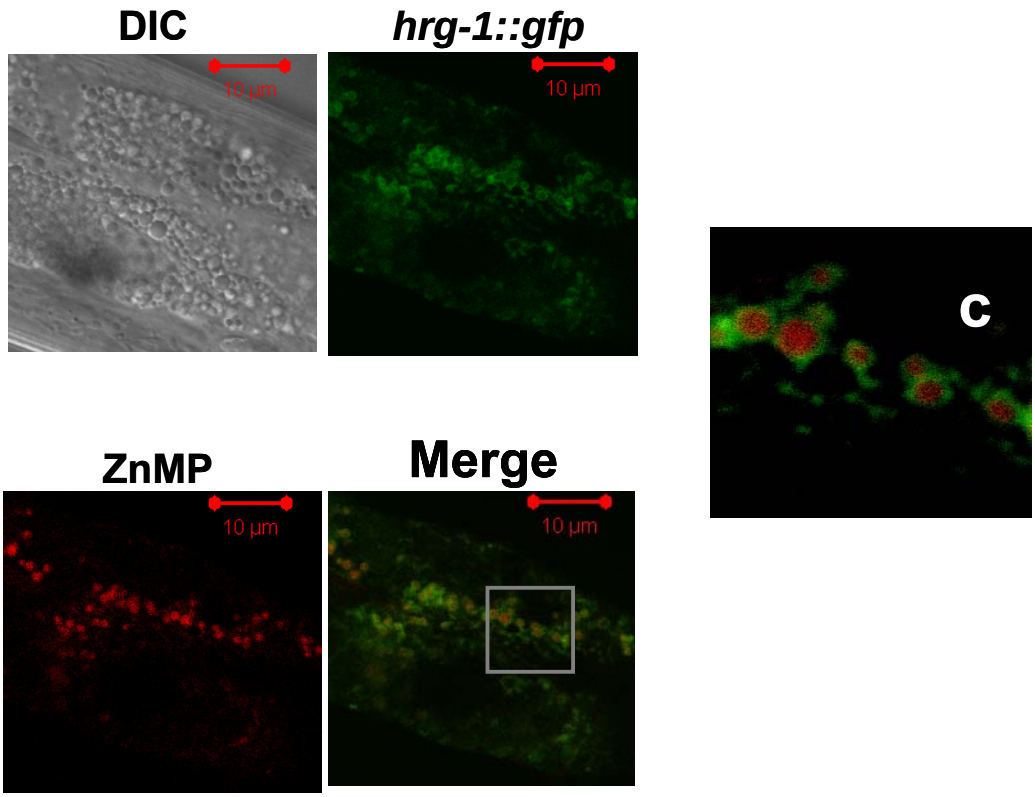
DIC
hrg-1::gfp
ZnMP
Merge
10 µm
c

Figure 3. HRG-4 localizes to the intestinal lumenal surface.

(a) Schematic representation of the *hrg-4::gfp* translational construct. **(b)** In the transgenic worms (IQ6141) stably expressing the HRG-4::YFP translational fusion construct, fluorescent heme analog ZnMP (red) localizes to a vesicular compartment in intestinal cells while HRG-4::YFP (green) localizes to the lumenal surface of the intestinal. **(c)** For clarity, the boxed region in the merge image has been enlarged to show that ZnMP and HRG-4::YFP are found in different regions of the intestine. Images were obtained with a Zeiss 510 confocal microscope. (Scale Bar = 10 μm)

a

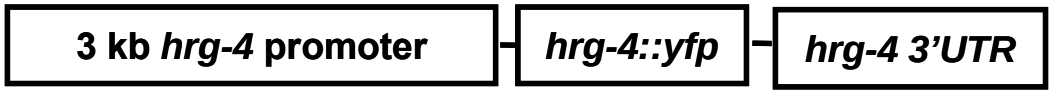
3 kb *hrg-4* promoter
hrg-4::yfp
hrg-4 3'UTR

b

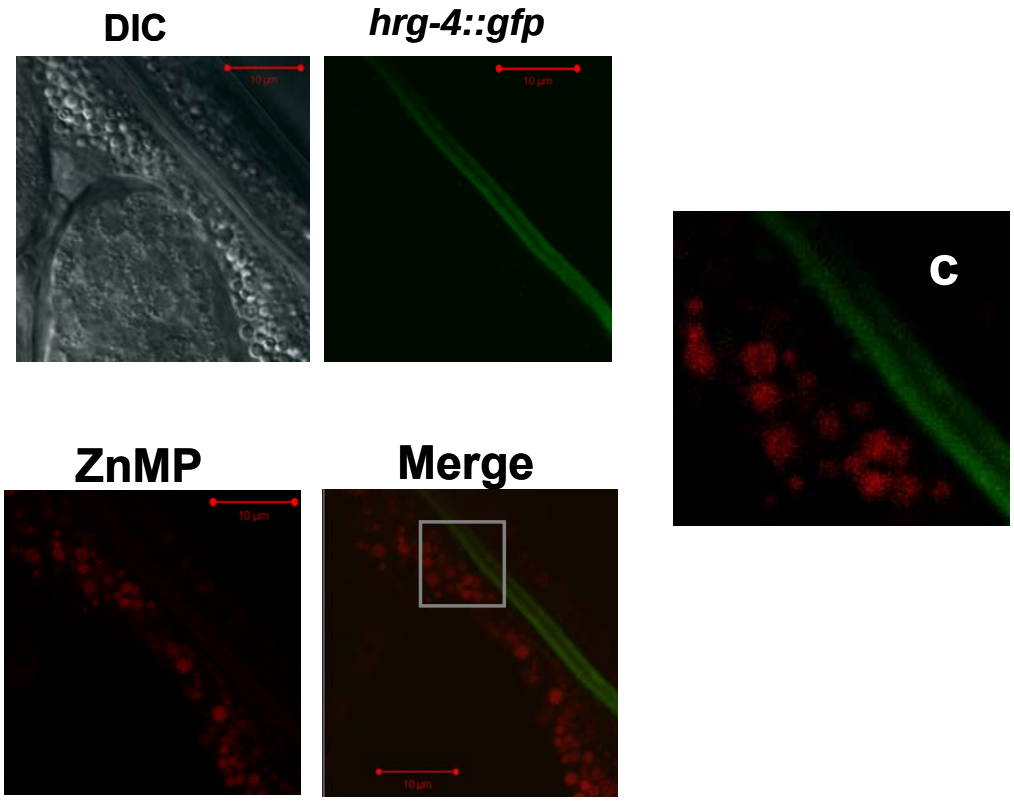
DIC
hrg-4::gfp
ZnMP
Merge
c

Figure 4. Analysis of the Δ*hrg-1* (*tm3199*) and Δ*hrg-4* (*tm2994*) deletion strains.

(a) Schematic representation of *tm3199* and *tm2994*. Open boxes represent exons and lines indicate introns. The size of each exon and intron is indicated. The deletion region is also represented. The red arrows represent the primers that were used to screen for homozygous deletion animals. **(b)** PCR analysis of genomic DNA obtained from wild-type N2 worms (lanes 2 and 4) and homozygous mutants. *hr*g-*1* specific primers were used in lanes 2 and 3; *hrg-4* primers were used for lanes 4 and 5. **(c)** PCR screening of cDNA synthesized from total RNA isolated from wild-type N2 worms and homozygous mutants. The *hrg-1* primers were used for lanes 2 and 3; *hrg-4* primers were used for lanes 4 and 5. **(d)** DNA sequence for *tm2994* along with predicted amino acid sequence of the RT-PCR product. The boxed region indicates the new sequences that are added.

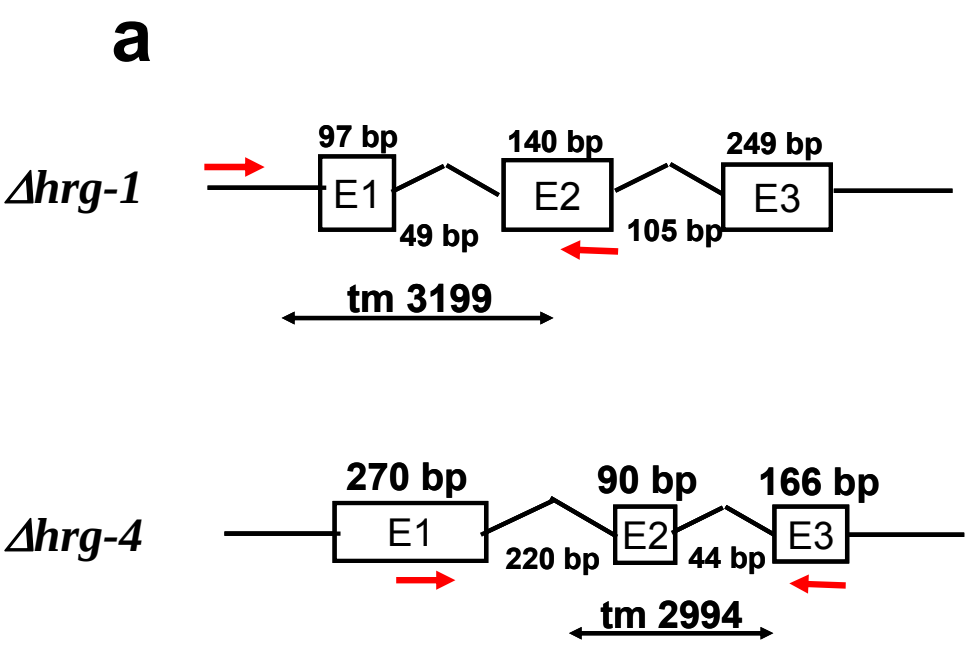
a
Δhrg-1
97 bp
140 bp
249 bp
E1
E2
E3
49 bp
105 bp
tm 3199
Δhrg-4
270 bp
90 bp
166 bp
E1
E2
E3
220 bp
44 bp
tm 2994

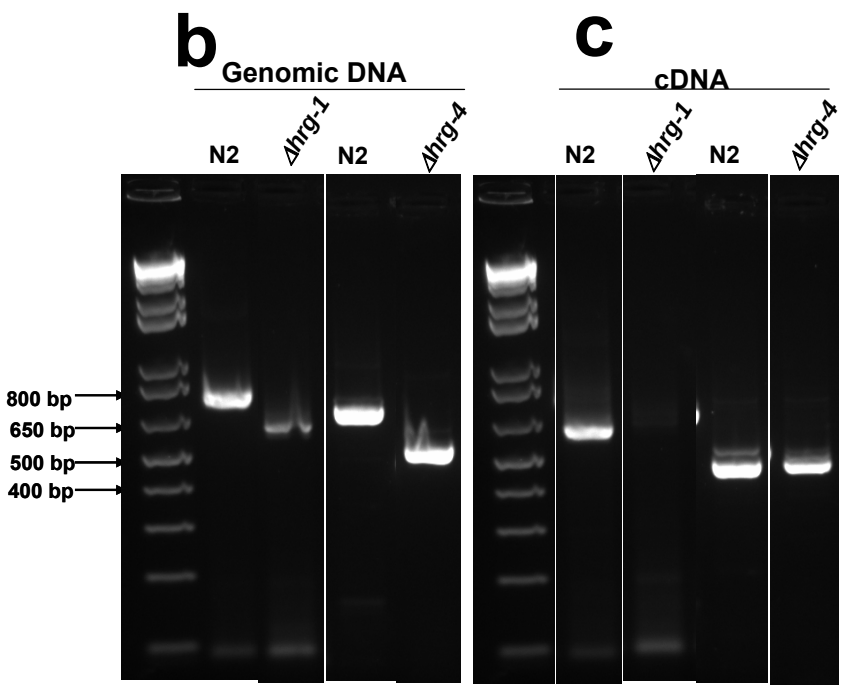
b
Genomic DNA
c
cDNA
N2
Δhrg-1
N2
Δhrg-4
N2
Δhrg-1
N2
Δhrg-4
800 bp
650 bp
500 bp
400 bp

d

```
M  T  A  E  N  R  G  F  C  Q  L  I  C  H  I  N  V
ATGACTGCTGAAAATCGAGGATTCTGTCAACTGATTTGTCATATAAACGTC

R  I  G  W  T  I  F  G  I  V  F  G  I  S  A  I  L
GAATTGGATGGACAATATTTGGAATTGTTTTTGGAATATCTGCAATTTTTA

T  Y  A  I  K  F  H  N  W  S  A  T  A  T  T  A  I
ACATATGCAATCAAATTTCATAATTGGTCAGCCACAGCAACAACTGCTATT

A  T  L  F  A  C  E  T  L  Y  L  Y  W  A  L  K  K
GCTACACTTTTTGCGTGTGAAACATTGTATTTGTATTGGGCTTTGAAGAAA

N  T  I  V  N  W  K  S  S  T  F  Q  L  M  I  W  P
AATACAATTGTTAACTGGAAGAGTAGTACTTTTCAGTTGATGATATGGCCA

S  E  Y  S  N  S  *  *  I  T  C  I  N  *  *  S  R
AGTGAGTACTCTAATAGTTGATAAATTACATGCATCAATTGATAATCAAGA

F  C  V  H  N  L  N  S  N  *  L  Q  F  G  F  R  *
TTTTGCGTACACAATCTGAATTCTAATTGATTGCAATTTGGCTTAAGATGA

F  F  N  N  N  C  R  M  G  H  R  L  L  Y  A  I  F
TTTTTTAATAACAACTGTAGAATGGGACATAGATTGCTTTATGCAATTTTT

F  *  M  E  R  I  F  G  L  L  D  H  G  V  L  *  S
TTTTGAATGGAGAGAATCTTTGGTTTACTGGATCATGGAGTCTTGTGATCA

L  N  G  L  G  K  M  H  S  L  P  E  N  T  S  T  K
CTAAATGGACTTGGCAAAATGCATTCTTTGCCAGAAAATACCTCAACAAAA

L  E  Q  L  P  K  M  E  T  L  M  M  T  M  L  K  S
TTGGAACAGCTTCCGAAGATGGAGACATTGATGATGACGATGTTGAAGTCA

L  K  V
TTAAAAGTT AA
```

While RNAi of *hrg-1* and *hrg-4* in IQ6011 or N2 did not reveal any discernable developmental defects, we reasoned that since the deletion strains lack HRG-1 heme transporters, the deletion animals might exhibit growth and/or developmental defects. This is a reasonable argument because we have previously demonstrated that heme is essential for worm reproduction and development. Therefore, abolishing heme uptake and transport could have an effect on growth and development of worms. Using a Leica DMIRE2 epifluorescence/ DIC microscope, we analyzed the deletion worms for morphological defects. We found that only Δ*hrg-1* animals show embryonic defects. About 80% of these animals had defects including an inability to lay embryos, persistence of embryo-like structures and, in many cases, the animals would have only one or two 4-cell stage embryos (Fig. 7a and b).

We postulated that such embryonic defects in these animals might lead to lower fecundity and, therefore, conducted a brood size experiment to determine the total number of progeny. Ten individual worms were placed individually on NGM agar plates and were allowed to lay progeny for a period of 6 days. We counted the total number of progeny laid every two days. Although there was a decrease in the total number of progeny laid by Δ*hrg-1* animals, we found that the brood mate control animals also had a reduction in brood size (Fig. 8). Importantly, only ~20% of brood mate control animals exhibited embryonic defects similar to the Δ*hrg-1* worms (Fig. 7).

A possible explanation for the discrepancies observed in the phenotypes in deletion worms versus the depletion of *hrg-1* and *hrg-4* in N2 worms by RNAi is that there may be an adaptive response concomitant with a global change in the

expression profiles of genes involved in heme homeostasis in the *hrg-1* and *hrg-4* deletion strains. Sequence analysis of *hrg-4* had revealed two other paralogs in worms, *hrg-5* and *hrg-6*. Although *hrg-5* and *hrg-6* were not heme-responsive, we reasoned that these genes might be providing the compensatory mechanisms for heme uptake in the worms that lack *hrg-1* or *hrg-4*. Using RNA isolated from Δ*hrg-1*, Δ*hrg-4* and the wild-type brood mates, we performed qRT-PCR assay. There was a down regulation of *hrg-1*, *hrg-5*, or *hrg-6* in the Δ*hrg-4* worms, and a down regulation of the *hrg-6* mRNA levels Δ*hrg-1* strain (Fig. 9). This modest decrease in levels of *hrg-1*, *hrg-5* and *hrg-6* in the Δ*hrg-4* worms and the decrease in *hrg-6* levels in the Δ*hrg-1* worms do not explain why these worms have decreased ZnMP uptake and increased resistance to GaPPIX. Also, there is an increased expression of *hrg-6* in IQ6911 wild-type brood mate and an increase in the levels of all three *hrgs* in the case of IQ6909 (Fig. 9). This finding suggests that even after eight backcrosses there might still be other mutations in the background of these strains that are causing the differences between wild-type siblings and the wild-type N2 strain. It is also possible that the Δ*hrg-4* worms are upregulating some of the other heme-responsive genes that might be involved in heme uptake.

Discussion

From our heme microarray analysis, we have identified *Cehrg-1* and *hrg-4* as heme-responsive genes that were highly upregulated at lower heme conditions. Using various genetic, biochemical and cell biological approaches, we have characterized the HRG-1 and HRG-4 proteins as heme transporters. We have previously shown that

in mammalian cells HRG-4 localized to the plasma membrane and HRG-1 was found on endo-lysosomal compartments. In mammalian cells, HRG-1 co-localized with LAMP-1 and we found that HRG-1 bound heme under acidic pH. Using transgenic worms stably expressing HRG-1::GFP and HRG-4::YFP translational constructs, we showed that HRG-4 localized to the lumenal surface and HRG-1 was found on membranes of vesicles in the intestinal cells. These vesicular compartments might be the birefringent, autofluorescent intestinal organelles called gut granules [165]. The gut granules in worm intestine have been shown to be a lysosome-related organelle [166]. Several proteins including GLO-1, an intestine-specific Rab GTPase, VHA-11, a vacuolar-ATPase that has been shown to be involved in the acidification of cellular compartments, and LMP-1, the *C. elegans* homolog of mammalian lysosome-associated membrane protein or LAMP, have been shown to be associated with the granules [165-168]. Knock-down of gut granule associated proteins such as VHA-11 in the IQ6111 strain and analysis of the HRG-1::GFP localization might be important in determining the cellular components that are responsible for proper targeting of HRG-1 coincident with ZnMP localization.

While RNAi depletion of *hrg-4* resulted in decreased ZnMP uptake and resistance to toxic GaPPIX, the Δ*hrg-4* animals showed an increase in ZnMP fluorescence and were sensitive to GaPPIX. Contradicting results were also observed for Δ*hrg-1* animals that had lower level of ZnMP and showed resistance to GaPPIX. Although it is possible that the RNAi results were due to off target effects, our RNAi experiments were conducted with multiple RNAi constructs targeting different parts of *hrg-1* and *hrg-4*. Another possibility is that RNAi by feeding transiently knocks-

down genes that are not sustained through multiple generations. Knock-out of genes by deletion is permanent and provides an opportunity for the animals to adapt to abnormal changes in the environment. Thus, it is possible that these animals have developed other compensatory mechanisms for heme uptake and sequestration. Therefore, it would be very interesting to identify differences in gene expression profiles between these mutants and the wild type strain using a global transcriptional profiling study. It is also possible that there are gene rearrangements or duplications in addition to the deletion of either *hrg-1* or *hrg-4* in these mutants. Thus, the phenotypes of Δ*hrg-1* and Δ*hrg-4* animals may be synthetic to these other spurious deletions.

The Δ*hrg-4* mutants did not exhibit any morphological defects. This could be attributed to the fact that these animals are probably making a truncated form of HRG-4. An *in vitro* transcription-translation assay might be useful to determine whether a protein can be translated and if so is it stable or functional in yeast or *Xenopus* assays.

We observed that ~80% of Δ*hrg-1* homozygous animals showed embryonic defects including the "bag-of-worms" phenotype. We also observed that ~25% of the Δ*hrg-1* wild-type brood mate animals had similar phenotypes. It is possible that these mutants are still harboring other mutations in their background, despite eight backcrosses, that are causing these embryogenesis defects. Therefore, it is important to ensure that the phenotypes observed are due to the deletion in *hrg-1*. This can be done by injecting these animals with a *hrg-1* rescue construct containing the 3 kb *hrg-1* promoter, *hrg-1* gene (exons and introns) fused to GFP and the *unc-54* 3' UTR.

We have a *Mos-1* transposon insertion available for *hrg-4* (ttTi 10386) which encompasses the first intron and further characterization of this *Mos-1* insertion allele will provide clues as to whether the *tm3199* allele for *hrg-4* is a null strain or a hypomorph. We are generating Δ*hrg-1* and Δ*hrg-4* double mutants but there have been problems with mating these strains. It is possible that there might be defects in the development of males from these homozygous strains. Analysis of the Δ*hrg-1* and Δ*hrg-4* double mutant strain and experiments including heme dose-response assays for the single and double mutants need to be conducted in order to characterize the deletion strains completely. The double deletion strain might provide a tractable animal model of abnormal heme homeostasis that could be exploited to further understand organismal heme metabolism by transformation of this strain with HRG-1 and HRG-4 mutant and chimeric proteins.

Figure 5. Deletion strains have aberrant ZnMP uptake

Worms grown on NGM agar plates spotted with OP50 were transferred to liquid axenic mCeHR-2 medium with 2 μM heme and 10 μM ZnMP. After overnight incubation at 20ºC, worms were photographed using Leica DMIRE2 epifluorescence/ DIC microscope fitted with a 10X objective lens. Images were quantified using SimplePCI software (mean ± S.E.M, n= 100). The deletion strains were compared to the respective wild-type brood mate animals. Student-Neuman-Keul's was used to determine the p-values (* $p< 0.05$ and ** $p<0.01$)

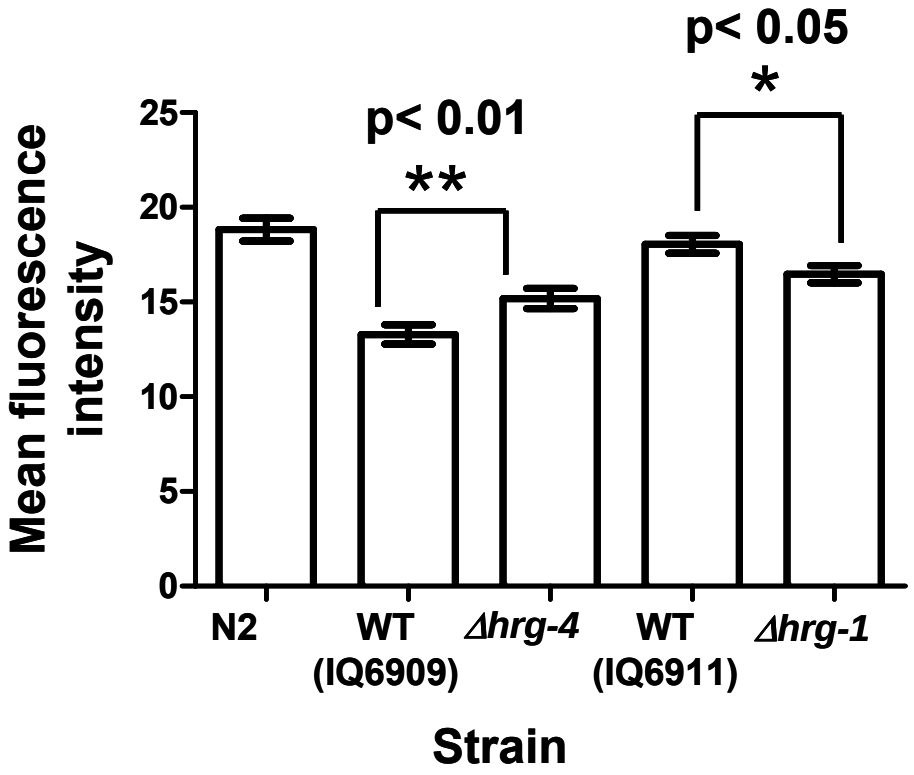
p< 0.05
*
p< 0.01
**
Mean fluorescence intensity
25
20
15
10
5
0
N2
WT (IQ6909)
Δhrg-4
WT (IQ6911)
Δhrg-1
Strain

Figure 6. Deletion strains show an abnormal response to GaPPIX

Fifteen L4 larval stage worms of the strains indicated, were added to each well in a 24-well plate containing NGM agar with 1 μM GaPPIX and spotted with OP50 bacteria. The total number of live progeny was counted 36 h after GaPPIX exposure. The experiment was performed in duplicate and the graph is represented as mean ± S.E.M

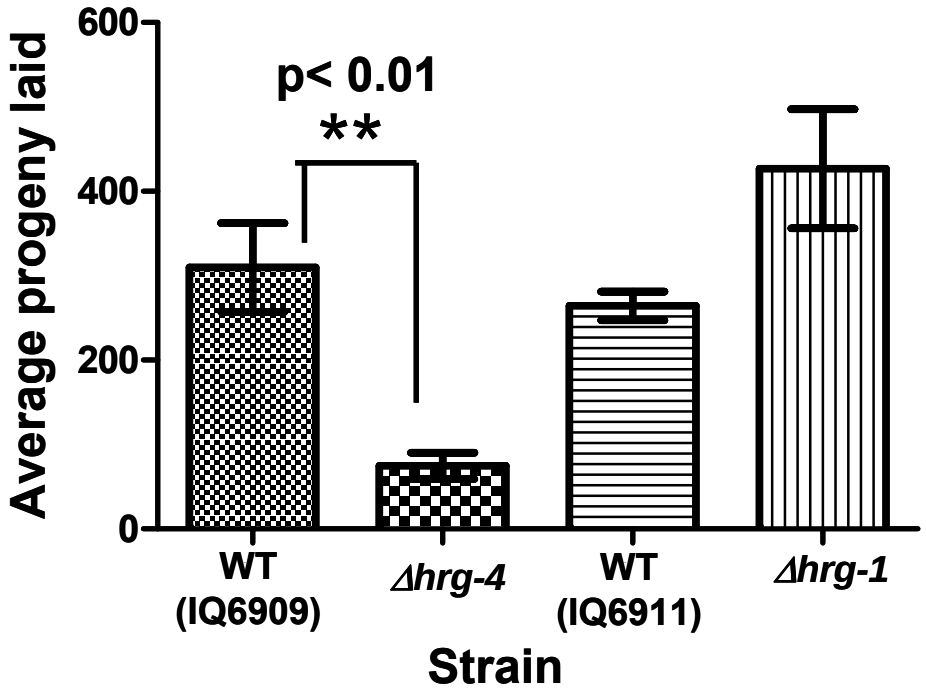
600
400
200
0
Average progeny laid
p< 0.01
**
WT
(IQ6909)
Δhrg-4
WT
(IQ6911)
Δhrg-1
Strain

Figure 7. Morphological defects in the deletion strains (a) N2, IQ6909, IQ6910, IQ6911 and IQ6912 worms were picked on to agar pads, anesthetized using 10 mM levamisole and analyzed using Leica DMIRE2 epifluorescence/ DIC microscope. DIC images of the morphological defects were obtained using a CCD camera fitted to the Leica DMIRE2 epifluorescence/ DIC microscope**.** Images were taken using 40X objective lens. Embryo-like structures (asterisk) and bag-of-worms (arrow heads) are indicated. (Scale Bar = 20 μm) **(b)** Each worm was scored for phenotypes indicated in the graph (n = 40-50 per strain). The percentage of number of worms with defects over total number of worms per strain was calculated.

a

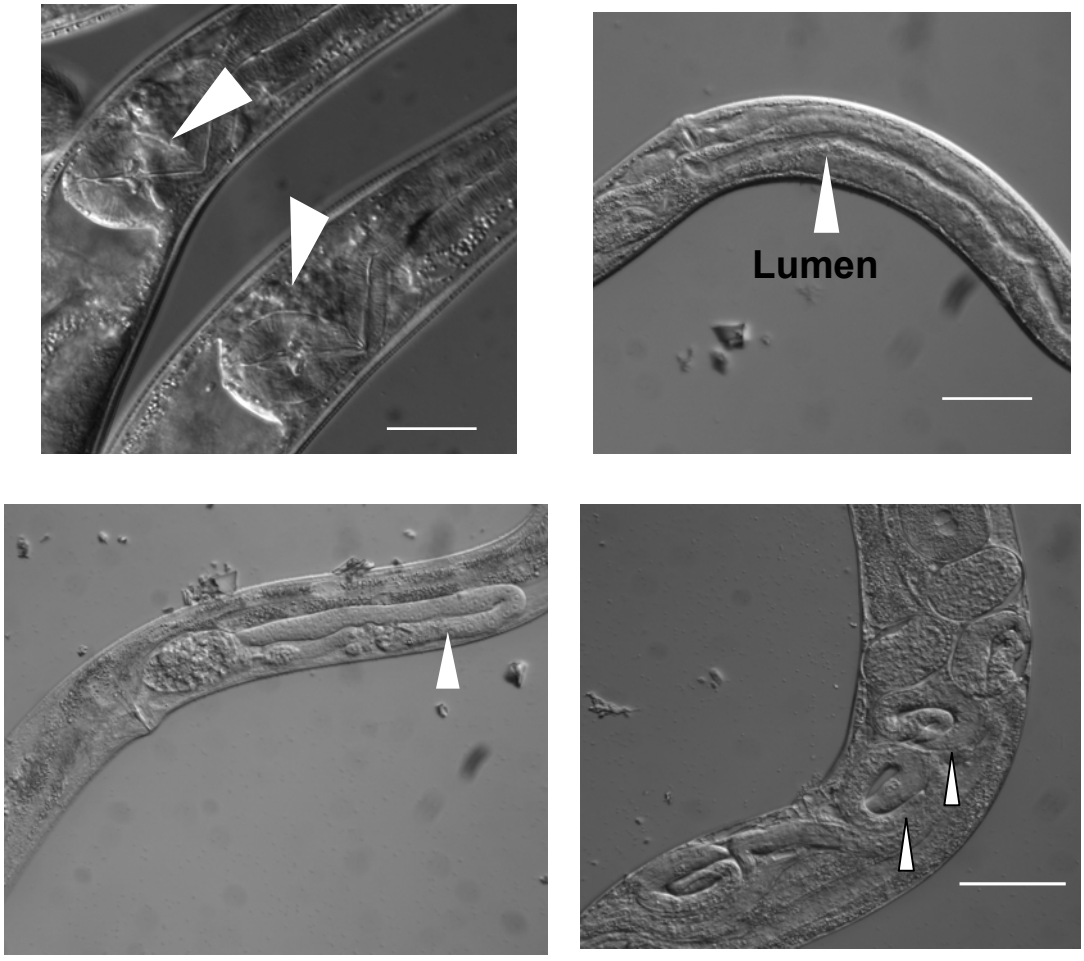

b

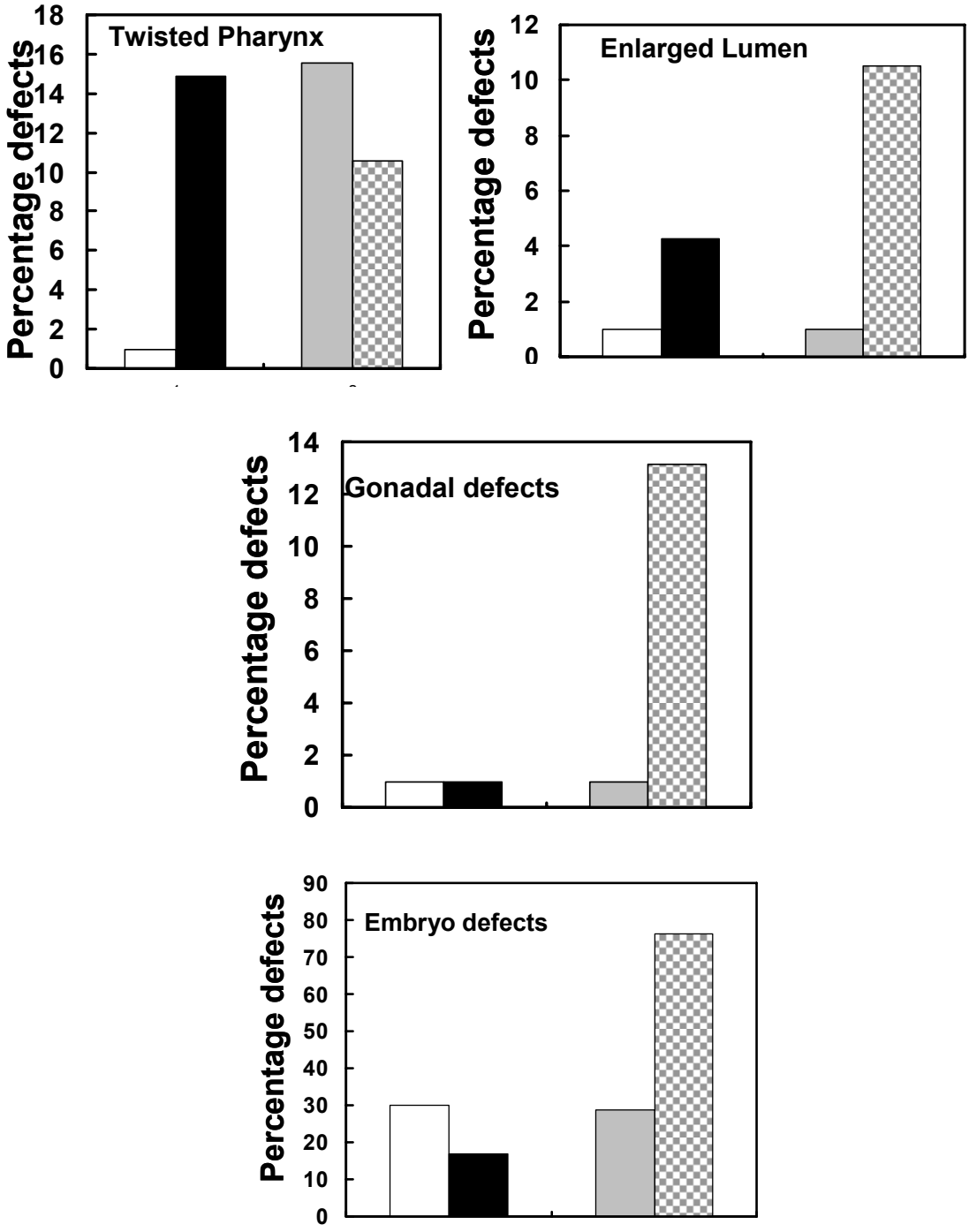
Twisted Pharynx
Percentage defects
0
2
4
6
8
10
12
14
16
18
Enlarged Lumen
Percentage defects
0
2
4
6
8
10
12
Gonadal defects
Percentage defects
0
2
4
6
8
10
12
14
Embryo defects
Percentage defects
0
10
20
30
40
50
60
70
80
90

Figure 8. Brood size of the deletion strains

Ten gravid worms from each of the strain as indicated in the graph, were placed individually on NGM agar plates spotted with OP50 grown in LB with no added heme (open bars) or in LB with 100 μM heme (gray bars). The worms were allowed to lay progeny for a period of 6 days. Total number of progeny was counted (mean ± S.E.M)

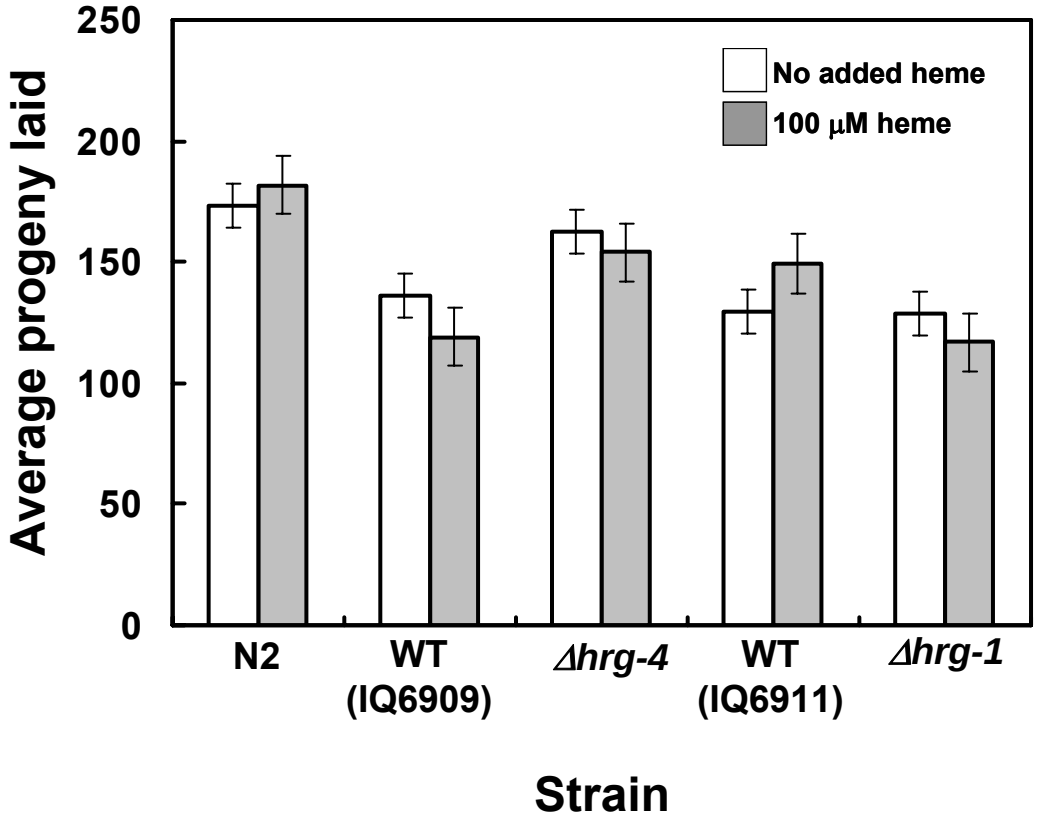
250
200
150
100
50
0
Average progeny laid
No added heme
100 μM heme
N2
WT
(IQ6909)
Δhrg-4
WT
(IQ6911)
Δhrg-1
Strain

Figure 9. Aberrant gene expression profiles of the *hrg-4* paralogs in the deletion strains

(a) Real-time PCR analysis of *hrg-1*, *hrg-5* and *hrg-6* in the following strains: N2, IQ6909 (Δ*hrg-4* wild-type brood mate) and Δ*hrg-4*. **(b)** Real-time PCR analysis of *hrg-4*, *hrg-5* and *hrg-6* in N2, IQ6911 (Δ*hrg-1* wild-type brood mate) and Δ*hrg-1*. Data were compared to *gpd-2* levels in each strain and the fold change was calculated using $2^{(-\Delta Ct)}$ method. The p-values were calculated using One-way ANOVA and Student-Neuman-Keul's multiple comparison tests.

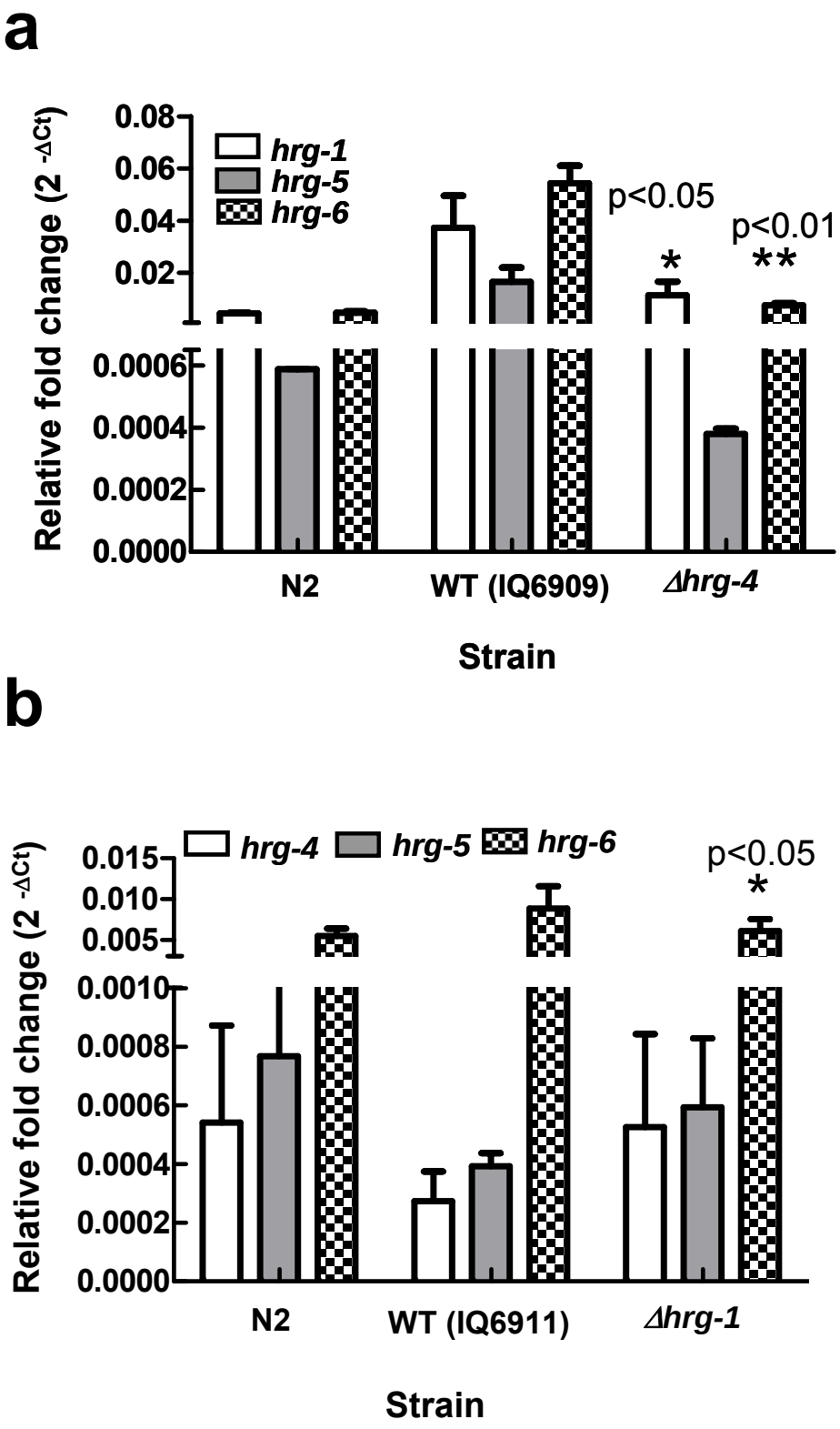
a
Relative fold change (2 -ΔCt)
0.08
0.06
0.04
0.02
0.0006
0.0004
0.0002
0.0000
hrg-1
hrg-5
hrg-6
p<0.05
p<0.01
*
**
N2
WT (IQ6909)
Δhrg-4
Strain
b
Relative fold change (2 -ΔCt)
0.015
0.010
0.005
0.0010
0.0008
0.0006
0.0004
0.0002
0.0000
hrg-4
hrg-5
hrg-6
p<0.05
*
N2
WT (IQ6911)
Δhrg-1
Strain

Chapter 6 Conclusions and future directions

Conclusions

The goal of this project was to identify specific molecules and pathways involved in heme uptake, transport and sequestration. *C. elegans* is a unique animal model in addressing questions related to regulation of heme homeostasis because it lacks the ability to synthesize heme and relies solely on exogenous heme for normal growth and development [93]. This unique aspect of *C. elegans* permitted, for the first time, the control of internal heme by dietary means, and we performed a genome-wide analysis using Affymetrix *C. elegans* whole genome arrays to identify genes that were regulated at a transcriptional level by heme. The major findings from this body of work are listed and discussed below.

1) Using the Affymetrix *C. elegans* whole genome arrays, we identified 288 heme-responsive genes (*hrgs*). Of these, 84 had homologs specific to humans. This finding is significant because it suggests that there might be pathways common to both worms and humans for maintaining intracellular levels of heme and the results from studies conducted using *C. elegans* as an animal model may be extrapolated to humans. We also identified 12 heme auxotroph-specific homologs. This is important because it suggests that the heme acquisition pathways may share commonalities between *C. elegans* and parasites that lack the ability to synthesize heme. Characterization of these

genes might enable the design of new drug targets to tackle parasitic infections that are a huge burden on public health and global agriculture.

2) From the heme microarrays, there were two genes, *hrg-1* and the paralog *hrg-4*, that were highly upregulated at low heme conditions. While *hrg-4* is specific to worms, *hrg-1* has homologs in vertebrates. Amino acid sequence comparison revealed that these genes have conserved amino acids, including histidines in TMD2 and the E2 loop and a FARKY motif in the C-terminus that might interact with the propionate side chains of heme.
3) Depletion of *hrg-1* by RNA-mediated interference resulted in increased GFP fluorescence in the "heme-sensor" IQ6011 strain at a heme concentration of 5 μM and increased ZnMP fluorescence. Depletion of *hrg-4* resulted in increased GFP fluorescence in the IQ6011 sensor strain in conditions where heme was in excess (25 μM), decreased ZnMP fluorescence and resistance to GaPPIX toxicity. These results indicate that knock-down of these genes lead to aberrant heme homeostasis. In addition the ZnMP staining pattern provides a clue to the intracellular localization, i.e. HRG-4 participated in heme uptake at the plasma membrane in the polarized intestinal cells of the worm while HRG-1 was involved in intracellular compartmentalization.
4) Ectopic expression in mammalian cells showed that HRG-4 localized to the plasma membrane and HRG-1 co-localized with endosomal (Rab 7 and Rab 11) and lysosomal markers (LAMP1). Human HRG-1 (SLC48A1) co-localized with CeHRG-1 greater than 80% of the time.

5) Amino acid sequence analysis reveals trafficking motifs within the C-terminus of worm and human HRG-1. A conserved tyrosine (YxxxØ in humans and YxxØ in worms) and acidic-dileucine (DxxIL in humans and ExxxLL in worms) based sorting motifs were found in HRG-1 but were absent in HRG-4. This observation is consistent with the localization studies because the tyrosine and acidic-dileucine based sorting motifs have been shown to be involved in targeting of proteins to endosomes and lysosome-related organelles.

6) HRG-4 bound heme over a broader pH range as compared to HRG-1 (both worm and human), which bound heme better only at lower pH. Thus, the studies corroborate the intracellular location and function of HRG-1 within an acidic compartment.

7) Injection of cRNA for *Cehrg-1*, *hHRG1* or *Cehrg-4* into *Xenopus* oocytes resulted in significant heme-mediated inward currents. Given that HRG-1 proteins are permeases, it is likely that these transporters may translocate the negatively charged heme coupled to a pre-established ionic gradient. An example of a counter-ion would be the Na+ gradient established by the Na/K ATPase at the plasma membrane. Nevertheless, our results clearly indicate that HRG-1 and HRG-4 function as transporter across membranes.

8) To understand the role of HRG-1 proteins in mediating heme homeostasis, morpholinos were used to knock-down zebrafish *hrg-1*. Zebrafish has been used extensively as a model organism to study hematopoiesis because the embryos are transparent and have a beating heart and visible erythrocytes by

24 hpf. While a reduction in *hrg-1* led to mild anemia as demonstrated by the MO1 phenotypes, a severe knock-down of *hrg-1* resulted in a striking anemic phenotype with developmental defects, including a curved body with shortened yolk sac and hydrocephalus. The lack of any developmental defects in worms depleted of *hrg-1* or *hrg-4* might be due to incomplete RNAi or other compensatory mechanisms. HRG-1 is important for the maintenance and hemoglobinization of hematopoietic cells in zebrafish and not for cell type specification. Importantly, the worm ortholog fully rescued all the genetic defects due to knock-down of zebrafish *hrg-1*.

9) *Cehrg-4* has two other paralogs, *hrg-5* and *hrg-6*, that were not heme-responsive. The identification of these other paralogs suggests that there might be redundant mechanisms for heme uptake and transport in worms. This could explain why we did not observe any discernable developmental phenotypes due to *hrg-1* and *hrg-4* depletion in worms.

10) In worms, both HRG-1 and HRG-4 are found in the intestinal cells. The two proteins have very different localization patterns. HRG-4 is found on the lumenal surface while HRG-1 localized to vesicles found in the intestinal cells.

11) Analysis of Δ*hrg-1* (*tm3199*) and Δ*hrg-4* (*tm2994*) worm strains revealed that the Δ*hrg-1* strain is a null mutant and the Δ*hrg-4* strain expresses a truncated form of *hrg-4* mRNA and may, therefore, be a hypomorph. Results from ZnMP uptake and GaPPIX toxicity assays in the deletion worms were contradictory to our results observed from *hrg-1* or *hrg-4* RNAi in N2 worms.

It is possible that even after eight backcrosses, the animals are still carrying other spurious deletions. This is demonstrated by the differences in *hrg-1*, *-4*, *-5* and *-6* gene expression in the brood mate controls. Another reasonable argument is that the deletion strains are upregulating other mechanisms of heme uptake and transport to compensate for the loss of *hrg-1* or *hrg-4*. The recent availability of a Mos transposon insertion line in the *hrg-4* locus (Ti10386) will permit us to verify the results from the *hrg-4* deletion mutant.

Significance

The goals of this dissertation were to identify genes that are transcriptionally regulated by heme and to characterize the role of one or more genes in mediating heme homeostasis. Prior to this work, the presence of molecules involved in intestinal heme uptake and transport of heme from the mitochondria where it is synthesized to other cellular compartments where hemoproteins reside has been widely speculated. The identification of such molecules has been stymied by the inability to dissociate the tightly regulated processes of heme biosynthesis and degradation from heme uptake and intracellular transport. *C. elegans* provided the unique opportunity to modulate intracellular heme levels by changing environmental heme levels in the liquid growth medium.

This dissertation provides, for the first time, insights into the mechanisms of heme uptake and transport in eukaryotes. The studies performed in this body of work using *C. elegans* as an animal model of heme auxotrophy, certainly provide a starting point for such nutrient-gene interaction studies, the results of which can then be

extrapolated to other vertebrates including mammals. The tools and reagents developed during the course of this dissertation will be useful to address some of the critical questions related to heme uptake, transport and sequestration but also questions regarding the mechanisms by which the heme moiety is incorporated into hemoproteins.

Future studies

In vivo analysis of HRG-1 proteins

While detailed studies have been conducted to characterize the role of HRG-1 and HRG-4 in mediating heme homeostasis, not much is known about the role of HRG-5 and HRG-6. We postulate that, since worms rely solely on exogenous heme for their growth and development, they have additional mechanisms for heme acquisition that might include HRG-5 and HRG-6. Therefore, spatial and temporal expression patterns, along with the intracellular location need to be determined for HRG-5 and HRG-6. Functional assays including heme-binding studies need to be performed to understand the role that these paralogs might play in heme homeostasis. Interestingly, while cloning *hrg-5*, we observed that there were discrepancies between the genomic DNA and the cDNA sequences. Further studies conducted on *hrg-5* in worms suggest that this gene might undergo RNA editing (Xiaojing Yuan and Iqbal Hamza, unpublished observations). Investigating the effects of heme on *hrg-5* editing and analyzing *hrg-5* genomic DNA and mRNA in the *C. elegans* ADAR mutants (Adenosine deaminase acting on RNA; this enzyme is responsible for the conversion of adenosines to inosines) will provide a better understanding of the post-transcriptional control of *hrg-5* [169].

The different localization pattern of HRG-1 and HRG-4 proteins has raised questions about how these paralogs might be regulated. Jason Sinclair, a graduate student in the lab, is conducting experiments to identify *cis*-elements that might be involved in the heme-mediated transcriptional regulation of *hrg-1* and *hrg-4*. Scott Severance, a post-doctoral fellow, has undertaken a genome-wide RNAi analysis looking for modulators of *hrg-1::gfp* expression in the "heme-sensor" strain in the presence and absence of heme. He has already identified 53 modulators of heme homeostasis by performing an RNAi screen using all the *hrgs* that were identified from the heme microarrays. This analysis may reveal novel molecules involved in organismal heme homeostasis.

Transgenic lines stably expressing *hrg-4::yfp* translational reporter constructs with either the *unc-54* 3' UTR or the *hrg-4* 3' UTR were generated. While lines containing the translational construct with *hrg-4* 3' UTR had YFP expression, there was no fluorescence in the worms expressing *hrg-4::yfp* with *unc-54* 3' UTR. This observation is preliminary, but it suggests that the 3' UTR might be important for the regulation of *hrg-4*. It has been shown before that 3' UTRs are important for the down regulation of mRNA levels [170].

These findings reveal the possibility of a complex regulatory circuit involving *hrg* paralogs. The differences in regulation of individual *hrgs* could provide molecular insights into the functional aspects of these *hrgs* and their contribution to heme homeostasis.

Structure-function analysis of HRG-1 proteins

As mentioned above, there are conserved residues shared between the CeHRG-1 and CeHRG-4 proteins. One such motif is the FARKY motif, which might be involved in stabilizing the heme moiety by interacting with the propionate side chains [153, 155, 171]. Human and the worm HRG-1 proteins have an invariant histidine in TMD 2 and the E2 loop and tyrosine- and acidic-dileucine-based sorting motifs at the C-terminus. Studies are underway to delineate the structural elements that are important for localization and function of HRG-1 proteins. For example, domain-swapping experiments done by Caitlin Hall revealed that the C-terminus of HRG-1 is important for its localization to endo-lysosomal compartments. Xiaojing Yuan is using PCR-based site-directed mutagenesis to mutate the conserved residues to alanine. These constructs will then be examined for differences in their intracellular localization patterns and heme transport abilities.

The HRG-1 and HRG-4 proteins share some of the features of tetraspanins including cysteines in the transmembrane domains that are important for membrane-proximal palmitoylation. It will be interesting to mutate the cysteine residues in the TMDs of these proteins and analyze the stability of the HRG-1 proteins. Tetraspanins are found in small microdomains called tetraspanin-enriched microdomains (TEM) [164]. A main biochemical feature of the TEM is that it is resistant to non-denaturating detergent treatments, a feature that has been observed for HRG-1 proteins. An interesting experiment would be to deplete cholesterol from the cells and then analyze the oligomerization pattern of HRG-1 proteins.

Identification of interacting partners

Heme uptake and transport in bacteria have been shown to involve complex molecular networks. Hence, we speculate that the HRG-1 proteins might also be a part of an elaborate network of molecules regulating heme uptake, transport and storage. To identify these additional molecules, genome-wide RNA-mediated interference assay will be performed in the strain IQ6111 (transgenic worms stably expressing *hrg-1::gfp* translational construct) to detect aberrant localization of HRG-1::GFP and/ or ZnMP. The genetic interaction between the candidate genes from the RNAi assay and either *hrg-1*, *hrg-4*, or both can be studied using the *hrg-1* and *hrg-4* single and double mutants. Furthermore, transcriptional profiling experiments of the *hrg-1* and *hrg-4* deletion animals grown under different heme concentrations might identify genes that are dysregulated due to disruption in heme homeostasis.

Speculations

There are still many unanswered questions. What is the physiologically relevant ligand for these proteins? Haptoglobin, hemopexin, serum albumin and lipoproteins (HDL and LDL) have been shown to physiologically sequester heme [172]. It would not be surprising if protein-bound heme is the ligand for HRG-1 proteins. How do these proteins function? It is possible that these proteins might function similarly to *lac* permeases in that the transport of heme could be coupled to a proton gradient [173]. This hypothesis can be tested by depleting the 19 V-type ATPases (these proteins have been shown to actively transport protons into organelles and extracellular compartments thereby generating a proton gradient) by RNAi in

IQ6111 worms and analyze the differences in localization of HRG-1::GFP and/or ZnMP uptake [174]. What is the role of human HRG-1 in mediating heme homeostasis? It has been shown that some of the heme released within the macrophages after phagocytosis of senescent red blood cells can be exported by FLCVR [88]. Although the fate of this exported heme is unclear, it is likely that it is being sequestered in an acidic compartment. This is a reasonable argument because it has been suggested that sequestration of metals or metal-containing groups such as heme in acidic compartments such as lysosomes may help avoid their toxic effects [175]. There is also evidence supporting the involvement of lysosomes in the recycling pathways for metals such as iron. A study conducted by Radisky and Kaplan has demonstrated that lysosomal degradation of ferritin is one of the mechanisms by which iron can reutilized [176]. The results from their study also suggest the possibility of soluble iron being stored in the lysosomes. We have shown that HRG-1 localizes to acidic endo-lysosomal compartments. So it might be possible that when there is a huge demand for heme, such as in developing erythrocytes, HRG-1 mobilizes free heme out of these acidic compartments. It is also likely that HRG-1 may be involved in intercellular transport of heme by redistributing heme from heme-rich tissues (red blood cells, bone marrow and liver) to other tissues with a greater requirement for heme transiently during embryonic and organ development. This argument is reasonable because loss of function of HRG-1 in zebrafish causes severe developmental defects concomitant with anemia.

Appendices

Appendix A

HRG-1 is essential for erythropoiesis in zebrafish

a) Zebrafish *hrg-1* expression in the 15-somite stage (left) and 24 h after fertilization (right). **b)** Knockdown of zebrafish *hrg-1* by using morpholinos MO1 and MO2 against zebrafish *hrg-1* results in either mild (MO1) or severe anemia (MO2) with very few *o*-dianisidine-positive red cells (arrows, right panel), hydrocephalus, curved body and shortened yolk sac (arrows, left panel). **c)** Schematic representation of zebrafish *hrg-1* genomic structure indicating the locations of MO1 and MO2 morpholinos and primers used for RT-PCR analysis. **d)** RNA extracted from embryos injected with MO1 and MO2 was used to perform RT-PCR. Left panel- top arrow indicates the misspliced mRNA isoform generated by MO1. Right panel- bottom arrow indicates the product of exon skipping generated by MO2. *Cehrg-1* cRNA injected along with MO2 rescues anemia as indicated by an increase in *o*-dianisidine-positive red cells **(e)** and completely rescues the developmental defects (f, arrows)

Julio Amigo and Barry Paw conducted the studies in zebrafish.

(Adapted from Rajagopal *et al*, 2008)

a

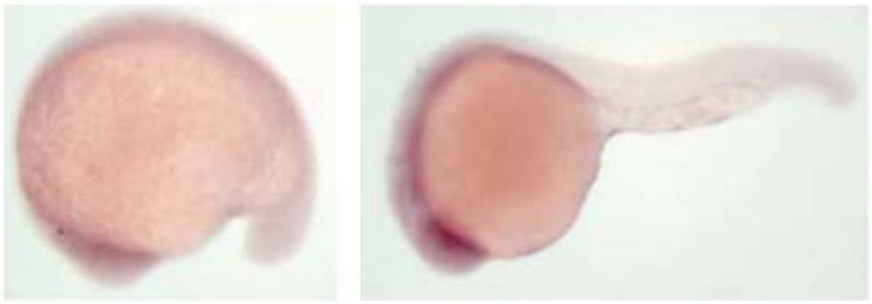

b

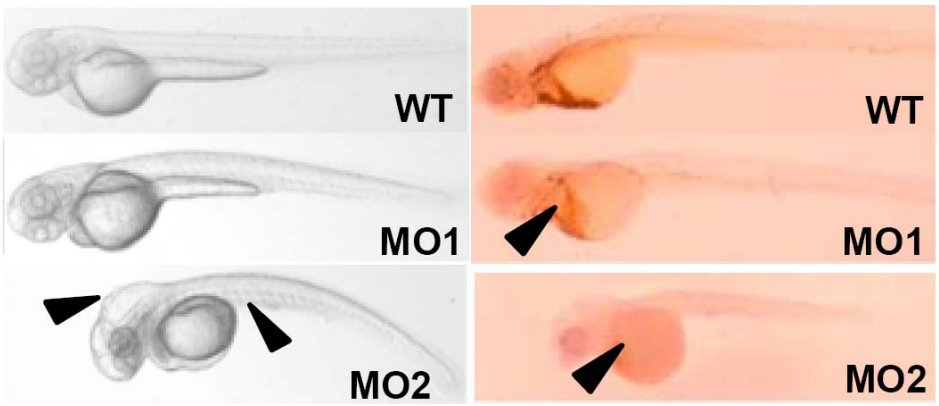
WT
WT
MO1
MO1
MO2
MO2

c


650bp
Ex1F
MO1
MO2
Ex3R
Ex4F
400 bp
Ex4R
250bp
Exon
Coding seq.
Intron
MO's

d

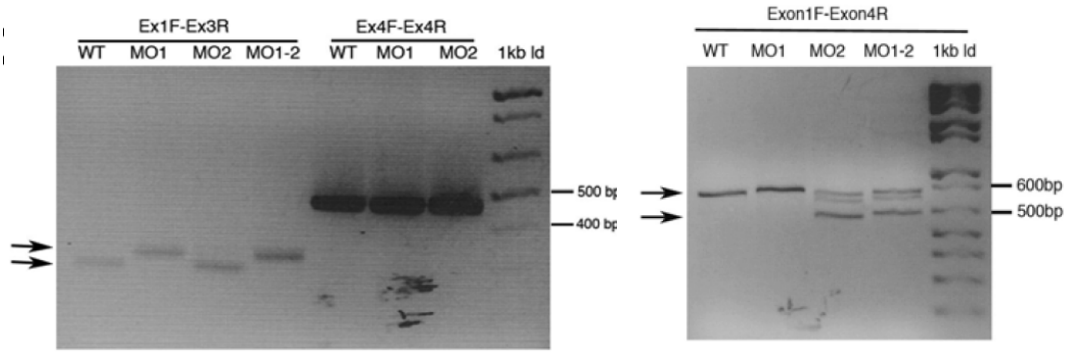
Ex1F-Ex3R
Ex4F-Ex4R
WT MO1 MO2 MO1-2 WT MO1 MO2 1kb ld
500 bp
400 bp
Exon1F-Exon4R
WT MO1 MO2 MO1-2 1kb ld
600bp
500bp

e

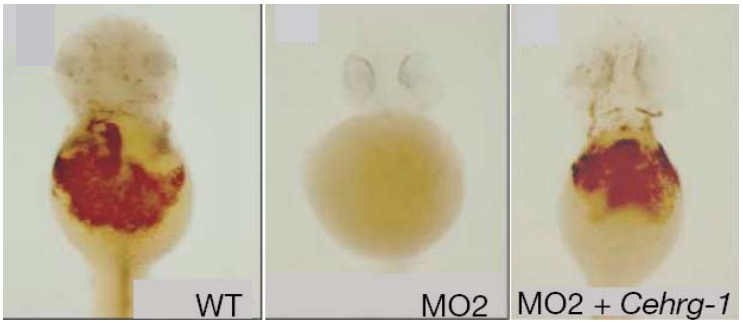
WT
MO2
MO2 + Cehrg-1

f

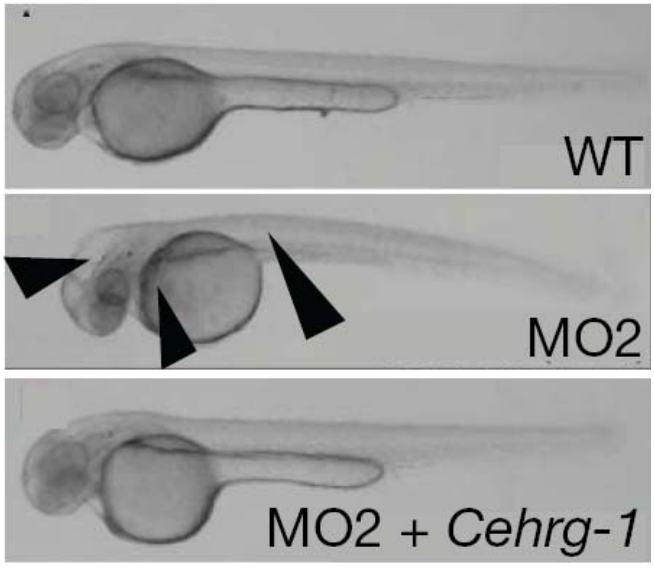
WT
MO2
MO2 + Cehrg-1

Appendix B

HRG-1 proteins bind heme

Cell lysates (lanes 1 and 4, one-tenth of total protein) from HEK 293 cells transfected with plasmids expressing either CeHRG-4 (60 μg), CeHRG-1 (60 μg), hHRG1 (60 μg) or hZIP-4 (360 μg) tagged with the HA epitope were incubated with 300 nmol of heme agarose. Samples were resolved by SDS-PAGE, transferred to nitrocellulose and detected with antibodies against the HA epitope. Wash (lanes 2 and 5) represents the final wash before elution (lanes 3 and 6). Samples were resolved by SDS-PAGE followed by immunoblotting with anti-HA antibody.

(Anita Rao and Iqbal Hamza performed the heme binding experiment)

(Adapted from Rajagopal *et al*, 2008)

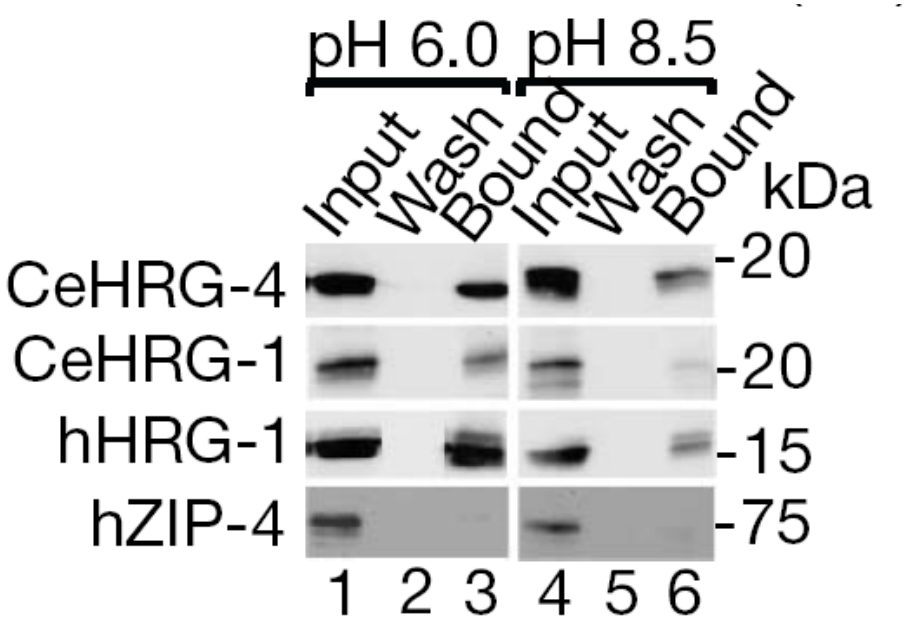
pH 6.0
pH 8.5
Input
Wash
Bound
Input
Wash
Bound
kDa
CeHRG-4
CeHRG-1
hHRG-1
hZIP-4
-20
-20
-15
-75
1 2 3 4 5 6

Appendix C

HRG-1 proteins transport heme

Electrophysiological currents (mean ± S.D., n = 4) from *Xenopus* oocytes injected with cRNA encoding the indicated protein when clamped at -110 mV in the presence of 20 μM heme. Y-axis represents the difference in the current in the presence and absence of heme, normalized to current observed in the absence of heme. Values with different letter labels are significantly different within each treatment compared to control, hKv1.1 ($P < 0.05$).

(Sanjeev.K.Upadhyay and M.Matthew conducted the transport studies in *Xenopus*)

(Adapted from Rajagopal *et al*, 2008)

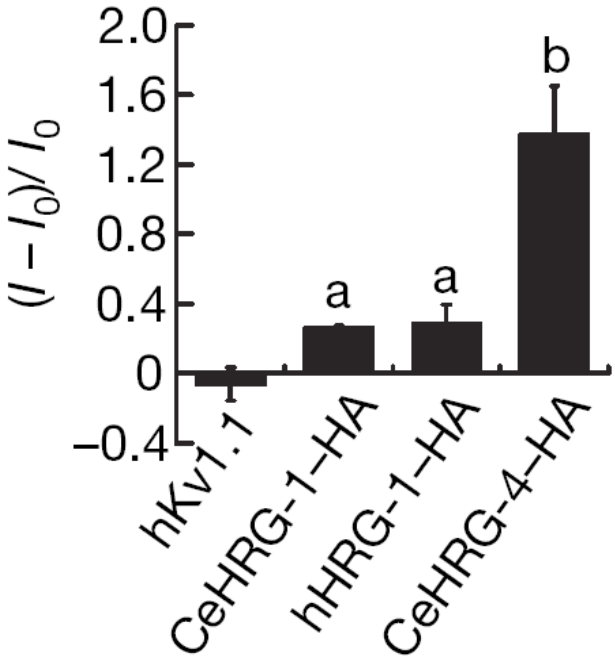
2.0
1.6
1.2
0.8
0.4
0
–0.4
(I – I0)/ I0
a
a
b
hKv1.1
CeHRG-1–HA
hHRG-1–HA
CeHRG-4–HA

Appendix D

qRT-PCR primers and primers for screening of *hrg-1* and *hrg-4* deletion strains.

C. elegans **qRT-PCR primers**	
5'qCehrg-1	**AATGGCAGGATGGTCAGAAAC**
3'qCehrg-1	**CGATGAATGAAAGGAACGATACG**
5'qhrg-4	**TTATTGGTCTTCTCGGACTTCTC**
3'qhrg-4	**CTGGCAAAGAATGCATTTTGC**
5'qhrg-5	**TCTTGGATTTCTTGCTCTAGGATG**
3'qhrg-5	**GTACTTTGTGATTGCTGTTGCC**
5'qhrg-6	**TGCTGGCTGCTACTAAACATC**
3'qhrg-6	**GGCTCCTCTGGGTGAATAATTG**
5'qgpd-2	**TGCTCACGAGGGAGACTAC**
3'qgpd-2	**CGGTGGACTCAACGACATAG**

Human qRT-PCR primers	
5'qhHRG1	**CTTCGTGGGCGTCCTCTTCTC**
3'qhHRG1	**GAAATCGCTGAGGATGCTGATGTC**
5-qhHMOX1	**ATGACACCAAGGACCAGAGC**
3-qhHMOX1	**TAAGGACCCATCGGAGAAGC**
5-qhTFR	**TGAATTGAACCTGGACTATGAGAG**
3-qhTFR	**CTGGAAGTAGCACGGAAGAAG**
5-qhAlas1	**TGAGACAGATGCTAATGGATGC**
3-qhAlas1	**CGTAGGGTAATTGATTGCTTGC**

Mouse qRT-PCR primers	
5'qmouseHrg-1	CTGGCACTGTGGGTCTTGG
3'qmouseHrg-1	GCGTAGAGGCTAAGTAGGAAGG
5'qmouseHbb-b1	TGCTGAGAAGGCTGCTGTC
3'qmouseHbb-b1	TTGAGGCTGTCCAAGTGATTC
5'qmouseHbb-a1	AAGGGTCACGGCAAGAAGG
3'qmouseHbb-a1	GGCAAGGAATTTATCCAGAGAGG
5'qmouseAlas-2	AAGAGCAAGATTGTGCAGAGG
3'qmouseAlas-2	ACGGTAGGTGTGGTCCTGTT
5'qmouseActinB	GCACCACACCTTCTACAATGAG
3'qmouseActinB	CGTGAGGGAGAGCATAGCC
5'qmouseGAPDH	AAGGTGGTGAAGCAGGCATC
3'qmouseGAPDH	TGGTCCAGGGTTTCTTACTCC

C. elegans deletion primers	
tm3199_external_f	GGCACAAGGTCCAATAGTTA
tm3199_external_b	AGTCGAGCCATATGGTGCAA
5'hrg-4_del	CAATCAAATTTCATAATTGGTCAGC
3'hrg-4_del	TTAACTTTTAATGACTTCAACATCGTC

Appendix E

Worm strains and their descriptions.

Name	Construct	Vector
IQ 6011	*hrg-1* promoter	pPD95.67
IQ 6041	*hrg-4* PRM::NLSGFP::*hrg-4* 3' UTR	pDESTR4R3
IQ 6111	*hrg-1* PRM::*hrg-1* gene+ *gfp* gene::*hrg-1* 3' UTR	pDESTR4R3
IQ 6141	*hrg-4* PRM::*hrg-4* gene+*yfp* gene::*hrg-4* 3' UTR	pDESTR4R3
IQ 6909	brood mate for *hrg-4* homozygous deletion worms	none
IQ 6910	*hrg-4* homozygous deletion	none
IQ 6911	brood mate for *hrg-1* homozygous deletion worms	none
IQ 6912	*hrg-1* homozygous deletion	none

References

1. Assesssing the iron status of populations. Report of a Joint World Health Organization/ Center for Disease Control and Prevention Technical Consultation on the Assessment of Iron Status at the population level [online], Geneva, Swtzerland From URL: http://http://libdocwhoint/publications/2004/9241593156_engpdf 6-8 April 2004.
2. Bungiro R, Cappello M: Hookworm infection: new developments and prospects for control. Current Opinion in Infectious Diseases 2004, 17(5):421.
3. Menendez C, Kahigwa E, Hirt R, Vounatsou P, Aponte JJ, Font F, Acosta CJ, Schellenberg DM, Galindo CM, Kimario J: Randomised placebo-controlled trial of iron supplementation and malaria chemoprophylaxis for prevention of severe anaemia and malaria in Tanzanian infants. Lancet 1997, 350(9081):844.
4. Molyneux ME, Looareesuwan S, Menzies IS, Grainger SL, Phillips RE, Wattanagoon Y, Thompson RPH, Warrell DA: Reduced Hepatic Blood Flow and Intestinal Malabsorption in Severe Falciparum Malaria. The American Journal of Tropical Medicine and Hygiene 1989, 40(5):470.
5. Weatherall DJ, Abdalla S: THE ANAEMIA OF PLASMODIUM FALCIPARUM MALARIA. British Medical Bulletin 1982, 38(2):147-152.
6. Spiro TG, Bates G, Saltman P: Hydrolytic polymerization of ferric citrate. II. Influence of excess citrate. Journal of the American Chemical Society 1967, 89(22):5559-5562.

7. Conrad ME, Umbreit JN: Iron absorption and transport-an update. American Journal of Hematology 2000, 64(4):287-298.

8. Uzel C, Conrad ME: Absorption of heme iron. Seminars in Hematology 1998, 35(1):27-34.

9. Carpenter CE, Mahoney AW: Contributions of heme and nonheme iron to human nutrition. Crit Rev Food Sci Nutr 1992, 31(4):333-367.

10. Weintraub LR, Conrad ME, Crosby WH: Absorption of hemoglobin iron by the rat. Proceedings of the Society for Experimental Biology and Medicine 1965, 120(3):840-843.

11. Conrad ME, Benjamin BI, Williams HL, Foy AL: Human absorption of hemoglobin-iron. Gastroenterology 1967, 53(1):5-10.

12. Wyllie JC, Kaufman N: An electron microscopic study of heme uptake by rat duodenum. Laboratory Investigation 1982, 47(5):471-476.

13. Tsiftsoglou AS, Tsamadou AI, Papadopoulou LC: Heme as key regulator of major mammalian cellular functions: Molecular, cellular, and pharmacological aspects. Pharmacology and Therapeutics 2006, 111(2):327-345.

14. Nakajima O, Takahashi S, Harigae H, Furuyama K, Hayashi N, Sassa S, Yamamoto M: Heme deficiency in erythroid lineage causes differentiation arrest and cytoplasmic iron overload. The EMBO Journal 1999, 18(22):6282-6289.

15. Ogawa K, Sun J, Taketani S, Nakajima O, Nishitani C, Sassa S, Hayashi N, Yamamoto M, Shibahara S, Fujita H, Igarashi K: Heme mediates derepression

of Maf recognition element through direct binding to transcription repressor Bach1. The EMBO Journal 2001, 20(11):2835-2843.

16. Tang XD, Xu R, Reynolds MF, Garcia ML, Heinemann SH, Hoshi T: Haem can bind to and inhibit mammalian calcium-dependent Slo1 BK channels. Nature 2003, 425(6957):531-535.

17. Balla G, Vercellotti GM, Muller-Eberhard U, Eaton J, Jacob HS: Exposure of endothelial cells to free heme potentiates damage mediated by granulocytes and toxic oxygen species. Laboratory Investigation 1991, 64(5):648-655.

18. Barros MH, Nobrega FG, Tzagoloff A: Mitochondrial Ferredoxin Is Required for Heme A Synthesis in Saccharomyces cerevisiae. Journal of Biological Chemistry 2002, 277(12):9997-10002.

19. Moraes CT, Diaz F, Barrientos A: Defects in the biosynthesis of mitochondrial heme c and heme a in yeast and mammals. BBA-Bioenergetics 2004, 1659(2-3):153-159.

20. Cornah JE, Terry MJ, Smith AG: Green or red: what stops the traffic in the tetrapyrrole pathway? Trends in Plant Science 2003, 8(5):224-230.

21. Papenbrock JaG, B.: Regulatory network of tetrapyrrole biosynthesis-studies of intracellular signalling involved in metabolic and developmental control of plastids. planta 2001, 213:667-681.

22. Vavilin DV, Vermaas WFJ: Regulation of the tetrapyrrole biosynthetic pathway leading to heme and chlorophyll in plants and cyanobacteria. Physiologia Plantarum 2002, 115(1):9-24.

23. Hamza I, Chauhan S, Hassett R, O'Brian MR: The Bacterial Irr Protein Is Required for Coordination of Heme Biosynthesis with Iron Availability. Journal of Biological Chemistry 1998, 273(34):21669-21674.

24. Lai LC, Kosorukoff AL, Burke PV, Kwast KE: Metabolic-State-Dependent Remodeling of the Transcriptome in Response to Anoxia and Subsequent Reoxygenation in Saccharomyces cerevisiae. Eukaryotic Cell 2006, 5(9):1468-1489.

25. Keng T: HAP1 and ROX1 form a regulatory pathway in the repression of HEM13 transcription in Saccharomyces cerevisiae. Molecular and Cellular Biology 1992, 12(6):2616-2623.

26. Verdiere J, Gaisne M, Labbe-Bois R: CYP 1(HAP 1) is a determinant effector of alternative expression of heme-dependent transcription in yeast. MGG Molecular & general genetics 1991, 228(1-2):300-306.

27. Todd BL, Stewart EV, Burg JS, Hughes AL, Espenshade PJ: Sterol Regulatory Element Binding Protein Is a Principal Regulator of Anaerobic Gene Expression in Fission Yeast†. Molecular and Cellular Biology 2006, 26(7):2817-2831.

28. Riddle RD, Yamamoto M, Engel JD: Expression of delta-aminolevulinate synthase in avian cells: separate genes encode erythroid-specific and nonspecific isozymes. Proceedings of the National Academy of Sciences USA 1989, 86(3):792.

29. Kaasik K, Lee CC: Reciprocal regulation of haem biosynthesis and the circadian clock in mammals. Nature 2004, 430(6998):467-471.

30. Christoph Handschin JL, James Rhee, Anne-Kathrin Peyer, Sherry Chin, Pei-Hsuan Wu, Urs A. Meyer and Bruce M. Spiegelman: Nutritional Regulation of Hepatic Heme Biosynthesis and Porphyria through PGC-1α. Cell 2005, 122(4):505-515.

31. Han L, Lu J, Pan L, Wang X, Shao Y, Han S, Huang B: Histone acetyltransferase p300 regulates the transcription of human erythroid-specific 5-aminolevulinate synthase gene. Biochemical and Biophysical Research Communications 2006, 348(3):799-806.

32. Cooperman SS, Meyron-Holtz EG, Olivierre-Wilson H, Ghosh MC, McConnell JP, Rouault TA: Microcytic anemia, erythropoietic protoporphyria, and neurodegeneration in mice with targeted deletion of iron-regulatory protein 2. Blood 2005, 106(3):1084.

33. Melefors O, Goossen B, Johansson HE, Stripecke R, Gray NK, Hentze MW: Translational control of 5-aminolevulinate synthase mRNA by iron-responsive elements in erythroid cells. Journal of Biological Chemistry 1993, 268(8):5974-5978.

34. Ajioka RS, Phillips JD, Kushner JP: Biosynthesis of heme in mammals. BBA-Molecular Cell Research 2006, 1763(7):723-736.

35. Takahashi S, Taketani S, Akasaka JE, Kobayashi A, Hayashi N, Yamamoto M, Nagai T: Differential regulation of coproporphyrinogen oxidase gene between erythroid and nonerythroid cells. Blood 1998, 92(9):3436-3444.

36. Sellers VM, Wu CK, Dailey TA, Dailey HA: Human ferrochelatase: characterization of substrate-iron binding and proton-abstracting residues. Biochemistry 2001, 40(33):9821-9827.

37. Wu CK, Dailey HA, Rose JP, Burden A, Sellers VM, Wang BC: The 2.0 Å structure of human ferrochelatase, the terminal enzyme of heme biosynthesis. Nature Structural Biology 2001, 8:156-160.

38. Yoon T, Cowan JA: Frataxin-mediated Iron Delivery to Ferrochelatase in the Final Step of Heme Biosynthesis. Journal of Biological Chemistry 2004, 279(25):25943.

39. Taketani S, Adachi Y, Nakahashi Y: Regulation of the expression of human ferrochelatase by intracellular iron levels. In., vol. 267: FEBS; 2000: 4685-4692.

40. Liu YL, Ang SO, Weigent DA, Prchal JT, Bloomer JR: Regulation of ferrochelatase gene expression by hypoxia. Life Sciences 2004, 75(17):2035-2043.

41. James MFM, Hift RJ: Porphyrias. British Journal of Anaesthesia 2000, 85(1):143-153.

42. http://www.nlm.nih.gov/medlineplus/ency/article/001208.htm#Symptoms.

43. http://www.porphyriafoundation.com/about_por/types/index.html.

44. Elder G: Molecular basis of disorders of heme biosynthesis. Journal of Clinical Pathology 1993, 46(11):977-981.

45. Raimo Tenhunen HSM, and Rudi Schmid: Microsomal heme oxygenase-Characterization of the enzyme. Journal of Biological Chemistry 1969, 244(23):6388-6394.

46. Mense SM, Zhang L: Heme: a versatile signaling molecule controlling the activities of diverse regulators ranging from transcription factors to MAP kinases. Cell Research 2006, 16:681-692.

47. William K. McCoubrey Jr. TJHaMDM: Isolation and characterization of a cDNA from the rat brain that encodes hemoprotein heme oxygenase-3. European Journal of Biochemistry 1997, 247:725- 732.

48. Hong Pyo Kim XW, Ferruccio Galbiati, Stefan W. Ryter and Augustine M. K. Choi: Caveolae compartmentalization of heme oxygenase-1 in endothelial cells. The FASEB Journal 2004, 18:1080-1089.

49. Lin Q, Weis S, Yang G, Weng YH, Helston R, Rish K, Smith A, Bordner J, Polte T, Gaunitz F: Heme Oxygenase-1 Protein Localizes to the Nucleus and Activates Transcription Factors Important in Oxidative Stress. Journal of Biological Chemistry 2007, 282(28):20621.

50. Shan Y, Lambrecht RW, Ghaziani T, Donohue SE, Bonkovsky HL: Role of Bach-1 in Regulation of Heme Oxygenase-1 in Human Liver Cells: Insights from studies with small interferin RNAs. Journal of Biological Chemistry 2004, 279(50):51769.

51. Ryter SW, Alam J, Choi AMK: Heme Oxygenase-1/Carbon Monoxide: From Basic Science to Therapeutic Applications. Physiological Reviews 2006, 86(2):583-650.

52. Richardson DR, Ponka P: The molecular mechanisms of the metabolism and transport of iron in normal and neoplastic cells. BBA-Reviews on Biomembranes 1997, 1331(1):1-40.

53. Eisenstein RS, Garcia-Mayol D, Pettingell W, Munro HN: Regulation of ferritin and heme oxygenase synthesis in rat fibroblasts by different forms of iron. Proceedings of the National Academy of Sciences USA 1991, 88(3):688.

54. Vile GF, Tyrrell RM: Oxidative stress resulting from ultraviolet A irradiation of human skin fibroblasts leads to a heme oxygenase-dependent increase in ferritin. Journal of Biological Chemistry 1993, 268(20):14678-14681.

55. Vile GF, Basu-Modak S, Waltner C, Tyrrell RM: Heme oxygenase 1 mediates an adaptive response to oxidative stress in human skin fibroblasts. Proceedings of the National Academy of Sciences USA 1994, 91(7):2607.

56. Furchgott RF, Jothianandan D: Endothelium-dependent and-independent vasodilation involving cyclic GMP: relaxation induced by nitric oxide, carbon monoxide and light. Blood Vessels 1991, 28(1-3):52-61.

57. Wandersman C, Stojiljkovic I: Bacterial heme sources: the role of heme, hemoprotein receptors and hemophores. Current Opinion in Microbiology 2000, 3(2):215-220.

58. Stojiljkovic I, Perkins-Balding D: Processing of heme and heme-containing proteins by bacteria. DNA Cell Biology 2002, 21(4):281-295.

59. Stojiljkovic I, Hantke K: Transport of haemin across the cytoplasmic membrane through a haemin-specific periplasmic binding-protein-dependent

transport system in Yersinia enterocolitica. Molecular Microbiology 1994, 13(4):719-732.

60. Wandersman C: Protein and peptide secretion by ABC exporters. Research in Microbiology 1998, 149(3):163-170.

61. Létoffé S, Omori K, Wandersman C: Functional Characterization of the HasAPF Hemophore and Its Truncated and Chimeric Variants: Determination of a Region Involved in Binding to the Hemophore Receptor. Journal of Bacteriology 2000, 182(16):4401.

62. Letoffe S, Redeker V, Wandersman C: Isolation and characterization of an extracellular haem-binding protein from Pseudomonas aeruginosa that shares function and sequence similarities with the Serratia marcescens HasA haemophore. Molecular Microbiology 1998, 28(6):1223-1234.

63. Letoffe S, Nato F, Goldberg ME, Wandersman C: Interactions of HasA, a bacterial haemophore, with haemoglobin and with its outer membrane receptor HasR. Molecular Microbiology 1999, 33(3):546-555.

64. DeCarlo AA, Paramaesvaran M, Yun PLW, Collyer C, Hunter N: Porphyrin-Mediated Binding to Hemoglobin by the HA2 Domain of Cysteine Proteinases (Gingipains) and Hemagglutinins from the Periodontal Pathogen Porphyromonas gingivalis. Journal of Bacteriology 1999, 181(12):3784.

65. Otto BR, van Dooren SJM, Nuijens JH, Luirink J, Oudega B: Characterization of a Hemoglobin Protease Secreted by the Pathogenic Escherichia coli Strain EB1. Journal of Experimental Medicine 1998, 188(6):1091-1103.

66. Genco CA, Dixon DW: Emerging strategies in microbial haem capture: MicroReview. Molecular Microbiology 2001, 39(1):1-11.

67. Olczak T, Simpson W, Liu X, Genco CA: Iron and heme utilization in Porphyromonas gingivalis. FEMS Microbiology Reviews 2005, 29(1):119-144.

68. Skaar EP, Humayun M, Bae T, DeBord KL, Schneewind O: Iron-source preference of Staphylococcus aureus infections. Science 2004, 305(5690):1626-1628.

69. Brickman TJ, Vanderpool CK, Armstrong SK: Heme Transport Contributes to In Vivo Fitness of Bordetella pertussis during Primary Infection in Mice. Infection and Immunity 2006, 74(3):1741.

70. Weissman Z, Kornitzer D: A family of Candida cell surface haem-binding proteins involved in haemin and haemoglobin-iron utilization. Molecular Microbiology 2004, 53(4):1209-1220.

71. Navarro-Garcia F, Sanchez M, Nombela C, Pla J: Virulence genes in the pathogenic yeast Candida albicans. FEMS Microbiology Reviews 2001, 25(2):245-268.

72. Pendrak ML, Chao MP, Yan SS, Roberts DD: Heme Oxygenase in Candida albicans Is Regulated by Hemoglobin and Is Necessary for Metabolism of Exogenous Heme and Hemoglobin to {alpha}-Biliverdin. Journal of Biological Chemistry 2004, 279(5):3426.

73. Santos R, Buisson N, Knight S, Dancis A, Camadro JM, Lesuisse E: Haemin uptake and use as an iron source by Candida albicans: role of CaHMX1-

encoded haem oxygenase. In., vol. 149: Society of General Microbiology; 2003: 579-588.

74. Grasbeck R, Kouvonen I, Lundberg M, Tenhunen R: An intestinal receptor for heme. Scandinavian Journal of Haematology 1979, 23(1):5-9.

75. Worthington MT, Cohn SM, Miller SK, Luo RQ, Berg CL: Characterization of a human plasma membrane heme transporter in intestinal and hepatocyte cell lines. American Journal of Physiology- Gastrointestinal and Liver Physiology 2001, 280:G1172-G1177.

76. Tenhunen R, Grasbeck R, Kouvonen I, Lundberg M: An intestinal receptor for heme: its parital characterization. International Journal of Biochemistry 1980, 12(5-6):713-716.

77. Shayeghi M, Latunde-Dada GO, Oakhill JS, Laftah AH, Takeuchi K, Halliday N, Khan Y, Warley A, McCann FE, Hider RC: Identification of an Intestinal Heme Transporter. Cell 2005, 122(5):789-801.

78. McKie AT, Marciani P, Rolfs A, Brennan K, Wehr K, Barrow D, Miret S, Bomford A, Peters TJ, Farzaneh F: A Novel Duodenal Iron-Regulated Transporter, IREG1, Implicated in the Basolateral Transfer of Iron to the Circulation. Molecular Cell 2000, 5(2):299-309.

79. Qiu A, Jansen M, Sakaris A, Min SH, Chattopadhyay S, Tsai E, Sandoval C, Zhao R, Akabas MH, Goldman ID: Identification of an Intestinal Folate Transporter and the Molecular Basis for Hereditary Folate Malabsorption. Cell 2006, 127(5):917-928.

80. Hamza I: Intracellular trafficking of porphyrins. ACS Chemical Biology 2006, 1:627-629.

81. Krishnamurthy PC, Du G, Fukuda Y, Sun D, Sampath J, Mercer KE, Wang J, Sosa-Pineda B, Murti KG, Schuetz JD: Identification of a mammalian mitochondrial porphyrin transporter. Nature 2006, 443(7111):586-589.

82. Kabe Y, Ohmori M, Shinouchi K, Tsuboi Y, Hirao S, Azuma M, Watanabe H, Okura I, Handa H: Porphyrin Accumulation in Mitochondria Is Mediated by 2-Oxoglutarate Carrier. Journal of Biological Chemistry 2006, 281(42):31729.

83. Shirihai OS, Gregory T, Yu C, Orkin SH, Weiss MJ: ABC-me: a novel mitochondrial transporter induced by GATA-1 during erythroid differentiation. The EMBO Journal 2000, 19(11):2492-2502.

84. Pondarre C, Campagna DR, Antiochos B, Sikorski L, Mulhern H, Fleming MD: Abcb7, the gene responsible for X-linked sideroblastic anemia with ataxia, is essential for hematopoiesis. Blood 2007, 109(8):3567-3569.

85. Quigley JG, Burns CC, Anderson MM, Lynch ED, Sabo KM, Overbaugh J, Abkowitz JL: Cloning of the cellular receptor for feline leukemia virus subgroup C (FeLV-C), a retrovirus that induces red cell aplasia. Blood 2000, 95(3):1093-1099.

86. Weiss RA, Tailor CS: Retrovirus receptors. Cell 1995, 82(4):531-533.

87. Quigley JG, Yang Z, Worthington MT, Phillips JD, Sabo KM, Sabath DE, Berg CL, Sassa S, Wood BL, Abkowitz JL: Identification of a human heme exporter that is essential for erythropoiesis. Cell 2004, 118(6):757-766.

88. Keel SB, Doty RT, Yang Z, Quigley JG, Chen J, Knoblaugh S, Kingsley PD, De Domenico I, Vaughn MB, Kaplan J: A Heme Export Protein Is Required for Red Blood Cell Differentiation and Iron Homeostasis. Science 2008, 319(5864):825.

89. Knutson MD, Oukka M, Koss LM, Aydemir F, Wessling-Resnick M: Iron release from macrophages after erythrophagocytosis is up-regulated by ferroportin 1 overexpression and down-regulated by hepcidin. Proceedings of the National Academy of Sciences 2005, 102(5):1324-1328.

90. Krishnamurthy P, Schuetz JD: The ABC Transporter Abcg2/Bcrp: Role in Hypoxia Mediated Survival. BioMetals 2005, 18(4):349-358.

91. Jonker JW, Buitelaar M, Wagenaar E, van der Valk MA, Scheffer GL, Scheper RJ, Plosch T, Kuipers F, Elferink RPJ, Rosing H: The breast cancer resistance protein protects against a major chlorophyll-derived dietary phototoxin and protoporphyria. Proceedings of the National Academy of Sciences 2002, 99(24):15649.

92. Krishnamurthy P, Ross DD, Nakanishi T, Bailey-Dell K, Zhou S, Mercer KE, Sarkadi B, Sorrentino BP, Schuetz JD: The Stem Cell Marker Bcrp/ABCG2 Enhances Hypoxic Cell Survival through Interactions with Heme. Journal of Biological Chemistry 2004, 279(23):24218.

93. Rao AU, Carta LK, Lesuisse E, Hamza I: Lack of heme synthesis in a free-living eukaryote. Proceedings of the National Academy of Sciences 2005, 102(12):4270.

94. Chitwood DJ: Research on plant-parasitic nematode biology conducted by the United States Department of Agriculture-Agricultural Research Service. Pest Management Science 2003, 59(6-7):748-753.

95. Colley DG, LoVerde PT, Savioli L: INFECTIOUS DISEASE: Medical Helminthology in the 21st Century. In., vol. 293; 2001: 1437-1438.

96. Gilleard JS: Understanding anthelmintic resistance: The need for genomics and genetics. International Journal for Parasitology 2006, 36(12):1227-1239.

97. Roos MH, Kwa MSG, Grant WN: New genetic and practical implications of selection for anthelmintic resistance in parasitic nematodes. Parasitology Today 1995, 11(4):148-150.

98. Held MR, Bungiro RD, Harrison LM, Hamza I, Cappello M: Dietary Iron Content Mediates Hookworm Pathogenesis In Vivo. Infection and Immunity 2006, 74(1):289.

99. Ghedin E, Wang S, Foster JM, Slatko BE: First sequenced genome of a parasitic nematode. Trends in Parasitology 2004, 20(4):151-153.

100. Foster J, Ganatra M, Kamal I, Ware J, Makarova K: The Wolbachia Genome of Brugia malayi: Endosymbiont Evolution within a Human Pathogenic Nematode. PLoS Biology 2005, 3(4):e121.

101. Brenner S: The genetics of Caenorhabditis elegans. Genetics 1974, 77(1):71-94.

102. Chalfie M: Genome sequencing. The worm revealed. Nature 1998, 396(6712):620-621.

103. The_C_elegans_Sequencing_Consortium: Genome sequence of the nematode C. elegans: a platform for investigating biology. Science 1998, 282(5396):2012-2018.

104. Nass R, Hamza I: The nematode C. elegans as an animal model to explore toxicology in vivo: solid and axenic growth culture conditions and compound exposure parameters. In: Current Protocols in Toxicology. Edited by Maines MD, Costa LG, Hodgson E, Reed DJ, Sipes IG. New York: John Wiley & Sons, Inc.; 2007: 1.9.1-1.9.17.

105. Timmons L, Court DL, Fire A: Ingestion of bacterially expressed dsRNAs can produce specific and potent genetic interference in Caenorhabditis elegans. Gene 2001, 263(1-2):103-112.

106. Irizarry RA, Hobbs B, Collin F, Beazer-Barclay YD, Antonellis KJ, Scherf U, Speed TP: Exploration, normalization, and summaries of high density oligonucleotide array probe level data. Biostatistics 2003, 4(2):249-264.

107. Ellestad LE, Carre W, Muchow M, Jenkins SA, Wang X, Cogburn LA, Porter TE: Gene expression profiling during cellular differentiation in the embryonic pituitary gland using cDNA microarrays. Physiological Genomics 2006, 25(3):414-425.

108. Livak KJ, Schmittgen TD: Analysis of relative gene expression data using real-time quantitative PCR and the $2^{-\Delta\Delta C}$T Method. Methods 2001, 25(4):402-408.

109. Evans TC: Transformation and microinjection. In: WormBook. Edited by The *C. elegans* Research Community W, doi/10.1895/wormbook.1.7.1, http://www.wormbook.org.; 2005.

110. Praitis V, Casey E, Collar D, Austin J: Creation of Low-Copy Integrated Transgenic Lines in Caenorhabditis elegans. Genetics 2001, 157(3):1217-1226.

111. Zhu YH, Hon T, Ye WZ, Zhang L: Heme deficiency interferes with the Ras-mitogen-activated protein kinase signaling pathway and expression of a subset of neuronal genes. Cell Growth & Differentiation 2002, 13(9):431-439.

112. Ponka P, Borova J, Neuwirt J, Fuchs O: Mobilization of iron from reticulocytes. Identification of pyridoxal isonicotinoyl hydrazone as a new iron chelating agent. FEBS Letters 1979, 97(2):317-321.

113. Medlock AE, Dailey HA: Regulation of mammalian heme biosynthesis. In: Tetrapyrroles. Edited by Warren M, Smith AG. Austin: Landes Bioscience and Springer Science + Business Media; 2007: 116-127.

114. Reinke V, Smith HE, Nance J, Wang J, Van Doren C, Begley R, Jones SJM, Davis EB, Scherer S, Ward S: A Global Profile of Germline Gene Expression in C. elegans. Molecular Cell 2000, 6(3):605-616.

115. www.bioconductor.org.

116. Irizarry RA, Bolstad BM, Collin F, Cope LM, Hobbs B, Speed TP: Summaries of Affymetrix GeneChip probe level data. Nucleic Acids Research 2003, 31(4):e15.

117. Altschul SF, Madden TL, Schaffer AA, Zhang J, Zhang Z, Miller W, Lipman DJ: Gapped BLAST and PSI-BLAST: a new generation of protein database search programs. Nucleic Acids Research, 25(17):3389-3402.

118. Berriman M, Ghedin E, Hertz-Fowler C, Blandin G, Renauld H, Bartholomeu DC, Lennard NJ, Caler E, Hamlin NE, Haas B, Bohme U, Hannick L, Aslett MA, Shallom J, Marcello L *et al*: The genome of the African trypanosome Trypanosoma brucei. Science 2005, 309(5733):416-422.

119. Koster W: ABC transporter-mediated uptake of iron, siderophores, heme and vitamin B12. Research in Microbiology 2001, 152(3-4):291-301.

120. Lee BC: Quelling the red menace: haem capture by bacteria. Molecular Microbiology 1995, 18(3):383-390.

121. Cousins RJ, Liuzzi JP, Lichten LA: Mammalian Zinc Transport, Trafficking, and Signals. Journal of Biological Chemistry 2006, 281(34):24085.

122. Dunn LL, Rahmanto YS, Richardson DR: Iron uptake and metabolism in the new millennium. Trends in Cell Biology 2007, 17(2):93-100.

123. Prohaska JR, Gybina AA: Intracellular copper transport in mammals. Journal of Nutrition 2004, 134(5):1003-1006.

124. Sonnhammer EL, von Heijne G, Krogh A: A hidden Markov model for predicting transmembrane helices in protein sequences. Proceedins of the International Conference on Intelligent Systems for Molecular Biology 1998, 6:175-182.

125. Rojek A, Praetorius J, Frokiaer J, Nielsen S, Fenton RA: A Current View of the Mammalian Aquaglyceroporins. Annual Review of Physiology 2008, 70:301.

126. Kulas J, Schmidt C, Rothe M, Schunck WH, Menzel R: Cytochrome P450-dependent metabolism of eicosapentaenoic acid in the nematode Caenorhabditis elegans. Archives of Biochemistry and Biophysics 2008.

127. Rajagopal A, Rao AU, Amigo J, Tian M, Upadhyay SK, Hall C, Uhm S, Mathew MK, Fleming MD, Paw BH, Krause M, Hamza I: Haem homeostasis is regulated by the conserved and concerted functions of HRG-1 proteins. Nature 2008, 453(7198):1127-1131.

128. Ashburner M, Ball CA, Blake JA, Botstein D, Butler H, Cherry JM, Davis AP, Dolinski K, Dwight SS, Eppig JT: Gene ontology: tool for the unification of biology. The Gene Ontology Consortium. Nature Genetics 2000, 25(1):25-29.

129. Arakawa K: KEGG-Based Pathway Visualization Tool for Complex Omics Data. In Silico Biology 2005, 5(4):419-423.

130. Kim JK, Gabel HW, Kamath RS, Tewari M, Pasquinelli A, Rual JF, Kennedy S, Dybbs M, Bertin N, Kaplan JM: Functional Genomic Analysis of RNA Interference in C. elegans. In., vol. 308: American Association for the Advancement of Science; 2005: 1164-1167.

131. Rual JF, Ceron J, Koreth J, Hao T, Nicot AS, Hirozane-Kishikawa T, Vandenhaute J, Orkin SH, Hill DE, van den Heuvel S: Toward Improving

Caenorhabditis elegans Phenome Mapping With an ORFeome-Based RNAi Library. In., vol. 14: Cold Spring Harbor Lab; 2004: 2162-2168.

132. Sönnichsen B, Koski LB, Walsh A, Marschall P, Neumann B, Brehm M, Alleaume AM, Artelt J, Bettencourt P, Cassin E: Full-genome RNAi profiling of early embryogenesis in Caenorhabditis elegans. Nature 2005, 434:462-469.

133. Kamath RS, Fraser AG, Dong Y, Poulin G, Durbin R, Gotta M, Kanapin A, Le Bot N, Moreno S, Sohrmann M: Systematic functional analysis of the Caenorhabditis elegans genome using RNAi. Nature 2003, 421:231-237.

134. Simmer F, Moorman C, Linden AM, Kuijk E, Berghe PVE, Kamath RS, Fraser AG, Ahringer J, Plasterk RHA: Genome-wide RNAi of C. elegans using the hypersensitive rrf-3 strain reveals novel gene functions. PLoS Biology 2003, 1(1):e2.

135. Hieb WF, Stokstad EL, Rothstein M: Heme requirement for reproduction of a free-living nematode. Science 1970, 168(927):143-144.

136. Cinar H, Keles S, Jin Y: Expression Profiling of GABAergic Motor Neurons in Caenorhabditis elegans. Current Biology 2005, 15(4):340-346.

137. Cui Y, McBride SJ, Boyd WA, Alper S, Freedman JH: Toxicogenomic analysis of Caenorhabditis elegans reveals novel genes and pathways involved in the resistance to cadmium toxicity. Genome Biology 2007, 8(6):R122.

138. Hill AA, Hunter CP, Tsung BT, Tucker-Kellogg G, Brown EL: Genomic analysis of gene expression in C. elegans. Science 2000, 290(5492):809-812.

139. O'Rourke D, Baban D, Demidova M, Mott R, Hodgkin J: Genomic clusters, putative pathogen recognition molecules, and antimicrobial genes are induced

by infection of C. elegans with M. nematophilum. Genome Research 2006, 16(8):1005.

140. Perally S, Lacourse EJ, Campbell AM, Brophy PM: Heme Transport and Detoxification in Nematodes: Subproteomics Evidence of Differential Role of Glutathione Transferases. Journal of Proteome Research 2008, 7(10):4557-4565.

141. Faller M, Matsunaga M, Yin S, Loo JA, Guo F: Heme is involved in microRNA processing. Nature Structural and Molecular Biology 2007, 14(1):23-29.

142. Shoubridge EA: Cytochrome c oxidase deficiency. American Journal of Medical Genetics (Semin Med Genet) 2001, 106:46-52.

143. Suzuki H, Tashiro S, Hira S, Sun J, Yamazaki C, Zenke Y, Ikeda-Saito M, Yoshida M, Igarashi K: Heme regulates gene expression by triggering Crm1-dependent nuclear export of Bach1. The EMBO Journal 2004, 23:2544-2553.

144. Wenger RH: Mammalian oxygen sensing, signalling and gene regulation. Journal of Experimental Biology 2000, 203(Pt 8):1253-1263.

145. Yin L, Wu N, Curtin JC, Qatanani M, Szwergold NR, Reid RA, Waitt GM, Parks DJ, Pearce KH, Wisely GB: Rev-erb {alpha}, a Heme Sensor That Coordinates Metabolic and Circadian Pathways. Science's STKE 2007, 318(5857):1786.

146. Colley DG, LoVerde PT, Savioli L: Infectious disease. Medical helminthology in the 21st century. Science 2001, 293(5534):1437-1438.

147. Lara FA, Sant'Anna C, Lemos D, Laranja GAT, Coelho MGP, Reis Salles I, Michel A, Oliveira PL, Cunha-e-Silva N, Salmon D: Heme requirement and intracellular trafficking in Trypanosoma cruzi epimastigotes. Biochemical and Biophysical Research Communications 2007, 355(1):16-22.

148. Patel N, Singh SB, Basu SK, Mukhopadhyay A: Leishmania requires Rab7-mediated degradation of endocytosed hemoglobin for their growth. Proceedings of the National Academy of Sciences USA 2008, 105(10):3980.

149. www.wormbase.org.

150. Hamza I, Prohaska J, Gitlin JD: Essential role for Atox1 in the copper-mediated intracellular trafficking of the Menkes ATPase. Proceedings of the National Academy of Sciences U S A 2003, 100(3):1215-1220.

151. Harrison PM, Arosio P: The ferritins: molecular properties, iron storage function and cellular regulation. BBA-Bioenergetics 1996, 1275(3):161-203.

152. Bonifacino JS, Traub LM: Signals for sorting of transmembrane proteins to endosomes and lysosomes. Annual Reviews in Biochemistry 2003, 72:395-447.

153. Goldman BS, Beck DL, Monika EM, Kranz RG: Transmembrane heme delivery systems. Proceedings of the National Academy of Sciences U S A 1998, 95(9):5003-5008.

154. Eakanunkul S, Lukat-Rodgers GS, Sumithran S, Ghosh A, Rodgers KR, Dawson JH, Wilks A: Characterization of the Periplasmic Heme-Binding Protein ShuT from the Heme Uptake System of Shigella dysenteriae. Biochemistry(Washington) 2005, 44(39):13179-13191.

155. Pellicena P, Karow DS, Boon EM, Marletta MA, Kuriyan J: Crystal structure of an oxygen-binding heme domain related to soluble guanylate cyclases. Proceedings of National Academy of Sciences U S A 2004, 101(35):12854-12859.

156. Schmidt PM, Rothkegel C, Wunder F, Schroder H, Stasch JP: Residues stabilizing the heme moiety of the nitric oxide sensor soluble guanylate cyclase. European Journal of Pharmacology 2005, 513(1-2):67-74.

157. Berezikov E, Bargmann CI, Plasterk RH: Homologous gene targeting in Caenorhabditis elegans by biolistic transformation. Nucleic Acids Research 2004, 32(4):e40.

158. Shafizadeh E, Paw BH: Zebrafish as a model of human hematologic disorders. Current Opinion in Hematology 2004, 11(4):255-261.

159. Fleming MD, Trenor CC, Su MA, Foernzler D, Beier DR, Dietrich WF, Andrews NC: Microcytic anaemia mice have a mutation in Nramp2, a candidate iron transporter gene. Nature Genetics 1997, 16:383-386.

160. Gunshin H, Mackenzie B, Berger UV, Gunshin Y, Romero MF, Boron WF, Nussberger S, Gollan JL, Hediger MA: Cloning and characterization of a proton-coupled mammalian metal-ion transporter. Nature 1997, 388:482-488.

161. Howe CL, Granger BL, Hull M, Green SA, Gabel CA, Helenius A, Mellman I: Derived Protein Sequence, Oligosaccharides, and Membrane Insertion of the 120-kDa Lysosomal Membrane Glycoprotein (lgp120): Identification of a Highly Conserved Family of Lysosomal Membrane Glycoproteins.

Proceedings of the National Academy of Sciences USA 1988, 85(20):7577-7581.

162. Rodman JS: Rab GTPases coordinate endocytosis. In: Journal of Cell Science. vol. 113; 2000: 183-192.

163. Goodwin DC, Rowlinson SW, Marnett LJ: Substitution of tyrosine for the proximal histidine ligand to the heme of prostaglandin endoperoxide synthase 2: implications for the mechanism of cyclooxygenase activation and catalysis. Biochemistry 2000, 39(18):5422-5432.

164. Hemler ME: Targeting of tetraspanin proteins - potential benefits and strategies. Nature Reviews in Drug Discovery 2008, 7(9):747-758.

165. Clokey GV, Jacobson LA: The autofluorescent "lipofuscin granules" in the intestinal cells of Caenorhabditis elegans are secondary lysosomes. Mechanisms of Ageing and Development 1986, 35(1):79-94.

166. Hermann GJ, Schroeder LK, Hieb CA, Kershner AM, Rabbitts BM, Fonarev P, Grant BD, Priess JR: Genetic analysis of lysosomal trafficking in Caenorhabditis elegans. Molecular Biology of the Cell 2005, 16(7):3273-3288.

167. Kostich M, Fire A, Fambrough DM: Identification and molecular-genetic characterization of a LAMP/CD68-like protein from Caenorhabditis elegans. Journal of Cell Science 2000, 113 (Pt 14):2595-2606.

168. Oka T, Futai M: Requirement of V-ATPase for ovulation and embryogenesis in Caenorhabditis elegans. Journal of Biological Chemistry 2000, 275(38):29556-29561.

169. Keegan LP, Leroy A, Sproul D, O'Connell MA: Adenosine deaminases acting on RNA (ADARs): RNA-editing enzymes. Genome Biology 2004, 5(2):209.

170. Merritt C, Rasoloson D, Ko D, Seydoux G: 3' UTRs Are the Primary Regulators of Gene Expression in the C. elegans Germline. Current Biology 2008.

171. Schmidt PM, Schramm M, Schroder H, Wunder F, Stasch JP: Identification of residues crucially involved in the binding of the heme moiety of soluble guanylate cyclase. Journal of Biological Chemistry 2004, 279(4):3025-3032.

172. Ascenzi P, Bocedi A, Visca P, Altruda F, Tolosano E, Beringhelli T, Fasano M: Hemoglobin and heme scavenging. IUBMB Life 2005, 57(11):749-759.

173. Kaback HR, Frillingos S, Jung H, Jung K, Prive GG, Ujwal ML, Weitzman C, Wu J, Zen K: The lactose permease meets Frankenstein. Journal of Experimental Biology 1994, 196:183-195.

174. Muller V, Gruber G: ATP synthases: structure, function and evolution of unique energy converters. Cell and Molecular Life Sciences 2003, 60(3):474-494.

175. Holtzman E: *Lysosomes.* Cellular organelles New York: Plenum Press.; 1989.

176. Radisky DC, Kaplan J: Iron in cytosolic ferritin can be recycled through lysosomal degradation in human fibroblasts. Biochemical Journal 1998, 336 (Pt 1):201-205.